2026

Final Report SPR-FY24(036)

Assessment of Truck Parking Demand and Safety During Normal and Severe Weather Conditions in Nebraska

Nathan Huynh, Ph.D.
Director, Nebraska Transportation Center
Professor, Department of Civil & Environmental Engineering
University of Nebraska-Lincoln

Li Zhao, Ph.D.
Research Assistant Professor
Department of Civil & Environmental Engineering
University of Nebraska-Lincoln

Zhenghong Tang, Ph.D.
Professor
Community and Regional Planning Program
University of Nebraska-Lincoln

Aida Riahifar
Graduate Research Assistant
Department of Civil & Environmental Engineering
University of Nebraska-Lincoln

Jahangeer Jahangeer, Ph.D.
Research Assistant Professor
Community and Regional Planning Program
University of Nebraska-Lincoln

Nebraska Department of Transportation Research
Headquarters Address
1400 Nebraska Parkway
Lincoln, NE 68509
ndot.research@nebraska.gov
(402) 479-4697
https://dot.nebraska.gov/business-center/research/

Nebraska Transportation Center
262 Prem S. Paul Research Center at Whittier School
2200 Vine Street
Lincoln, NE 68583-0851
(402) 472-1932
http://ntc.unl.edu

This report was funded in part through grant from the U.S. Department of Transportation Federal Highway Administration. The views and opinions of the authors expressed herein do not necessarily state or reflect those of the U.S. Department of Transportation.

Assessment of Truck Parking Demand and Safety During Normal and Severe Weather Conditions in Nebraska

Nathan Huynh, Ph.D.
Director, Nebraska Transportation Center
Professor, Department of Civil & Environmental Engineering
University of Nebraska-Lincoln

Aida Riahifar
Graduate Research Assistant
Department of Civil & Environmental Engineering
University of Nebraska-Lincoln

Li Zhao, Ph.D.
Research Assistant Professor
Department of Civil & Environmental Engineering
University of Nebraska-Lincoln

Jahangeer Jahangeer, Ph.D.
Research Assistant Professor
Community and Regional Planning Program
University of Nebraska-Lincoln

Zhenghong Tang, Ph.D.
Professor
Community and Regional Planning Program
University of Nebraska-Lincoln

A Report on Research Sponsored by

Nebraska Department of Transportation

and

Nebraska Transportation Center
University of Nebraska–Lincoln

January 2026

Technical Report Documentation Page

1. Report No. SPR-FY24(036)	2. Government Accession No.	3. Recipient's Catalog No.
4. Title and Subtitle Assessment of Truck Parking Demand and Safety During Normal and Severe Weather Conditions in Nebraska		5. Report Date: January 2026 6. Performing Organization Code
7. Author(s) Nathan Huynh, Li Zhao, Zhenghong Tang, Aida Riahifar, and Jahangeer Jahangeer		8. Performing Organization Report No.
9. Performing Organization Name and Address Nebraska Transportation Center University of Nebraska–Lincoln 2200 Vine Street, Prem S. Paul Research Center at Whittier School Lincoln, NE 68583-0851		10. Work Unit No. (TRAIS) 11. Contract or Grant No. FY24(036)
12. Sponsoring Agency Name and Address Nebraska Department of Transportation (NDOT) Headquarters Address 1400 Nebraska Parkway Lincoln, NE 68509		13. Type of Report and Period Covered 7/1/2023 – 1/31/2026 14. Sponsoring Agency Code NDOT
15. Supplementary Notes		

16. Abstract

This project examined truck parking capacity, demand, and utilization patterns along I-80 in Nebraska. The objectives were to (1) document the capacity of public and private truck parking facilities along I-80, (2) analyze spatial and temporal trends in parking demand, (3) develop models to predict occupancy at parking facilities, (4) identify clusters of undesignated parking during inclement weather, and (5) assess whether truck parking shortages contribute to truck-involved crashes. Within a one-mile buffer of I-80, 21 public facilities and 49 private facilities were identified. The spatiotemporal analysis of these public and private truck parking facilities using the National Agriculture Imagery Program and Google Earth Imagery data between 2010 and 2022 showed a higher parking occupancy rate at private facilities, with several private facilities experiencing 100% occupancy or higher. Public facilities near Omaha had a consistently high occupancy rate. To enable NDOT to estimate the occupancy rate of a facility, public or private, expansion factors were first developed using the 2022 ATRI GPS data. The number of trucks parked at public and private facilities was then estimated by multiplying the number of GPS-identified trucks that remained stationary for more than 60 minutes by the corresponding expansion factor. Building on these estimates, a hybrid Bayesian modeling framework was developed to predict occupancy. Parking facilities were clustered based on their inter-facility distances, resulting in groups containing either single or multiple facilities. Accordingly, a dynamic time series model was developed for individual facilities, while a panel model with time fixed effects and distance-based spatial lags was developed for multi-facility clusters. Results indicate that lagged occupancy is the strongest predictor, with spatial effects also significant in the panel model. Both models achieved strong predictive performance. During inclement weather, trucks were found to park in four locations: facility entry and exit areas, off-road sites, ramps, and shoulders. Lastly, statistical analysis showed no significant relationship between truck-involved crashes and parking shortages.

17. ORCID No. of each Researcher	18. Distribution Statement
Huynh: 0000-0002-4605-5651; Zhao: 0000-0003-1914-1041; Tang: 0000-0001-7603-0394; Riahifar: 0000-0001-8478-1040, and Jahangeer: 0000-0002-5070-1265	

19. Security Classif. (of this report)	20. Security Classif. (of this page)	21. No. of Pages	22. Price
Unclassified	Unclassified	149	

Table of Contents

List of Figures

List of Tables

List of Abbreviations

FHWA	Federal Highway Administration
NDOT	Nebraska Department of Transportation
NTC	Nebraska Transportation Center
USDOT	United States Department of Transportation
TAC	Technical Advisory Committee

Acknowledgments

The project team greatly appreciates the guidance and assistance from the following Technical Advisory Committee (TAC) members and NDOT Research Program staff:

- Ryan Huff (Lead TAC member)
- Jarrod Walker (Lead TAC member)
- Walter Moy
- Don Butler
- Justin Luther
- Lieska Halsey

Disclaimer

The contents of this report reflect the views of the authors, who are responsible for the facts and the accuracy of the information presented herein. The contents do not necessarily reflect the official views or policies of either the Nebraska Department of Transportation or the University of Nebraska-Lincoln. This report does not constitute a standard, specification, or regulation. Trade or manufacturers' names, which may appear in this report, are cited only because they are considered essential to the objectives of the report.

The United States (U.S.) government and the State of Nebraska do not endorse products or manufacturers. This material is based upon work supported by the Federal Highway Administration under SPR-FY24(036). Any opinions, findings, and conclusions or recommendations expressed in this publication are those of the authors and do not necessarily reflect the views of the Federal Highway Administration.

This report has been reviewed by the Nebraska Transportation Center for grammar and context, formatting, and compliance with Section 508 of the Rehabilitation Act of 1973.

Executive Summary

This project seeks to enhance understanding and management of truck parking along Interstate 80 (I-80), a nationally critical freight corridor. The objectives are to: (1) document the capacity and availability of public and private truck parking facilities, (2) analyze actual parking demand and identify geographic hotspots of overutilization, (3) develop predictive models of parking occupancy that account for spatial and temporal dynamics, (4) evaluate unauthorized parking during inclement weather, and (5) investigate whether parking shortages contribute to increased truck-involved crash risk.

Using a one-mile buffer (0.5 mile on each side) along I-80 in Nebraska, 20 public parking facilities (10 eastbound, 10 westbound) and 46 private facilities (18 eastbound, 28 westbound) were identified. Public facilities are generally small, with most offering fewer than 20 spaces (e.g., Kearney EB has only seven spaces), while private facilities range widely from fewer than 10 spaces to large truck stops exceeding 200 spaces (e.g., Pilot Travel Center has 400 spaces). This distribution indicates the important role private facilities provide in meeting truck parking demand, with state-operated rest areas serving a complementary function along the corridor.

Building on this inventory, spatiotemporal analysis of National Agriculture Imagery Program and Google Earth imagery (2010–2022) showed persistently high occupancy at both public and private facilities. Many public rest areas regularly operated at or above capacity, particularly those located eastbound near Omaha and westbound in central Nebraska. Several private facilities in eastern and central Nebraska also experienced repeated over-capacity conditions, with some eastbound sites operating near full utilization (often exceeding 80–100% of available spaces). These trends indicate that demand is concentrated in specific geographic

hotspots rather than evenly distributed across the corridor, highlighting growing strain on existing infrastructure and the need for targeted capacity improvements.

While the spatiotemporal analysis described truck parking patterns observed in 2022, these findings cannot directly predict future conditions at specific facilities. To address this need, a hybrid Bayesian framework was developed to predict parking occupancy by jointly capturing temporal dynamics and spatial dependencies. The framework consists of two components: dynamic Bayesian time-series models for individual (i.e., isolated) facilities, and dynamic Bayesian panel models with time fixed effects and spatial lags for clusters of facilities within 19 miles. The analysis used more than 350 million GPS records from 2022, scaled with expansion factors derived from seven Automatic Traffic Recorder (ATR) stations. The results showed that lagged occupancy was the most influential predictor, with spatial effects enhancing the model's predictive accuracy. Both models achieved strong predictive performance, with R^2 values between 0.66 and 0.89 and RMSE values ranging from 0.05 to 0.27.

Weather-related disruptions were also examined to determine how severe conditions and road closures affected truck parking behavior along the I-80 corridor. GPS data from these periods showed that many drivers stopped in undesignated locations. Among all recorded events, most of the undesignated parking occurred at off-road locations such as Walmart parking lots (~93%), followed by ramps (5.2%), shoulders (1.4%), and entry/exit areas (0.1%). Further spatial analysis revealed that these events were concentrated on recurring hotspots rather than evenly distributed along the corridor. The largest clusters occurred near major urban centers such as Lincoln and Omaha, and in central Nebraska around North Platte and Kearney, which together accounted for about 60% of all undesignated parking during severe weather. In many of these areas, trucks remained parked for more than 100 minutes on average, suggesting that drivers often waited until conditions improved before resuming travel. Although fewer weather events were recorded in western Nebraska in 2022, several smaller clusters were identified.

Finally, the project rigorously assessed whether truck parking shortages were statistically associated with truck-involved crashes along the I-80 corridor. In 2022, 1,610 truck-involved crashes were recorded, including 38 within parking facilities and 795 within 10-mile downstream buffers. Two matched sample strategies were implemented: one examined crashes within 10-mile downstream segments of parking facilities, and the other examined inter-facility segments along I-80. In both cases, all statistical tests, including Phi coefficients (0.000 and 0.0007, with $p = 1.000$ and $p = 0.654$, respectively), Matthews Correlation Coefficients (near-zero), and Spearman rank-order correlations (-0.000013 and 0.0009; $p \approx 1.0$), indicated no significant association between full parking occupancy and the occurrence of truck-involved crashes. Additionally, penalized logistic regression models found no statistically significant relationship between parking occupancy and crash occurrence in both models ($p = 0.993$ and $p = 0.562$), with odds ratios close to 1 and wide confidence intervals. These consistent findings indicate that full parking conditions were not a meaningful predictor of truck-involved crashes along I-80 in 2022.

Chapter 1 Introduction

Freight movement in the United States has grown steadily over the past three decades and is projected to continue increasing well into the future. Between 2020 and 2050, as shown in Figure 1.1, freight tonnage is expected to rise by nearly 50 percent, reaching about 29 billion tons, while the total value of shipments will double to more than $36 trillion (Hwang et al. 2021). Trucks are expected to remain the dominant mode of freight transportation, carrying approximately 65 percent of all tonnage across the nation (Hwang et al. 2021). As freight activity and truck traffic volumes continue to increase, the demand for safe and reliable truck parking infrastructure has become increasingly pressing for both drivers and transportation agencies.

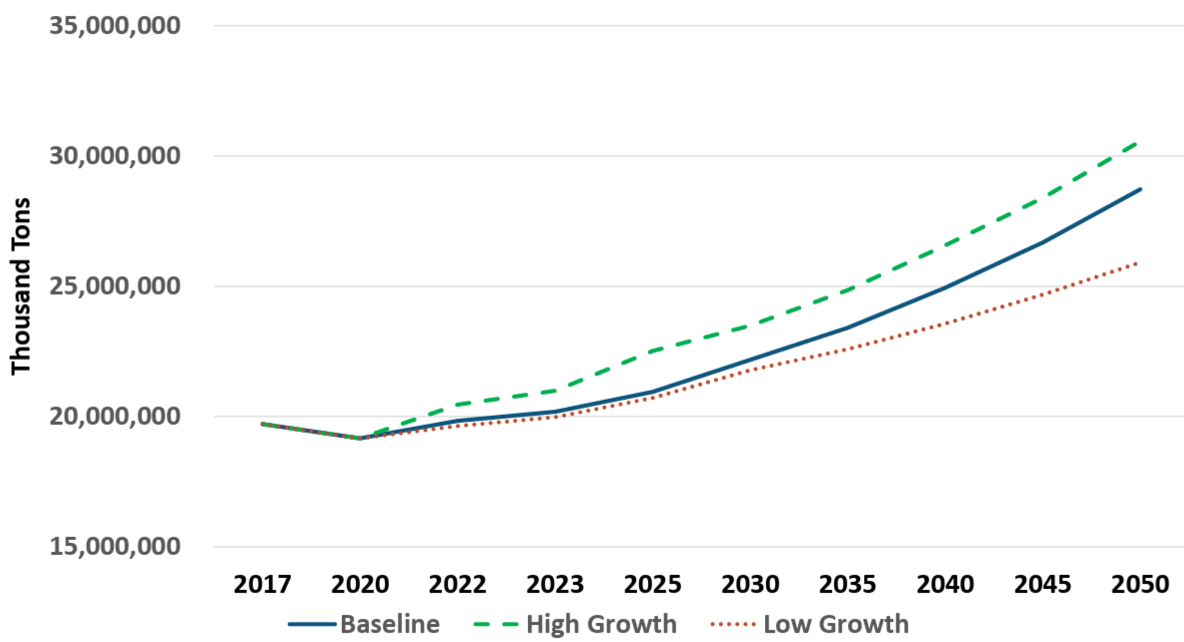

Figure 1.1 Freight Analysis Framework (version 5) Freight Growth Scenarios by the Year 2050. Source: Bureau of Transportation Statistics (Hwang et al. 2021)

The shortage of truck parking has been identified as one of the most pressing concerns in the trucking industry. In annual surveys conducted by the American Transportation Research

Institute (ATRI), this issue consistently ranks among the top five industry challenges (ATR 2023). Recognizing the national importance of this issue, Section 1401 of the Moving Ahead for Progress in the 21st Century Act (MAP-21), also known as Jason's Law, established a national priority to address the shortage of long-term truck parking on the National Highway System to improve safety for commercial drivers and the traveling public. This shortage is directly tied to federal Hours-of-Service (HOS) regulations, which limit the number of hours commercial motor vehicle drivers can drive and require them to take mandatory rest breaks, all of which are monitored by onboard electronic logging devices. When safe parking is unavailable, drivers may be forced to stop earlier than required or spend excessive time searching for spaces, leading to lost productivity and income. Drivers are estimated to lose about $4,600 annually in wages from stopping early due to inadequate parking (Boris and Brewster 2016). Inadequate parking also forces drivers to park in unauthorized areas such as ramps, shoulders, or other undesignated areas, thereby introducing safety risks for both CMV drivers and the traveling public.

In Nebraska, truck parking shortages are a growing concern along I-80, the backbone of the state's freight network and one of the most critical east–west freight corridors in the nation. Nebraska moves more than 440 million tons of goods annually, and freight volumes are projected to grow substantially in the coming decades, driven by agriculture, food manufacturing, and other freight-intensive industries (Nebraska Department of Transportation 2023). The 2023 Nebraska State Freight Plan noted that all 20 public truck parking facilities in the state are located along I-80 and that they have limited parking places. Consequently, private facilities play a critical role in meeting overall parking demand. Feedback from Nebraska stakeholders gathered during the development of the 2023 State Freight Plan indicated that inadequate parking not only disrupts freight efficiency but may also compromise safety, particularly when drivers are forced to stop in undesignated areas. While these concerns are widely recognized, they remain largely anecdotal, underscoring the need for data-driven analysis to quantify parking demand and guide investment strategies.

Previous research has examined truck parking issues at the national and state levels; however, none has focused specifically on Nebraska. For the Nebraska Department of Transportation (NDOT), several important questions remain unexplored and were beyond the scope of the 2023 State Freight Plan. These include how public truck parking facilities differ from private ones in terms of available spaces, amenities, and utilization; the magnitude and spatial distribution of parking demand across the state; and the feasibility of developing predictive models to support future planning and investment decisions. NDOT was also interested in understanding how severe weather affects parking behavior, for example, where drivers choose to park when I-80 is closed or during snowstorms and other extreme weather events. Finally, NDOT sought to determine whether limited truck parking availability contributes to truck-involved crashes along I-80.

To address these questions, this project was undertaken to provide NDOT with data-driven insights into truck parking needs along I-80. The study advances five interrelated objectives, closely aligned with priorities in NDOT's State Freight Plan:

1. To develop a complete inventory of public and private parking facilities, including capacities and amenities, addressing the gap in supply data.
2. To analyze one year of truck GPS data, scaled with traffic counts, to quantify utilization patterns and identify demand hotspots under both normal and severe weather conditions.
3. To build predictive models of parking occupancy that account for temporal persistence and spatial interactions, advancing beyond conventional facility-based approaches.

4. To identify clusters of unauthorized parking, particularly those arising during inclement weather, to guide emergency preparedness.
5. To examine whether truck-involved crashes are associated with parking shortages under two scenarios: (1) crashes occurring within ten miles downstream of a facility, and (2) crashes occurring between one facility and the next, thereby clarifying the safety concerns raised by stakeholders.

The remainder of this report is organized as follows. Chapter 2 reviews the relevant literature on truck parking demand prediction, weather-related impacts on parking behavior, and the relationship between parking availability and truck-involved crashes. Chapter 3 describes the datasets used in the analysis, including GPS data, Automatic Traffic Recorder (ATR) counts, weather data, and crash records. Chapter 4 presents the modeling frameworks and analytical methods applied in this study. Chapter 5 presents the empirical results derived from these analyses, and Chapter 6 concludes with a summary of key findings and practical recommendations for NDOT.

Chapter 2 Literature Review

The literature on truck parking is extensive and multidisciplinary, encompassing regulatory, operational, economic, behavioral, and technological perspectives. Research topics range from compliance with HOS regulations and electronic logging device implementation to routing, dispatching, and the economics of facility provision and pricing. Studies have examined public–private partnerships, land-use constraints, and the siting and design of truck stops and rest areas. On the technology front, an important body of work focuses on Truck Parking Information and Management Systems, which integrate sensors, communication networks, and traveler information platforms to provide real-time updates on parking availability. These systems, often implemented through federal and state partnerships, aim to improve parking efficiency, reduce search times, and enhance safety. Other areas of research address environmental impacts, community and equity considerations, electrification and charging needs, and infrastructure resilience during severe weather or emergencies. However, despite this breadth, few studies have comprehensively analyzed the spatial and temporal patterns of public and private truck parking facilities across an entire state over an extended period. This study directly addresses that gap by examining long-term trends in truck parking along a major interstate corridor (Objective 2).

Given the broad research landscape on truck parking, the present review focuses specifically on three research domains most relevant to this project: (1) prediction of truck parking demand, (2) weather-related impacts on undesignated parking, and (3) the relationship between parking availability and commercial motor vehicle crashes.

2.1 Prediction of Truck Parking Demand

2.1.1 Statistical and Econometric Models

The earliest stream of research on truck parking demand utilized statistical and econometric frameworks such as linear regression, Poisson regression, and negative binomial models. These approaches were attractive because they offered interpretable coefficients, were computationally tractable, and aligned with the type of survey and count data typically available in transportation studies.

Guerrero et al. (2023) developed linear regression and negative binomial models to estimate truck parking demand in Phoenix. Their study revealed that demand is strongly concentrated around locations associated with heavy machinery and industrial activity, underscoring how land-use characteristics shape parking needs. The use of the negative binomial framework was particularly valuable because it accounted for overdispersion in parking count data, a feature often encountered in real-world settings.

Similarly, Haque et al. (2017) examined truck parking utilization in Tennessee using Poisson and negative binomial models. The inclusion of time-of-day dummy variables in the regression specification allowed the authors to statistically capture diurnal variation in parking behavior. Significant positive coefficients for late-night hours (e.g., 12–1 a.m., 2–3 a.m., and 9–10 p.m.) indicated a higher probability of truck accumulation during these periods, whereas negative coefficients for afternoon hours (particularly 3–4 p.m.) reflected lower utilization. Elasticity estimates further confirmed that parking demand during the hour past midnight was approximately 11% greater than the average, while afternoon values declined. These results, derived directly from the model parameters rather than descriptive trends, provided one of the first empirical demonstrations that truck parking demand is temporally dynamic, exhibiting systematic and predictable daily cycles with clear nighttime peaks. Vital, Ioannou, and Gupta (2020), in their comprehensive survey on intelligent truck parking, discussed the application of non-homogeneous Poisson process (NHPP) models as an extension of classical count models. By allowing the intensity parameter to vary over time, NHPP approaches can capture the dynamic nature of parking demand more effectively than static Poisson or negative binomial models. Their review further emphasized that prediction-based statistical models, including NHPP, consistently outperformed naive historical averages, reinforcing the operational value of even relatively simple econometric forecasting tools for planners.

Collectively, these studies established three important insights. First, econometric models are well-suited to quantify the effects of observable factors such as land use, facility characteristics, and time of day. Second, truck parking demand is highly variable and subject to overdispersion, necessitating models more flexible than standard Poisson regression. Third, statistical methods offered the first baseline forecasts that agencies could use to understand capacity shortages.

Yet, despite their contributions, econometric approaches faced important limitations. These models relied on specific statistical assumptions about how the data are distributed; for example, the Poisson model assumes that the mean and variance of parking counts are equal, while the negative binomial model assumes a fixed form of overdispersion. Such restrictive model assumptions limit their ability to capture more complex, nonlinear relationships between predictors and demand. For instance, increases in truck traffic volumes may not translate linearly into higher demand once facilities approach capacity, but traditional linear and count-based models are ill-suited to represent this saturation effect. Moreover, these models typically analyzed each facility in isolation, ignoring potential spillover effects whereby overflowing from one site influences utilization at neighboring facilities. Finally, they provided little insight into the temporal persistence of demand—whether high utilization during one hour raises the likelihood of continued congestion in subsequent hours. Collectively, these limitations suggest the need for more flexible, data-driven approaches made possible by the growing availability of large-scale GPS datasets.

2.1.2 GPS-Based and Observational Approaches

Given the limitations of applying statistical models, some researchers turned to empirical datasets that could provide direct evidence of truck parking behavior. The expansion of GPS tracking for commercial vehicles and field-based monitoring of facilities marked an important shift in the literature. These studies moved beyond abstract parameter estimates to capture the where and when of parking demand with greater fidelity.

Torrey IV & Murray (2017) offered one of the first systematic efforts to use truck GPS data in Minnesota to evaluate the balance between supply and demand. Their analysis showed that demand for parking consistently outpaced both public and private supply, confirming industry concerns that existing infrastructure was insufficient. The strength of this study was its ability to highlight regional hot spots and temporal spikes in demand that conventional regression approaches could only approximate. However, while the GPS-based evidence provided a more accurate picture of utilization, the analysis was largely descriptive and case-specific, limiting its generalizability across broader freight corridors.

In another example, Bayraktar et al. (2015) examined truck parking utilization in Florida using Kalman filtering to track the dynamic distribution of facility usage. Kalman filters are well-suited for smoothing noisy time series data and provided valuable insights into overall utilization trends. However, this approach did not capture slot-level variations in occupancy, which are essential for understanding localized congestion and overflow phenomena. Despite these limitations, the study demonstrated how filtering techniques could enrich the analysis of field data and inspired hybrid approaches in subsequent research.

Together, these studies advanced the field in three important ways. First, they demonstrated the operational value of GPS and field observations for identifying temporal peaks and spatial imbalances in truck parking. Second, they highlighted the persistent mismatch between demand and available supply, underscoring the urgency of policy responses. Third, they showed that advanced filtering techniques can enhance data interpretation, particularly when observations are noisy or incomplete.

Nevertheless, GPS-based and observational approaches are not without shortcomings. Most analyses are constrained by localized case studies, raising concerns about the transferability of findings to other contexts. In addition, they rarely account for inter-facility interactions: overflow from one lot often affects nearby facilities, but such spatial spillovers were largely ignored. Finally, while GPS data can reveal patterns of movement and stop, their use for predictive modeling remained limited in this phase, motivating the subsequent adoption of machine learning approaches better equipped to handle nonlinearities and spatiotemporal dependencies.

2.1.3 Machine Learning Models

The growing availability of GPS data and advances in computational methods opened the door for the use of machine learning (ML) in truck parking demand prediction. Unlike traditional econometric approaches, which rely on predefined functional forms, ML algorithms are data-driven and flexible, making them better suited to capture nonlinearities and complex interactions among predictors. This shift represented a natural response to the limitations observed in statistical and observational studies: the need to model spatiotemporal dependencies, saturation effects, and diverse facility characteristics without imposing restrictive modeling assumptions.

Early ML studies applied relatively simple algorithms, such as support vector machines (SVM), regression trees, and ensemble methods, to predict truck parking. These models offered greater adaptability to heterogeneous datasets while remaining computationally manageable.

Zhao et al. (2020) tested regression and SVM methods in urban settings in China to forecast parking occupancy. Their findings demonstrated that SVM achieved more stable and accurate predictions across different facility types and sizes compared to conventional regression approaches. This was particularly important because it highlighted the value of ML in generalizing across diverse contexts, something traditional models often struggled with.

Slavova et al. (2022) extended this line of inquiry by evaluating a suite of machine learning algorithms, including decision trees, random forests, and gradient boosting, in the Netherlands. Their comparative analysis revealed that decision tree–based methods were especially effective for real-time applications, owing to their low computational overhead and ability to adapt to incoming data streams. The study also emphasized that ML approaches could scale better than econometric models when datasets grew larger and more complex.

Taken together, these early ML studies showed that classical algorithms could outperform regression-based approaches in both accuracy and scalability. However, they also exposed new challenges: many ML models still required extensive feature engineering to incorporate relevant predictors, and their capacity to account for sequential or spatial correlations was limited. These shortcomings set the stage for the adoption of deep learning architectures capable of directly learning such dependencies from the data.

2.1.4 Deep Learning Models

The limitations of classical ML approaches, particularly their inability to capture temporal persistence and inter-facility spillovers, prompted researchers to explore more sophisticated frameworks. For example, parking demand at one facility is often influenced by conditions at neighboring facilities, and occupancy levels at one point in time can strongly predict levels in subsequent hours. Classical ML techniques typically treat each data point as independent, making it difficult to model such dependencies. This realization motivated the application of deep learning (DL) architectures, including recurrent neural networks (RNNs) and graph-based frameworks, which are explicitly designed to address these challenges.

While classical ML approaches represented an important step forward by demonstrating that non-parametric, data-driven models could outperform traditional econometrics, their limitations in handling spatiotemporal dynamics and their dependence on manual feature selection highlighted the need for more advanced modeling strategies. The deep learning literature, discussed in the next section, reflects this progression.

The rapid advancement of computational power and the growing availability of high-frequency, high-volume datasets fundamentally transformed truck parking demand research. Building on the momentum of classical machine learning, DL approaches emerged as the leading paradigm for capturing nonlinear, spatiotemporal, and interdependent dynamics. Unlike regression or classical ML models, DL architectures can directly learn sequential patterns, spatial interactions, and latent features from raw data, reducing the need for extensive manual feature engineering.

Ludowieg et al. (2023) provided early evidence of the superiority of deep learning neural networks over traditional regression methods in Spain. Their comparative analysis of multilayer perceptron (MLP), long short-term memory (LSTM), and hybrid architectures against linear regression for loading-zone demand prediction demonstrated that these deep learning models substantially improved predictive accuracy. This finding was important because it highlighted the nonlinearity and heterogeneity of parking demand—a complexity that linear models could not adequately capture. The study reinforced the idea that parking demand is not only influenced by observable variables but also by latent interactions and unobserved behavioral factors that deep neural networks are better equipped to capture.

One of the most significant innovations in truck parking demand prediction has been the adoption of recurrent architectures, particularly long short-term memory (LSTM) networks, which are designed to capture temporal persistence in sequential data.

Shao et al. (2019) applied LSTM models in Australia to forecast truck parking availability, showing that their framework outperformed conventional baselines across multiple performance metrics. The study revealed that occupancy levels exhibit strong serial correlation, meaning that recent demand conditions are highly predictive of near-future demand. LSTM networks were able to exploit this dependency more effectively than classical ML, making them ideal for short-term prediction.

Building on this, Shao et al. (2024) combined LSTM regression models with K-shape clustering in Melbourne. Their hybrid approach first clustered parking facilities into homogeneous groups based on usage patterns, then applied LSTM within each cluster. The results showed that clustering substantially improved accuracy by tailoring predictions to the unique characteristics of each group. This study illustrated how hybrid methods could enhance the scalability and adaptability of DL approaches, particularly when applied to large heterogeneous facility networks.

Another innovative application of DL models came from Yang et al. (2022), who proposed the Smart Parking Data Management and Prediction (SPDMP) system using neural representation learning. By embedding facility attributes and usage data into latent vector representations, their model improved both accuracy and computational efficiency for real-time prediction. This study illustrated how DL could be integrated into larger decision-support systems, moving beyond standalone prediction toward actionable tools for transportation agencies.

Perhaps the most transformative contributions in recent years have been the application of graph-based learning. These methods explicitly model the spatial interdependence between facilities, allowing the prediction framework to account for spillover effects when one lot reaches capacity.

Sasaki et al. (2023) introduced a graph-to-sequence framework in Spain, demonstrating that their approach outperformed conventional sequence-to-sequence models for predicting truck parking availability. By directly encoding the spatial relationships between facilities, the graph-to-sequence model provided more realistic forecasts of demand redistribution.

Zhang et al. (2022) advanced this line of work with a hierarchical recurrent graph convolutional network (HRGCN) in China. Their framework combined graph convolution (for spatial dependencies) with recurrent layers (for temporal dynamics), outperforming seven benchmark models. Importantly, the HRGCN design reflected how truck parking demand is simultaneously shaped by local temporal cycles and broader network-level interactions.

Awan et al. (2020) provided further insights by testing recurrent neural networks (RNNs) in Spain. Interestingly, they found that simpler architectures sometimes performed as well as, or better than, more complex models. This finding raised critical questions about the trade-offs between model complexity, interpretability, and practical deployment, issues that remain central to the literature today. Collectively, deep learning studies delivered several breakthroughs. They validated the strong temporal persistence of parking demand and demonstrated the superiority of recurrent architectures in capturing it. They also highlighted the importance of facility heterogeneity, showing that clustering and hybrid methods could substantially improve scalability. In addition, these studies incorporated spatial interactions through graph-based methods, thereby addressing one of the most persistent gaps in earlier models. Finally, they opened pathways for real-time prediction and integration into operational systems, illustrating the potential of DL frameworks to support practical decision-making in transportation planning.

Despite these advances, limitations remain. DL approaches require large volumes of high-quality data, which may not always be available across corridors or states. They are also computationally demanding, raising concerns about scalability in real-world planning environments. Most importantly, DL models often function as "black boxes," offering little transparency for policymakers who need interpretable evidence to guide infrastructure investment. These limitations suggest the need for hybrid frameworks that combine the predictive strength of DL with the interpretability and policy relevance of more transparent models.

Table 2.1 synthesizes the reviewed studies across methodological categories, summarizing their key contributions and limitations. The progression highlights how the literature has evolved from interpretable but rigid econometric frameworks toward flexible, data-driven approaches capable of modeling nonlinear, temporal, and spatial dependencies.

Table 2.1 Summary of Literature on Truck Parking Demand Prediction

Category / Study	Model Type / Technique	Key Findings / Contributions	Main Limitations / Gaps
Statistical & Econometric Models			
Guerrero et al. (2023)	Linear and Negative Binomial Regression	Revealed that parking demand concentrates around industrial and heavy-machinery zones; land-use strongly shapes parking needs.	Static specification; ignored temporal persistence and spatial spillovers.
Haque et al. (2017)	Poisson and Negative Binomial Models	Identified clear diurnal cycles—overnight peaks and morning declines—showing parking demand is time-dependent.	Treated facilities independently; lacked temporal or spatial interaction modeling.
Vital, Ioannou, & Gupta (2021)	Non-Homogeneous Poisson Process (NHPP)	Demonstrated that NHPP models capture time-varying demand intensity better than static count models.	Required restrictive distributional assumptions; limited flexibility.
GPS-Based and Observational Approaches			
Torrey IV & Murray (2017)	GPS-Based Descriptive Analysis	Used GPS data to show chronic shortages and regional hot-spots, confirming persistent supply–demand imbalance.	Descriptive and case-specific; not generalizable or predictive.
Bayraktar et al. (2015)	Kalman Filtering	Applied Kalman filtering to smooth noisy occupancy data and reveal utilization trends over time.	Ineffective at slot-level variation; limited spatial detail.
Machine Learning Models			
Zhao et al. (2020)	Regression and Support Vector Machines (SVM)	Showed that SVM yields more accurate and stable occupancy forecasts than regression models across facility types.	Required heavy feature engineering; weak temporal and spatial correlation capture.
Slavova et al. (2022)	Decision Trees, Random Forest, Gradient Boosting	Found that tree-based ensembles perform efficiently for real-time truck-parking prediction at scale.	Could not represent temporal or inter-facility dependencies.

Deep Learning Models			
Ludowieg et al. (2023)	Neural Networks (Feedforward)	Confirmed neural networks outperform linear models in capturing nonlinear and heterogeneous demand patterns.	Limited interpretability; black-box behavior.
Shao et al. (2019)	Long Short-Term Memory (LSTM) Network	Demonstrated that LSTM models effectively capture temporal persistence in occupancy dynamics.	Data-intensive and computationally demanding.
Shao et al. (2024)	Hybrid: LSTM + K-Shape Clustering	Hybrid LSTM + K-shape clustering improved accuracy by tailoring predictions to facility groups.	Performance depends on correct clustering; transferability limited.
Yang et al. (2022)	Neural Representation Learning (SPDMP)	Developed SPDMP with neural representations, improving real-time predictive accuracy and efficiency.	Requires rich labeled data; corridor-specific calibration.
Sasaki et al. (2023)	Graph-to-Sequence Neural Network	Introduced graph-to-sequence network capturing spatial spillovers among facilities for realistic forecasts.	Complex structure; limited transparency for planning.
Zhang et al. (2022)	Hierarchical Recurrent Graph Convolutional Network (HRGCN)	Proposed HRGCN integrating temporal and spatial features, outperforming multiple benchmarks.	Computationally heavy; large data requirements.
Awan et al. (2020)	Recurrent Neural Network (RNN)	Found that simpler RNNs can match or exceed complex models, highlighting model-efficiency trade-offs.	Limited interpretability; context-specific results.

2.1.5 Summary

To date, no study has systematically addressed both spatial and temporal dependencies in forecasting truck parking occupancy at the corridor scale. Existing approaches tend to model either temporal patterns or spatial interactions in isolation, overlooking how these two dimensions interact in practice. For instance, high occupancy in one hour often signals congestion in the next, and shortages at one location frequently spill over into neighboring facilities. This omission reduces predictive accuracy and limits operational usefulness for corridor-level management. The present study fills this gap by introducing a hybrid Bayesian spatio-temporal framework that explicitly integrates temporal dynamics, spatial interdependence, and unobserved facility-level effects. In contrast to purely data-driven black-box models, the proposed Bayesian specification preserves coefficient interpretability, allowing direct assessment of how explanatory factors influence parking occupancy. Moreover, the model's Bayesian structure allows continual updating with new data, ensuring that estimated relationships remain interpretable, transferable, and statistically consistent over time.

2.2 Weather-Related Impacts on Undesignated Truck Parking

Severe weather has emerged as a critical yet underexplored factor shaping truck parking behavior. While much of the existing literature focuses on demand forecasting under normal conditions, evidence suggests that snowstorms, flooding, and other extreme weather events exacerbate shortages and significantly increase the prevalence of unauthorized off-road parking. These disruptions highlight that parking demand is not a static phenomenon but one that is highly sensitive to environmental shocks.

Early state freight plans and industry reports consistently observed that during heavy snow or facility closures, truck drivers diverted to highway shoulders, interchange ramps, or other unsafe areas (Minnesota Department of Transportation 2019). Pigman and Agent (1998) similarly reported that trucks parked on ramps and shoulders created safety conflicts, a problem aggravated under adverse weather conditions.

More recently, Shrestha (2023) provided some of the clearest empirical evidence linking weather-related disruptions to parking safety. Their analysis of rest area closures demonstrated that when facilities were forced offline by severe storms or other disruptions, drivers shifted to unauthorized roadside locations, leading to measurable increases in crash risks. This study highlighted that even temporary reductions in capacity can have cascading safety consequences, underscoring the importance of parking infrastructure resilience alongside baseline availability.

Systematic modeling of weather impacts remains rare. Most predictive studies either exclude weather variables entirely or treat them as minor controls, leaving limited quantitative understanding of how seasonal variation and severe storms influence demand peaks and unauthorized parking. This gap is particularly significant for states such as Nebraska, where frequent winter storms routinely disrupt travel and directly affect corridor safety.

2.3 Impact of Truck Parking on Truck-Involved Crashes

One of the most critical dimensions of the truck parking shortage is its potential connection to traffic safety. While much of the literature has focused on forecasting demand and utilization, several studies have explicitly examined whether inadequate parking contributes to risky behaviors and crash outcomes. This body of work is particularly relevant to policymakers, as it links infrastructure deficits to tangible safety consequences.

Early qualitative evidence indicates that insufficient truck parking capacity directly contributes to risky driver behavior. Boris and Brewster (2016), using truck-driver parking diaries, documented that drivers who struggled to find legal parking often resorted to unsafe alternatives such as freeway ramps, shoulders, or vacant lots. Although their study did not employ a statistical model, it revealed the behavioral mechanisms through which parking shortages escalate safety risks, highlighting the causal chain from limited capacity to increased exposure to hazards.

In parallel, Hernandez and Anderson (2017) identified the nationwide shortage of safe and adequate truck parking as a growing safety threat to highway users. Drawing on survey data from professional drivers across multiple northwestern states, they found that a majority of respondents experienced persistent difficulty finding safe parking along primary freight corridors, often leading to illegal or unsafe stopping behaviors. Their findings emphasized that chronic parking scarcity contributes to driver fatigue, stress, and schedule disruptions, thereby increasing the likelihood of unsafe parking and crash risk.

Building on this behavioral foundation, Anderson et al. (2018) conducted a quantitative analysis and by using a random-parameters binary logit model to examine survey data from long-haul drivers and identify factors influencing drivers' perceptions of parking adequacy and safety. Explanatory variables included roadway type, traffic density, access to rest-area amenities, distance between parking facilities, and time of day. Results indicated that drivers operating on high-traffic routes with longer spacing between facilities were significantly more likely to perceive parking as inadequate or unsafe, suggesting that perceived scarcity itself can influence driver decision-making and risk-taking behavior.

These behavioral and perceptual studies set the stage for empirical analyses linking parking shortages to actual crash outcomes. Boggs et al. (2019) conducted one of the first statistical examinations of this relationship using crash data from Tennessee. They analyzed 179 police-reported crashes involving illegally parked trucks across 1,221 rural and urban interstate ramps. To statistically test the relationship, the authors applied Bayesian binary logistic regression models, in three variants with different prior distributions, to estimate the odds of a truck-involved crash as a function of parking facility utilization and ramp characteristics. Explanatory variables included ramp length, geometric configuration (e.g., diamond vs. other types), presence of adjacent parking facilities, shoulder width, ramp type (on- vs. off-ramp), and parking utilization rate. Results showed that shorter entrance ramps, ramps adjacent to parking facilities operating at or above 90 percent utilization, diamond-shaped configurations, wider shoulders, and off-ramps were all significantly associated with higher odds of crashes involving illegally parked trucks. This study provided the first quantitative evidence directly linking parking inadequacy to safety risk at the ramp level.

More recently, Mathew et al. (2024) examined the effects of rest-area closures on truck parking availability and crash risk. Their results demonstrated that when rest areas were temporarily closed, drivers were substantially more likely to park in unsafe locations, producing measurable increases in crash rates. This finding suggested the system's sensitivity to sudden disruptions and reinforced the conclusion that parking capacity is not merely a matter of convenience but a fundamental component of highway safety infrastructure.

Collectively, the evidence indicates a consistent association between truck parking shortages and elevated crash risks. Behavioral accounts and empirical analyses alike show that when adequate parking is unavailable, drivers resort to unsafe alternatives, creating new conflict points and increasing crash risk.

Chapter 3 Data Description

This project utilized several data sources, including aerial imagery from the National Agriculture Imagery Program (NAIP) and Google Earth, truck parking facility websites, high-resolution truck GPS data, Automatic Traffic Recorder (ATR) counts, crash records, and NDOT monthly reports on weather conditions and highway closures. Truck parking facility websites and NDOT's State Freight Plan were used to document the facility locations, capacities, and amenities. Aerial imagery was used to analyze the spatial and temporal demand over time. Truck GPS data were used to determine truck parking locations and durations at truck parking facilities and undesignated parking locations, as well as truck trajectories. ATR data were used to determine expansion factors, which are the quotient of truck volume at the ATR and the corresponding number of GPS-equipped trucks. Crash records were used to determine the number of truck-involved crashes on I-80 downstream of public and private parking facilities. Lastly, NDOT weather reports were used to determine when I-80 was closed due to severe weather conditions.

3.1 Facility Inventory Data

A comprehensive inventory of truck parking facilities located within a one-mile (1.6 km) buffer along Nebraska's I-80 corridor was assembled. This inventory included both public and private facilities, as shown in Figure 3.1. The public facilities and their associated metadata, location, ID, and number of available parking spaces, were obtained from the Nebraska Department of Transportation's State Freight Plan (Nebraska Department of Transportation 2023). In contrast, private facilities were identified through two online sources: RoadNow[1] and TruckStopsAndServices.com[2], both of which provide locations of truck stops, parking

[1] https://roadnow.com/i80/truck-stops-nebraska
[2] https://www.truckstopsandservices.com/location_details.php?id=16262

availability, and amenities. Facility-level attributes such as directionality (eastbound, westbound, or both directions), parking capacity, and available services (e.g., restrooms, food, fuel) were manually verified using satellite imagery and site-specific information. Altogether, the inventory included 20 public and 46 private facilities along I-80; a complete listing of these facilities and their associated attributes is provided in Appendix A. The facilities are grouped into three geographic sections: Kimball–Lincoln (I), Lincoln–York (II), and York–Douglas (III). Figure 3.1 presents all parking facilities along I-80 at the state level, along with detailed views of Sections I, II, and III.

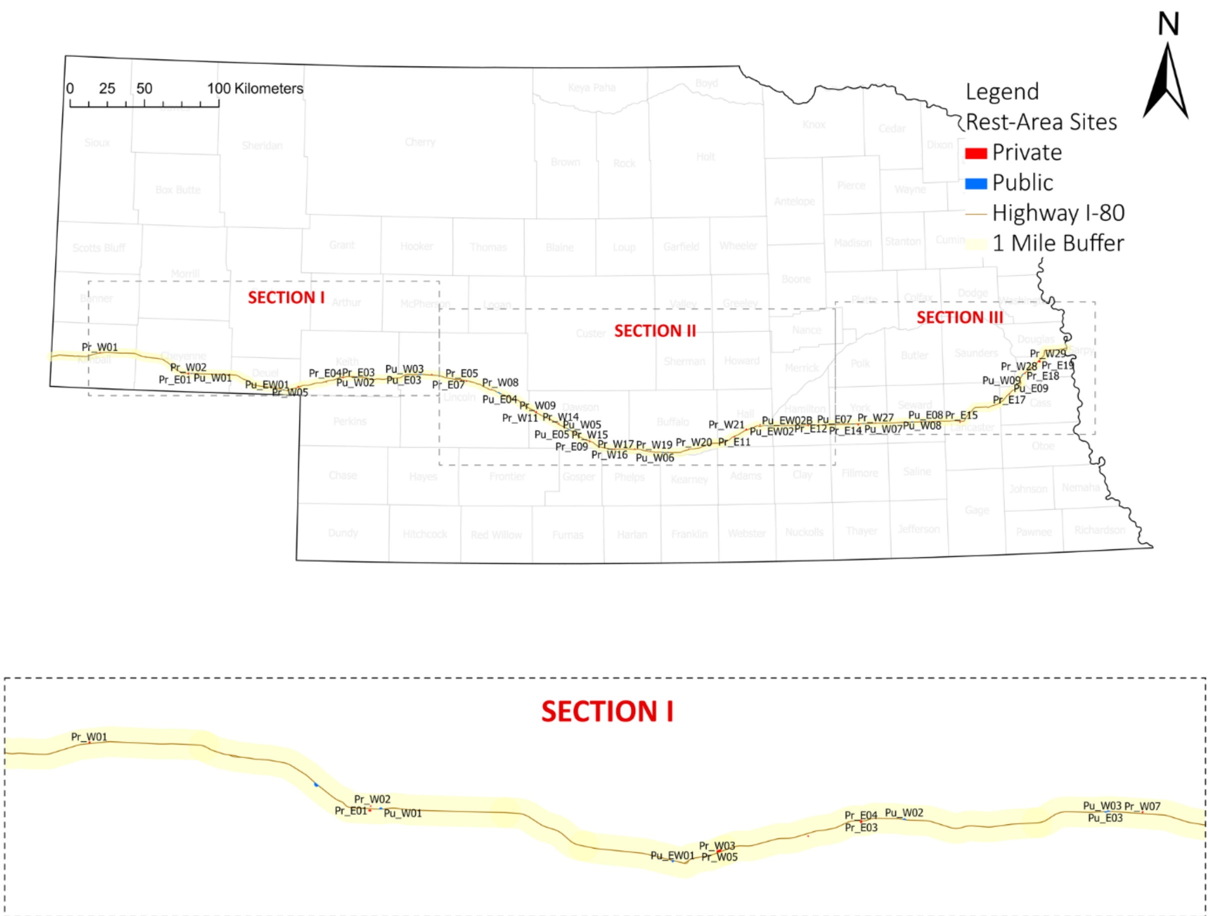

Figure 3.1 Public and private truck parking facilities within one mile of I-80 in Nebraska Map. Section I: Kimball County to Lincoln County, Section II: Lincoln County to York County, and Section III: York County to Douglas County

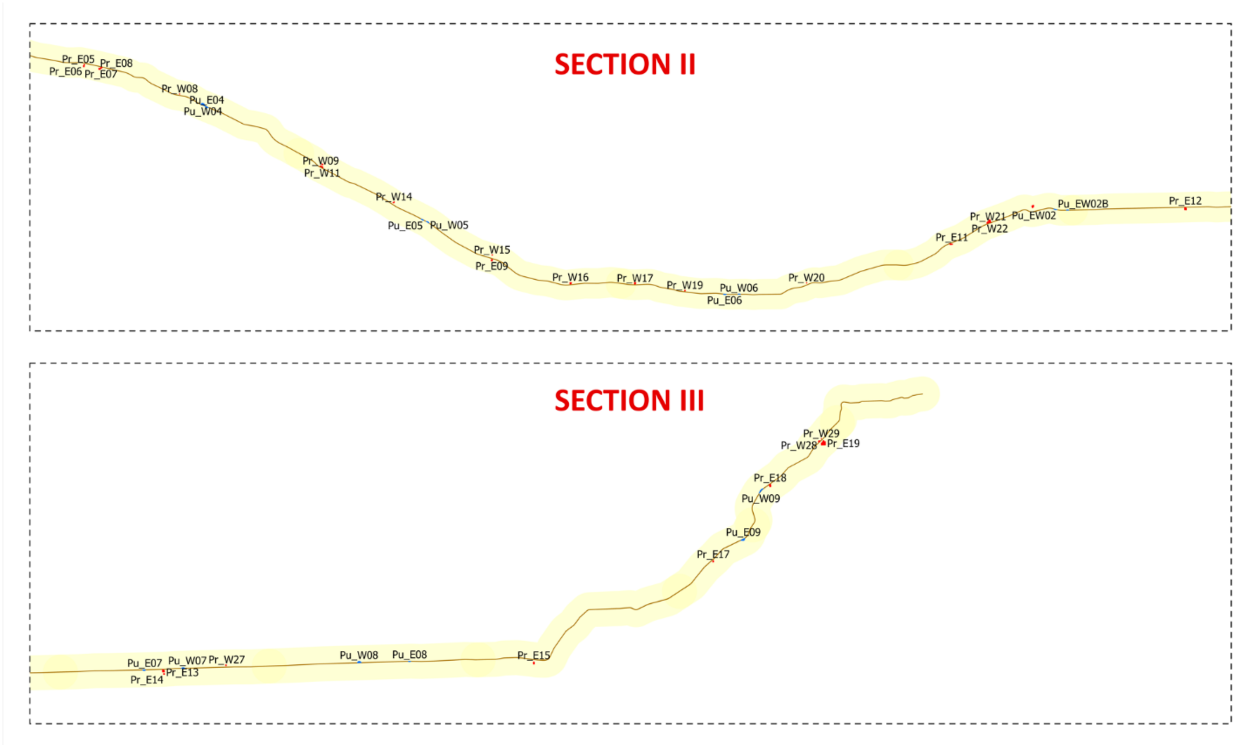

Figure 3.1 cont. Public and private truck parking facilities within one mile of I-80 in Nebraska Map. Section I: Kimball County to Lincoln County, Section II: Lincoln County to York County, and Section III: York County to Douglas County

A coding system was implemented to enable consistent reference to specific facilities throughout the analysis. The coding scheme adopted for public facilities used the prefix “Pu_E” for eastbound rest areas, “Pu_W” for westbound, and “Pu_EW” for those accessible from both directions. A similar directional coding was used for private facilities (e.g., “Pr_E01”). Table 3.1 provides a consolidated summary of the 66 identified facilities, including their IDs, names, directional access, and available parking spaces.

Table 3.1 List of public and private truck parking facilities along I-80 in Nebraska

Public Parking Facility					
ID	**Name**	**Spaces**	**ID**	**Name**	**Spaces**
Pu_E01	Sidney RA EB	34	Pu_E06	Kearney RA EB	7
Pu_W01	Sidney RA WB	7	Pu_W06	Kearney RA WB	7
Pu_EW01	Interchange 101 EB & WB	60	Pu_EW02	Grand Island RA EB	7
Pu_W02	Ogallala RA WB	7	Pu_EW02B	Grand Island RA WB	7
Pu_E03	Sutherland RA EB	7	Pu_E07	York RA EB	8
Pu_W03	Sutherland RA WB	7	Pu_W07	York RA WB	9
Pu_W04	Brady RA WB	22	Pu_W08	Goehner RA WB	56
Pu_E04	Brady RA EB	18	Pu_E08	Blue River RA EB	7
Pu_E05	Cozad RA EB	7	Pu_E09	Platte River RA EB	16
Pu_W05	Cozad RA WB	7	Pu_W09	Melia Hill RA WB	26
Private Parking Facility					
ID	**Name**	**Spaces**	**ID**	**Name**	**Spaces**
Pr_W01	Travel Shop	48	Pr_W13	Gas N Shop	5
Pr_E01	Love's Travel Stop #625	96	Pr_E13	Petro Stopping Center	250
Pr_W02	Sapp Brothers Travel Center	35	Pr_W14	Casey's General Store	0*
Pr_E02	Happy Jack	10	Pr_E14	Crossroads Fuel Stop	30
Pr_W03	Truck & Travel	6	Pr_W15	Ampride	20
Pr_E03	Travel Centers of America	94	Pr_E15	Shoemake's Travel Plaza	150
Pr_E04	Fat Dogs - Ogallala	15	Pr_W16	Jay Brothers	50
Pr_W05	Flying J Travel Center #904	244	Pr_W17	Pilot Travel Center #901	75
Pr_E05	Fat Dogs Gulf	65	Pr_E17	Rite Way 66	2
Pr_W06	Sapp Brothers	5	Pr_W18	Bosselmans Fuel Stop	20

Pr_E06	Time Saver #7	0	Pr_E18	Flying J Travel Plaza	150
Pr_W07	Western Convenience Truck Stop	80	Pr_W19	Sapp Brothers	65
Pr_E07	Love's Travel Stop #390	88	Pr_E19	Love's Travel Stop #730	107
Pr_E08	Flying J Travel Plaza	123	Pr_W20	Fort Kearney Trading Post -Gibbon	50
Pr_W08	Ranchland Convenience Store	20	Pr_W21	Travel Centers of America	12
Pr_W09	Cubby's	30	Pr_W22	Grand Maverick Truck Stop	82
Pr_E09	Nebraska Land Tire Truck Center	60	Pr_W23	Git 'N Split	6
Pr_W10	Plaza Shell	15	Pr_W24	Gas N Shop	6
Pr_E10	Bosselman Fuel Stop	10	Pr_W25	Pilot Travel Center #902 - Bosselman's	400
Pr_W11	Cubby's	24	Pr_W26	Bosselman Travel Center	0*
Pr_E11	Pilot Travel Center #912	29	Pr_W27	Sapp Brothers	25
Pr_W12	I - 80 Pit Stop	40	Pr_W28	Akal Travel Center	61
Pr_E12	Love's Travel Stop #309	54	Pr_W29	Sapp Brothers	150

* Zero dedicates no long-term truck parking spaces, but trucks stop here for amenities and services.

3.2 NAIP and Google Earth Data

To examine long-term spatial and temporal trends in truck parking demand, potentially influenced by evolving freight volume, infrastructure development, and policy shifts, aerial imagery was collected from two sources: NAIP and Google Earth. The study period of 2010 to 2022 was selected for two main reasons: (1) the availability of consistent, high-resolution imagery from both sources that met the analytical requirements of this study, and (2) the objective of capturing more than a decade of truck parking activity to identify stable patterns as well as emerging shifts. This timeframe also supports the examination of spatial and temporal trends potentially influenced by changes in freight volumes, infrastructure investments, and policy developments.

NAIP imagery was acquired biennially at a spatial resolution of one meter, primarily during June and July under clear weather conditions. In contrast, Google Earth updates its imagery on a rolling monthly basis; however, given the platform's segmented update schedule, it typically took approximately three years for imagery of all truck parking facilities to be fully refreshed. The spatial resolution of Google Earth imagery used in this study was 0.6 meters. Figure 3.2 shows representative examples from both sources. The final dataset included 490 NAIP images and 280 Google Earth images spanning the 2010–2022 period.

Figure 3.2 Images collected in the study from (a) NAIP and (b) Google Earth

3.3 Truck GPS Data

ATRI provided truck GPS data in ZIP format, with one file for each month in 2022. A breakdown of the file sizes and record counts is presented in Table 3.2. In total, the 12 files are approximately 60 GB in size and contain more than 350 million records. Each file includes the following attributes: readdate (timestamp), truckid (unique identifier), speed (in miles per hour), latitude, and longitude.

Table 3.2 Truck GPS file size and number of records

Month (2022)	Size (GB)	Rows (millions)
January	5.12	29.8
February	4.76	27.7
March	5.27	30.7
April	5.06	29.5
May	4.99	29.1
June	5.39	31.4
July	5.32	31.0
August	5.61	32.6
September	5.19	30.2
October	4.96	28.9
November	3.92	22.9
December	3.99	23.3

Processing the ATRI truck GPS dataset required extensive effort due to its scale and structure. A key challenge was the dataset's irregular sampling frequency. The time between consecutive records for the same truck could vary from seconds to several hours. This variability required careful processing to accurately reconstruct individual truck trajectories. In addition to the irregular temporal resolution, several data quality issues had to be overcome. The GPS data contained occasional outlier coordinates and inconsistent timestamps, which introduced spatial and temporal gaps. To ensure positional accuracy and consistency, extensive data cleaning and validation were performed using custom Python scripts designed to detect and correct anomalies across millions of records. The computational intensity of processing such a large dataset presented an additional challenge. With more than 350 million observations, tasks such as clustering, trajectory reconstruction, and aggregation were both memory and time intensive. Although a high-performance computing environment was used, it was necessary to partition the data into manageable chunks and process them in parallel.

3.4 Automatic Traffic Recorders Data

Automatic Traffic Recorders (ATRs) installed along I-80 in Nebraska (see Figure 3.3) continuously recorded hourly traffic counts for 13 FHWA vehicle classes throughout 2022. Each record contains metadata including the FIPS state code, ATR station ID, direction, lane, and timestamp (year, month, day, and hour). Hourly truck volumes, specifically Class 9 vehicles, were extracted and aggregated by ATR, day, hour, and direction. Records corresponding to federal holidays in 2022 were excluded, and a minimum threshold of 10 trucks per hour was applied to remove hours affected by missing or incomplete ATR data, ensuring that only reliable traffic records were used in the analysis.

Figure 3.3 Locations of ATRs along I-80 in Nebraska

The hourly average number of vehicles recorded each month was analyzed for all ATR stations, both for vehicles and for trucks. Figures 3.4 and 3.5, respectively show the average hourly patterns of total recorded vehicles and passing trucks for January and February 2022. Across all 12 months and ATR stations, and in both cases of total vehicles and trucks only, similar hourly patterns were observed. The results showed that the stations could be grouped based on the similarity of these patterns into different clusters, and this grouping held consistently for both total vehicles and heavy trucks. Accordingly, three spatial clusters were defined along I-80: West (#53, #31), Central (#43, #20, #54, and #45 through July, replaced by #38 thereafter), and East (#56). The clustering approach reduced redundancy in the estimation of expansion factors by grouping ATRs with comparable temporal patterns, thereby improving the robustness and spatial consistency of regional traffic dynamics captured in subsequent analyses.

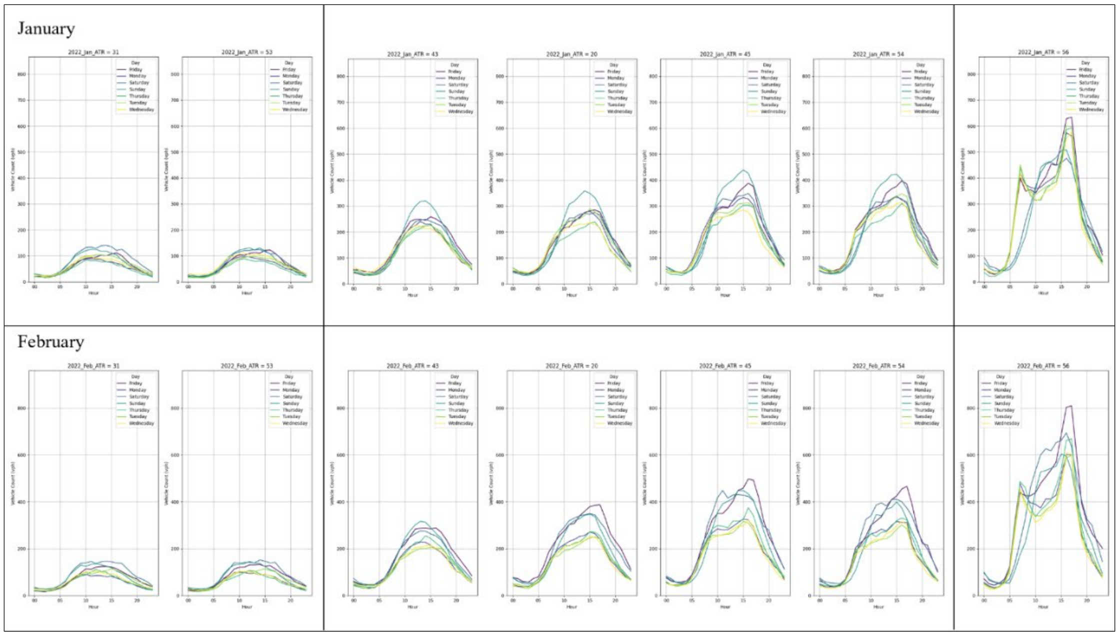

Figure 3.4 Average hourly traffic volumes (all vehicles) for January and February 2022

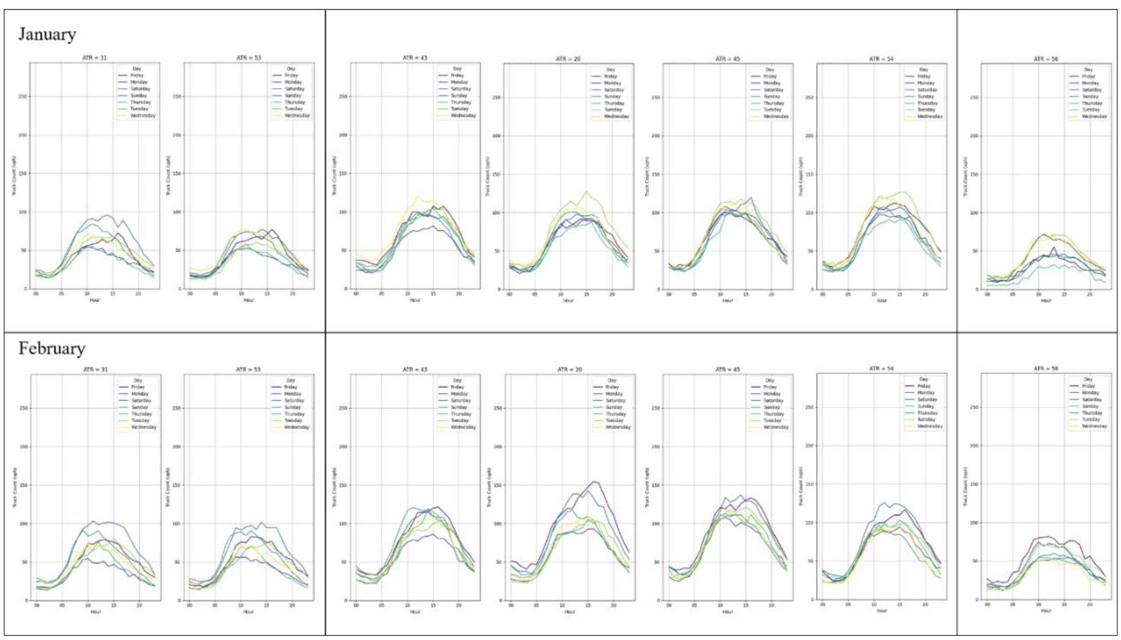

Figure 3.5 Average hourly truck volumes for January and February 2022

3.5 Expansion Factors

The expansion factor ($ExpFac$) was defined as the ratio of the number of trucks recorded in the ATR dataset to the number of trucks passing the same ATR location based on the GPS dataset during the same hour and direction:

$$ExpFac = \frac{ATR\_num\_trucks}{GPS\_num\_trucks} \quad (3.1)$$

The total number of trucks passing each station was aggregated by hour and month for ATR_num_trucks. Hourly volumes of Class 9 vehicles were used for this aggregation. Similarly, for GPS_num_trucks, the number of trucks passing each ATR station was identified based on the GPS dataset. To achieve this, truck trajectories were divided into continuous segments separated by time gaps greater than 60 minutes to mitigate irregular sampling effects. The 60-minute threshold was introduced because long time gaps between consecutive GPS records typically indicate that a truck has either stopped for an extended period, lost signal, or started a new trip. Segmenting trajectories at this threshold prevents the merging of non-continuous movements and ensures logical continuity in travel behavior. The travel direction within each segment was determined from the longitudinal coordinate trend—classified as eastbound when otherwise increasing and westbound. For each ATR station, centroid coordinates were stored, and geodesic distances between truck positions and the station centroid were computed. Trucks traveling at valid speeds (≥ 15 mph) and passing the ATR location were identified as valid pass events. The exact pass time for each event was refined using the 85th percentile speed within the segment to improve temporal precision. All computations were executed using parallel processing to efficiently handle the large-scale GPS dataset.

To stabilize estimates, multiple versions of the expansion factor were examined, including the hourly mean, the hourly median, and both mean and median values after removing outliers using the interquartile range (IQR) method. Additionally, K-means clustering was applied to the average hourly ATR truck volumes to classify each hour into low-, medium-, or high-traffic periods (see Figure 3.6). This categorization reduced fluctuations during low-volume hours and produced more stable and representative expansion factors for subsequent model calibration.

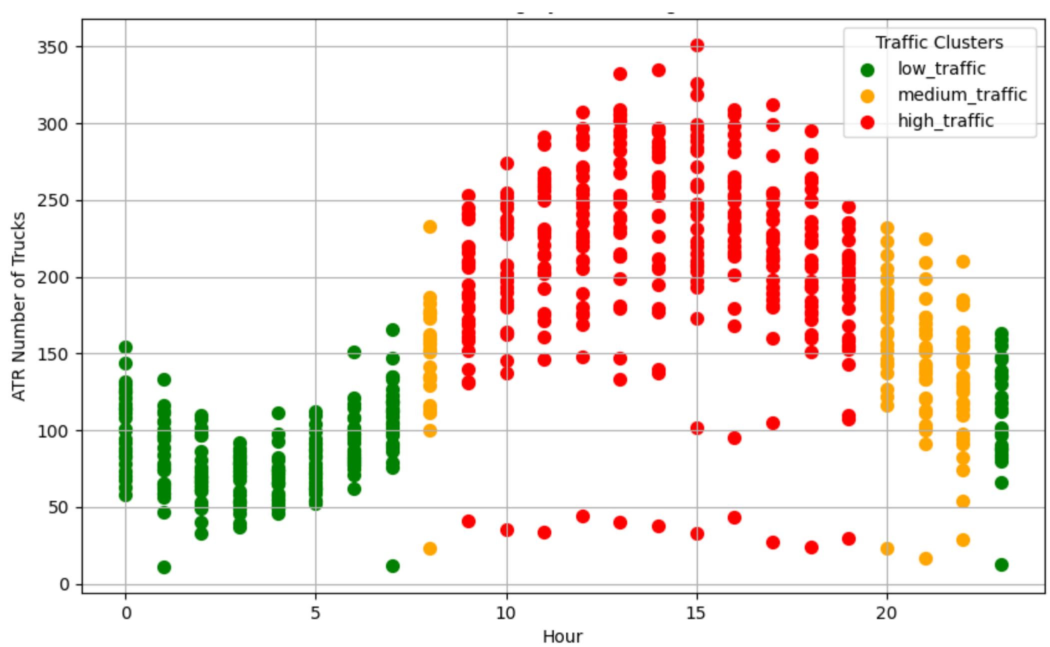

Figure 3.6 Traffic clustering hour using K-means

3.6 Truck parking area delineation and parking occupancy

To assess truck parking demand, it was first necessary to establish the spatial extent of truck parking facilities. Using ArcGIS, polygons were manually delineated for all 66 public and private facilities along Nebraska's I-80 corridor. However, twelve of these facilities exhibited zero occupancy for more than 90 percent of the observation period and were therefore excluded from subsequent analyses; a complete listing of these underutilized facilities is provided in

Appendix B. As a result, 54 facilities (25 eastbound and 29 westbound) were retained for detailed investigation.

The truck GPS records were then matched against these polygons. A preprocessing filter retained only those records where the reported speed equaled zero and the coordinates fell within a facility polygon, ensuring that only stationary events inside truck stops or rest areas were captured. A Python algorithm grouped consecutive zero-speed records by truck and polygon to define parking intervals. For each interval, the algorithm recorded the facility polygon name, truck ID, start and end timestamps, and stop duration. If a truck exited and reentered a facility, each stay was treated as a separate record. Finally, stops with a duration of at least 60 minutes were considered truck parking events, and only these events were retained in the final structured dataset.

To compute hourly occupancy rates for each facility, the observed GPS-equipped truck stops had to be expanded, using expansion factors described in the previous section, to represent the full truck population, since the GPS dataset contains only a sample of all trucks traveled on I-80. Hourly occupancy was then calculated by summing the total truck-hours of parking at each facility and hour, multiplying this value by the corresponding expansion factor, and dividing by facility capacity to yield a standardized occupancy percentage was obtained using Equation (3.2).

$$Occupancy_{i,t} = \frac{1}{C_i} \sum_{j \in P_{i,t}} Duration_j \times ExpFac_{g(i,t)} \tag{3.2}$$

where C_i is the facility capacity, $P_{i,t}$ is the set of parking events in facility i during hour t, $Duration_j$ is the stop duration of truck j expressed in hours, and $ExpFac_{g(i,t)}$ is the expansion factor corresponding to the facility's ATR group and time window.

Because GPS-equipped truck counts and scaling via expansion factors occasionally generated extremely high or low facility occupancy rates, particularly during early morning and late evening hours, box-plots were utilized to detect outliers. Observations outside the whisker bounds (maximums and minimums) were adjusted to the nearest whisker value to maintain internal consistency without suppressing genuine peaks. Figure 3.7 shows the occupancy rates for Pr_E15 for each hour during the month of March and illustrates how extremely high occupancy rates as detected by the box-plots have been removed.

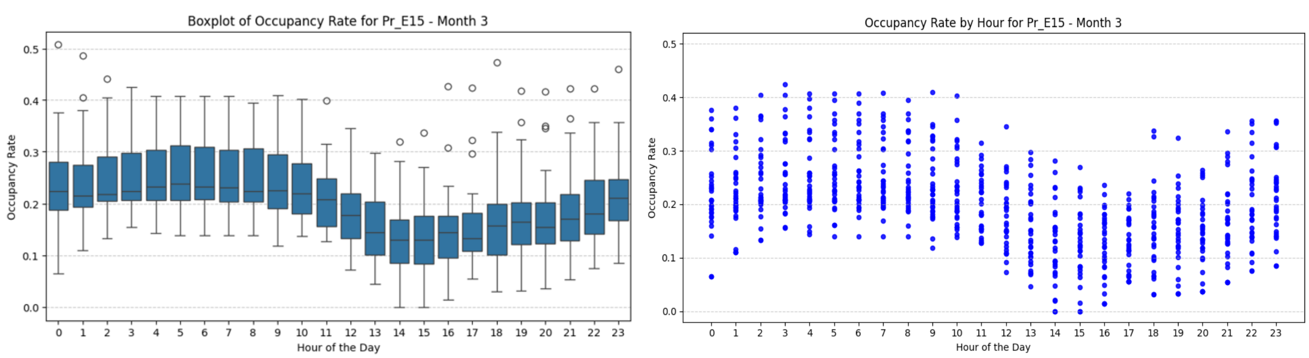

Figure 3.7 Hourly occupancy distribution for Pr_E15 in March: box-plot with outlier detection (left) and data after adjustment (right).

3.7 Truck Parking Facility Clusters

Facilities were organized into spatial clusters to capture regional interdependencies in truck parking behavior. All 54 public and private facilities were first classified by their direction (eastbound or westbound) and then spatially clustered based on their geographic proximity. A maximum threshold of 19 miles between adjacent facilities was applied to define cluster boundaries. This distance threshold was selected as a behaviorally and statistically reasonable limit: it reflects the average distance a truck driver can cover during the final 30–60 minutes before reaching the Hours-of-Service (HOS) limit, corresponding to a typical freeway speed range of 50–60 mph, and also ensures that spatial interactions remain meaningful before rapidly decaying with distance in spatial econometric terms.

This procedure resulted in 20 spatial clusters: five consisting of a single facility and fifteen containing multiple neighboring facilities. The five single-facility clusters consist of the following parking areas: Pr_E01, Pu_EW01, Pu_E06, Pr_W01, and Pu_W02. Table 3.3 presents the list of clusters and their associated facilities.

Table 3.3 Cluster Structure of Parking Facilities Along I-80

Cluster Name	Direction	Number of Facilities	Parking Facilities
E_cluster_1	East	2	Pr_E03, Pr_E04
E_cluster_2	East	6	Pr_E05, Pr_E07, Pr_E06, Pr_E08, Pu_E03, Pu_E04
E_cluster_3	East	2	Pr_E09, Pu_E05
E_cluster_4	East	3	Pu_EW02, Pr_E12, Pr_E11
E_cluster_5	East	3	Pu_E07, Pr_E14, Pr_E13
E_cluster_6	East	2	Pu_E08, Pr_E15
E_cluster_7	East	4	Pu_E09, Pr_E19, Pr_E18, Pr_E17
W_cluster_1	West	3	Pr_W29, Pu_W09, Pr_W28
W_cluster_2	West	3	Pu_W07, Pr_W27, Pu_W08
W_cluster_3	West	3	Pu_EW02B, Pr_W21, Pr_W22
W_cluster_4	West	10	Pr_W16, Pr_W20, Pr_W14, Pr_W17, Pr_W15, Pu_W06, Pr_W11, Pu_W05, Pr_W09, Pr_W19
W_cluster_5	West	2	Pr_W08, Pu_W04
W_cluster_6	West	2	Pr_W07, Pu_W03
W_cluster_7	West	2	Pr_W03, Pr_W05
W_cluster_8	West	2	Pr_W02, Pu_W01

3.8 Explanatory Variables

Explanatory variables used in the model for predicting hourly truck occupancy at a facility cluster included: lagged occupancy (1-hour), hour of day, day of week, month, holiday, road closure, average speed, truck volume within the one-mile upstream approach zone, and a spatial lag of occupancy calculated via inverse distance weighting over nearby facilities.

3.8.1 Truck volume

Truck volumes were derived from the GPS dataset to represent the number of trucks passing through the one-mile upstream buffer of each facility during every hour. To accomplish this, the Python-based geospatial algorithm described earlier in the Expansion Factor section was applied. In this process, truck positions obtained from continuous trajectory segments were matched with the one-mile upstream buffer of each facility to identify passing events. For each facility and hour, the number of passing trucks was then calculated and multiplied by the number of GPS-observed trucks corresponding to the same facility, month, and hour to obtain the hourly truck volume.

3.8.2 Truck speed

Average speed was computed to characterize the traffic flow conditions upstream of each facility. For this purpose, the same geospatial algorithm and one-mile upstream buffer used in the truck volume analysis were applied, and valid GPS points corresponding to trucks passing each facility during each hour were extracted. The direction of each trajectory segment was determined based on the longitudinal coordinate trend to ensure alignment with the facility’s orientation. For each facility–hour combination, the mean of all speeds within the one-mile upstream buffer was calculated to represent the average speed for that facility.

3.8.3 Road closure

By using ATR data, a binary indicator was created to identify hours when I-80 was effectively closed. This attribute was used to determine where trucks parked when I-80 was closed. For each ATR and hour, total traffic volume across both directions was aggregated. If this combined value was less than or equal to 50 vehicles, the hour was flagged as a closure event ($road\_closure = 1$); otherwise, it was coded as 0. Formally:

$$road\_closure_{a,t} = \begin{cases} 1 & if\ Total\_Volume_{a,t} \leq 50 \\ 0 & Otherwise \end{cases} \tag{3.3}$$

where $Total\_Volume_{a,t}$ is the sum of all vehicles observed at ATR during hour t.

3.8.4 Holiday

Another binary variable that was created for the truck prediction based on the official U.S. federal holiday calendar for 2022. If an observation fell on a federal holiday, it was coded as *holiday=1*; otherwise, it was coded as 0.

3.9 Undesignated parking areas

To capture undesignated parking behavior, GPS records falling outside of the predefined facility polygons were reprocessed. For each truck ID, stop intervals were reconstructed by identifying consecutive zero-speed events. Only intervals with a duration between 1 hour and 24 hours were retained to ensure that short incidental stops and long-term off-network storage were excluded.

A geospatial classification framework was then implemented using OpenStreetMap (OSM) network data and OSMnx. The I-80 corridor and its connected links were extracted, and roadway segments were categorized as motorway (mainline) or ramps. Entry/exit nodes, defined as junctions connecting ramps and motorways, were also identified. Around these features, spatial buffers were constructed (40 m for motorway shoulders, 35 m for ramps, and 120 m for entry/exit sites). Each undesignated parking point was mapped against these buffers and classified hierarchically as:

- **Entry/Exit Site** – stops within the buffered zones around ramp–motorway junctions,
- **Ramp** – stops located within ramp buffers,
- **Shoulder** – stops directly adjacent to the motorway mainline,
- **Off-Road** – all remaining stops outside these categories.

This classification ensured a consistent typology of undesignated parking events along the corridor. To manage computational scale, snapping and nearest-edge matching were applied where necessary, and duplicate stop records were removed. The output consisted of a georeferenced dataset with event duration, stop coordinates, distance to roadway edge, and assigned parking type for each unique truck stop.

In addition, monthly NDOT reports on road closures and severe weather conditions were utilized to filter undesignated parking records. Temporal windows and geographic ranges of closures were extracted from these reports, and only undesignated stops coinciding with such events were retained for subsequent analysis. This ensured that the final dataset captured undesignated parking specifically caused by weather disruptions or road closures, rather than ordinary off-facility stopping behavior

3.10 Analyzing the Relationship Between Parking Shortages and Crashes

Crash records in 2022 were provided by NDOT. This dataset includes detailed information on the time, location, injury severity, contributing factors, and the characteristics of vehicles, occupants, and roadways involved in each crash. For this project, only crashes involving heavy trucks were analyzed, identified using the VehicleBodyType attribute in the crash dataset, which indicates Truck Tractor. In total, there were 1610 truck-involved crashes on I-80 in 2022.

Each truck-involved crash was assigned to the corresponding highway direction (eastbound or westbound). To examine spatial relationships between crash locations and parking facilities, two spatial scenarios were defined. In the first scenario, crashes occurring within ten miles downstream of a truck parking facility were identified and linked to the nearest upstream facility. In the second scenario, crashes occurring between two consecutive facilities were associated with the upstream facility adjacent to the crash location. This procedure was applied to all truck-involved crashes.

After linking each truck-involved crash to its respective upstream parking facility, a panel dataset was constructed at the facility–hour level for the entire year of 2022, consisting of 365×24 hourly observations for each facility. Within this dataset:

- The crash_count column records the number of crashes occurring in the corresponding facility–hour (zero if no crash occurred).
- The parking_shortage column is a binary indicator equal to 1 if the facility was at or over capacity during that hour, and 0 otherwise.

Chapter 4 Methods

This chapter presents the methods used to address four of the five objectives of this study. Objective 1 involves straightforward documentation of truck parking facilities and does not require an analytical method. For Objective 2, visualization techniques were used to support spatiotemporal analysis of truck parking demand. For Objective 3, time-series and panel modeling approaches were used; the necessary background information is provided to enable understanding of these approaches. For Objective 4 clustering techniques were used to identify spatial patterns in truck parking activity. Lastly, Objective 5 was addressed using several correlation tests and a regression model to evaluate the relationship between parking conditions and truck-involved crashes.

To support Objective 2 and establish the foundation for subsequent analyses, several visualization tools were applied to explore both spatial and temporal patterns in truck parking activity. Bar charts were used to examine historical trends in truck parking demand by facility. To visualize spatial and temporal patterns more effectively, heatmaps were generated in ArcGIS to display the relative intensity of truck parking activity across time and location. A heatmap represents the density of observations using a color gradient. In this study, darker areas on the heatmap indicate truck parking locations with higher occupancy, allowing for quick visual identification of recurring hotspots in parking demand.

4.1 Predicting Truck Parking Demand

4.1.1 Model Framework

The objective of this section is to model and predict hourly truck occupancy rates at parking facilities along I-80 in Nebraska by incorporating a comprehensive set of explanatory variables. Two modeling strategies are adopted based on spatial clustering:

- For clusters with multiple parking facilities, we applied a dynamic Bayesian fixed-effects panel model with facility-level spatial effects and time-varying covariates.
- For clusters containing a single parking facility, the lack of cross-sectional variation renders a panel modeling approach inappropriate. Hence, a dynamic Bayesian time series model was employed to account for temporal dependencies in occupancy while excluding spatial interactions, which are not meaningful in the absence of neighboring facilities.

Facilities were first separated by direction (eastbound or westbound) and then grouped using a 19-mile maximum pairwise distance threshold. We used a 19-mile threshold for spatial interactions among parking facilities based on both behavioral evidence and spatial econometric principles. National reports by the American Transportation Research Institute (ATRI) and the Federal Highway Administration (FHWA) emphasize that truck drivers face significant difficulty finding available parking, particularly near the end of their Hours-of-Service (HOS) limits. According to (Boris and Brewster 2016), drivers lose, on average, 56 minutes of revenue-driving time each day searching for parking, indicating that a substantial portion of their behavioral response occurs close to the HOS deadline. While Jason's Law also highlights substantial time pressure due to parking shortages, it does not report the precise timing of search initiation. We assumed drivers will begin searching for parking approximately 30 to 60 minutes before HOS expiration, and using an average freeway speed of 50–60 mph, their spatial search radius would fall between 15 and 30 miles. A 19-mile cutoff represents a conservative and behaviorally realistic approximation. From a modeling perspective, inverse-distance-based spatial weight matrices (LeSage and Pace 2009) result is rapidly decaying weights as distance increases; beyond 19 miles, the influence of other facilities becomes negligible. Thus, the 19-mile threshold balances behavioral realism with statistical parsimony, restricting spatial interactions to facilities with meaningful geographic and behavioral relevance.

4.1.2 Variable Selection and Justification

The explanatory variables were selected based on both theoretical foundations in transportation and empirical evidence from prior studies on truck parking.

- **Truck Volume ($V_{i,t}$)** directly influences the likelihood of facility occupancy. Higher volumes naturally lead to increased demand for rest opportunities, as demonstrated in count-based statistical models (Haque et al. 2017) and confirmed in deep learning and graph-based frameworks (Shao et al. 2024; Yang et al. 2022).
- **Average Speed ($S_{i,t}$)** serves as a proxy for traffic flow efficiency and road conditions. Lower speeds may indicate congestion or inclement weather, both of which contribute to increased parking needs due to driver fatigue, regulatory compliance, or route disruption. Previous studies have found significant associations between reduced speed and illegal parking (Haque et al. 2017), as well as its relevance in short-term forecasting models (Sadek et al. 2020).
- **Lagged Occupancy ($y_{i,t-1}$)** captures the temporal inertia inherent in truck parking behavior. Since trucks tend to remain parked for several hours, current occupancy is strongly autocorrelated with previous values. Incorporating this lag improves forecast accuracy by accounting for dwell-time persistence (Yang et al. 2022; Zhao et al. 2020).
- **Spatial Lag ($SL_{i,t}$)** is included to model correlated demand across nearby facilities. As drivers may sequentially search for parking within a bounded radius, the occupancy at a given site is often influenced by conditions at adjacent locations. This spatial spillover is

well-documented in both GNN-based and regression-based spatial models (Shao et al. 2024; Zhang et al. 2022).

- **Temporal Indicators** such as hour of day, day of week, and month capture recurring behavioral patterns in parking usage. These cyclic trends reflect the nature of long-haul driving schedules, HOS regulations, and logistics cycles. For example, parking demand typically peaks during nighttime hours and weekdays, a phenomenon confirmed by both time-series and ML-based analyses (Sadek et al. 2020; Zhao et al. 2020).
- **Holiday Indicator** is the binary variable that is equal to 1 if a date falls on a U.S. federal holiday. Our hypothesis is that holidays may alter freight schedules and thus parking demand.
- **Road Closure Indicator** is the binary variable that is equal to 1 when the hourly truck volume in both directions is below 50, expected in inclement weather that necessitates road closure. This value was obtained through discussions with the Nebraska DOT traffic engineers.

4.1.3 Variable Preprocessing and Diagnostics

To ensure robust and interpretable model estimation, we conducted preprocessing as follows:

- Temporal Variation Requirement: For any variable $X_{i,t}$, it is required that

$$Var(X_{i,t}) > 0 \qquad for\ all\ i \tag{4.1}$$

to ensure within-entity temporal variation. Variables constant over time within any polygon were excluded.

- Multicollinearity Assessment: We computed the Variance Inflation Factor (VIF) for each variable: $VIF_j = 1/(1 - R_j^2)$. A conservative cutoff of $VIF < 10$ was used to exclude collinear predictors.

The only variables that met both criteria were (1) sufficient temporal variation and (2) acceptable multicollinearity, were retained for model estimation.

4.1.4 Model Specification

4.1.4.1 Dynamic Bayesian Fixed-Effects Panel Model

- **Panel Data Framework**

Truck parking occupancy data are inherently panel (longitudinal) in structure, consisting of repeated hourly observations ($t = 1, \dots, T$) for multiple facilities ($i = 1, \dots, N$). Panel models combine cross-sectional and time-series dimensions, allowing estimation of both between-facility and within-facility variation. Formally, the general panel regression can be expressed as:

$$y_{i,t} = \alpha_i + \beta X_{i,t} + \epsilon_{i,t} \tag{4.2}$$

where $y_{i,t}$ is the dependent variable (truck parking occupancy), $X_{i,t}$ is a vector of covariates, α_i captures unobserved facility-specific factors, and $\epsilon_{i,t}$ represents idiosyncratic errors. The advantage of panel data is that it accounts for individual heterogeneity and improves estimation efficiency relative to purely cross-sectional or time-series models (Baltagi 2021).

- **Fixed-Effects Specification**

Among panel estimators, the fixed-effects (FE) model is particularly suitable when the unobserved heterogeneity (α_i) is correlated with explanatory variables. In the context of truck parking, facility-specific attributes—such as design capacity, geometric configuration, surrounding land use, or access convenience—may systematically influence both parking occupancy and explanatory variables (e.g., truck volume or speed).

The FE model controls these time-invariant characteristics by estimating a unique intercept for each facility, effectively purging the bias from omitted but constant attributes. This approach captures within-facility dynamics, isolating temporal variations in occupancy driven by observable and lagged factors rather than static facility traits.

- **Bayesian Formulation**

The Bayesian extension of the fixed-effects panel model provides a probabilistic framework for parameter inference. Instead of relying on point estimates, Bayesian analysis treats all parameters, including facility effects, regression coefficients, and variance components, as random variables with prior distributions. Posterior inference is then based on the conditional probability:

$$p(\Theta|Y) \propto p(Y|\Theta)p(\Theta) \tag{4.3}$$

where $\Theta = \{\alpha_i, \beta, \sigma^2\}$. This formulation allows incorporation of prior knowledge, hierarchical structures, and uncertainty quantification through full posterior distributions. The hierarchical priors $\alpha_i \sim \mathcal{N}(\bar{\alpha}, \sigma_\alpha^2)$ enable partial pooling across facilities, striking a balance between complete independence (fixed effects) and complete sharing (random effects). The Bayesian approach also avoids incidental-parameter bias in short panels and provides richer uncertainty measures (credible intervals rather than asymptotic confidence intervals).

- **Dynamic Extension**

To capture temporal dependence in parking occupancy, a dynamic component was introduced through a lagged dependent variable. The dynamic panel model accounts for persistence over time, reflecting behavioral inertia—trucks parked in the previous hour often remain parked, and occupancy patterns evolve gradually. The inclusion of $y_{i,t-1}$ also helps capture dwell-time effects and short-term adjustment behavior. This specification follows the general form:

$$y_{i,t} = \alpha_i + \beta_1 y_{i,t-1} + \beta X_{i,t} + \epsilon_{i,t} \tag{4.4}$$

In the Bayesian framework, the dynamic panel structure is estimated jointly with all model parameters within a unified hierarchical model using Markov Chain Monte Carlo (MCMC) methods. This joint estimation accounts for the dependence between the lagged dependent variable $y_{i,t-1}$ and the facility-specific effects α_i, a common source of endogeneity in traditional fixed-effects estimators such as OLS or within-transformation approaches. By sampling from the joint posterior distribution of all unknown parameters, the Bayesian MCMC approach provides consistent and unbiased inference for the autoregressive coefficient β_1 even when the time dimension (T) of the panel is small. Moreover, the full posterior sampling framework naturally accommodates parameter uncertainty propagation, posterior shrinkage, and robust estimation of temporal persistence under short panels or irregular observation intervals.

- Complete Model Specification

Integrating the spatial, temporal, and hierarchical components yields the final specification for clusters with multiple parking facilities:

$$y_{i,t} \sim \mathcal{N}(\mu_{i,t}, \sigma^2)$$

$$\mu_{i,t} = \alpha_i + \gamma_{h(t)} + \delta_{d(t)} + \eta_{m(t)} + \beta_1 y_{i,t-1} + \beta_2 SL_{i,t} + \beta_3 V_{i,t} + \beta_4 S_{i,t} + \beta_5 H_{i,t} + \beta_6 R_{i,t} \tag{4.5}$$

The parameters of the model are defined as follows: the facility-specific effects are modeled hierarchically as $\alpha_i \sim \mathcal{N}(\bar{\alpha}, \sigma_\alpha^2)$, allowing partial pooling across facilities to capture unobserved heterogeneity such as design capacity or accessibility. Temporal fixed effects $\gamma_{h(t)}$, $\delta_{d(t)}$, and $\eta_{m(t)}$ represent hour-of-day, day-of-week, and month-specific influences, respectively, accounting for systematic temporal variations in truck parking behavior. The regression coefficients β_1 to β_6 quantify the marginal effects of the lagged occupancy, spatial lag, truck volume, average speed, holiday indicator, and road closure indicator. The spatial lag of occupancy denoted $SL_{i,t}$, captures demand spillover effects among neighboring facilities through the weighted average of adjacent occupancy levels. The explanatory variables $V_{i,t}$, $S_{i,t}$, $H_{i,t}$, and $R_{i,t}$ correspond to truck volume, average speed, holiday status, and road closure condition, respectively. All continuous variables were standardized prior to estimation, and the spatial weight matrix W_{ij} was constructed using inverse-distance weighting within a 19-mile threshold, with row normalization such that $\sum_j W_{ij} = 1$, ensuring comparability of spatial influence across facilities.

4.1.4.2 Dynamic Bayesian Time Series Model

- **Time-Series Framework**

When a cluster consists of only one parking facility, the data reduces to a univariate time series, representing hourly occupancy observations indexed by time $t = 1, \dots, T$. Unlike the panel structure, there is no cross-sectional variation; therefore, the model focuses exclusively on temporal dependencies within a single location. In general, a time-series model expresses a variable as a function of its past values and time-dependent covariates:

$$y_t = \mu_t + \epsilon_t, \qquad \epsilon_t \sim \mathcal{N}(0, \sigma^2) \tag{4.6}$$

where y_t denotes the observed series (hourly occupancy rate), μ_t is its conditional mean, and ϵ_t represents random innovations or shocks.

This framework captures serial correlation, meaning that observations closer in time are statistically dependent, a key property of parking demand, as occupancy tends to evolve gradually over consecutive hours rather than randomly fluctuating.

- **Bayesian Time-Series Formulation**

In a Bayesian context, the parameters of the time-series model are treated as random variables with prior distributions, and inference is based on their posterior distribution's conditional on the observed data:

$$p(\Theta|Y) \propto p(Y|\Theta)p(\Theta) \tag{4.7}$$

where $\Theta = \{\beta, \sigma^2\}$ denotes the set of unknown parameters. This probabilistic framework allows full quantification of uncertainty and facilitates regularization through prior beliefs, which is particularly valuable for relatively short or noisy series.

Weakly informative priors, such as $\beta_k \sim \mathcal{N}(0,1)$ and $\sigma \sim Half - Cauchy(0, 2.5)$, stabilize estimation and prevent overfitting while remaining sufficiently flexible to let the data dominate the posterior. Estimation proceeds via MCMC simulation, which samples from the joint posterior distribution, yielding entire distributions for each coefficient rather than single point estimates. This approach provides richer inference, robust uncertainty quantification, and straightforward credible intervals for parameters and predictions.

- **Dynamic Extension**

To represent persistence in truck parking occupancy, a dynamic autoregressive component is introduced through a lagged dependent variable:

$$y_t = \beta_1 y_{t-1} + \beta X_t + \epsilon_t \tag{4.8}$$

where the coefficient β_1 captures temporal inertia—the tendency for current occupancy to depend on the previous hour's level due to dwell time and gradual arrival/departure processes. By incorporating y_{t-1}, the model transitions from a static regression to a Dynamic Bayesian Time-Series Model, which can describe both short-term fluctuations and longer-term temporal patterns.

This specification effectively captures state dependence and helps forecast near-future occupancy by leveraging the system's own recent behavior.

- **Complete Model Specification**

Integrating these components yields the full specification for clusters with a single parking facility:

$$y_t \sim \mathcal{N}(\mu_t, \sigma^2)$$
$$\mu_t = \gamma_{h(t)} + \delta_{d(t)} + \eta_{m(t)} + \beta_1 y_{t-1} + \beta_3 V_t + \beta_4 S_t + \beta_5 H_t + \beta_6 R_t \tag{4.9}$$

Here, $\gamma_{h(t)}$, $\delta_{d(t)}$, and $\eta_{m(t)}$ are fixed temporal effects accounting for hourly, daily, and monthly cycles in parking demand. The coefficients β_3 to β_6 represent the marginal impacts of truck volume (V_t), average speed (S_t), holiday indicator (H_t), and road closure indicator (R_t). All continuous variables were standardized prior to estimation for numerical stability and comparability of effects.

4.1.5 Priors, Estimation, and Diagnostics

In the Bayesian paradigm, all model parameters, including regression coefficients, variance components, and hierarchical effects, are treated as random variables characterized by probability distributions. Estimation proceeds by specifying prior distributions $p(\Theta)$ for each parameter, which encode either prior knowledge or serve as weakly informative regularization to stabilize inference. Upon observing data Y, the model updates these beliefs via Bayes' theorem (Equation 6), producing a posterior distribution $p(\Theta|Y)$ that combines prior information with evidence from the data. Because the proposed models incorporate temporal lags, spatial interdependence, and hierarchical facility-specific effects, the resulting posterior is analytically intractable. Consequently, MCMC techniques are employed to approximate the posterior through iterative stochastic simulation.

Specifically, the No-U-Turn Sampler (NUTS), an adaptive extension of Hamiltonian Monte Carlo (HMC), was used as implemented in PyMC. NUTS automatically adjusts both step size and trajectory length during sampling, ensuring efficient exploration of high-dimensional parameter spaces while maintaining detailed balance. Each model was estimated using four independent chains, each initialized with dispersed starting values to enhance exploration and reduce dependence on initial conditions. A warm-up phase (4,000 tuning iterations per chain) was performed to allow adaptation of the mass matrix and step size, followed by 3,000 posterior draws per chain, yielding a total of 12,000 effective posterior samples. This configuration follows best practices recommended in the Bayesian literature (Bürkner 2017; Hoffman and Gelman 2014; Salvatier et al. 2016) and the official PyMC documentation, which advocate multiple chains and thousands of tuning and sampling steps for hierarchical and dynamic models. Priors were set as weakly informative to prevent overfitting while retaining flexibility:

$$:\beta_k \sim \mathcal{N}(0,1), \quad \sigma \sim Half - Cauchy(0, 2.5) \tag{4.10}$$

These priors shrink implausible coefficient magnitudes without imposing undue bias, a standard approach for models with temporal and spatial dependencies. For hierarchical intercepts, priors of the form $\alpha_i \sim \mathcal{N}(\bar{\alpha}, \sigma_\alpha^2)$ were adopted to enable partial pooling across facilities.

To guarantee the validity of posterior inference, multiple convergence diagnostics were evaluated, each targeting a distinct aspect of MCMC chain behavior:

- **Gelman–Rubin Statistic ($\hat{R} < 1.01$)**

The Gelman–Rubin diagnostic (also known as the Potential Scale Reduction Factor, PSRF) assesses inter-chain convergence by comparing the variance between chains to the variance within chains (Gelman & Rubin, 1992). When all chains have converged to the same stationary posterior distribution, their between-chain and within-chain variances should be nearly identical, yielding $\hat{R} \approx 1$. Values greater than 1.01 indicate that some chains have not yet stabilized, implying incomplete mixing or insufficient sampling. Achieving $\hat{R} < 1.01$ thus provides strong evidence that the Markov chains have converged to a common posterior region.

- **Effective Sample Size ($ESS > 400$)**

Although MCMC produces many draws, successive samples are autocorrelated, reducing the effective number of independent samples. The Effective Sample Size quantifies how many independent samples the correlated chain is equivalent to. It is computed as:

$$ESS = \frac{M}{1 + 2\sum_{k=1}^{\infty} \rho_k} \tag{4.11}$$

where M is the total number of samples and ρ_k is the autocorrelation at lag k. A higher ESS indicates better chain mixing and lower autocorrelation. Values above 400 per parameter are generally considered adequate for stable posterior summaries (Vehtari et al. 2021).

- **Bayesian Fraction of Missing Information ($BFMI \geq 0.9$)**

The BFMI measures how efficiently the Hamiltonian Monte Carlo (HMC) algorithm explores the posterior energy landscape by comparing the variance of the energy transitions in the Markov chain to the variance expected under the marginal energy distribution (Betancourt 2016). Low BFMI values (typically $< 0.3 - 0.5$) suggest poor exploration of the target distribution's energy levels, which may cause biased samples or slow mixing. A threshold of $BFMI \geq 0.9$ indicates that the sampler is effectively exploring the energy levels and that the momentum resampling process is functioning properly, ensuring accurate posterior estimation.

- **Trace Plots**

Trace plots display the sampled parameter values across iterations for each chain, serving as a visual diagnostic of chain mixing and stationarity. Well-behaved trace plots show multiple chains overlapping densely around a constant mean with no apparent trends or drifts. Visible divergence, long-term trends, or isolated trajectories indicate non-convergence or poor mixing. For hierarchical Bayesian models, trace plots are particularly useful to detect "stickiness" in variance parameters or slow-moving hierarchical effects.

- **Divergent Transition Checks**

In Hamiltonian Monte Carlo (HMC) and NUTS algorithms, divergent transitions occur when the numerical integration of Hamiltonian dynamics fails to maintain constant energy due to regions of high curvature in the posterior geometry. Each divergence signals potential numerical instability or poor geometry adaptation, often associated with overly tight priors, strong parameter correlations, or poorly scaled data. An acceptable model should have zero or minimal divergent transitions after tuning. When divergences occur, reparameterization (e.g., non-centered parameterization) or stronger regularizing priors are recommended to improve the geometry of the posterior manifold and restore stability.

Together, these diagnostics, quantitative ($\hat{R}$, ESS, $BFMI$) and qualitative (trace plots, divergence checks), ensure that posterior samples are both converged and efficiently representative of the target distribution, thereby validating the reliability of all subsequent inference and prediction.

4.1.6 Bayesian Model Fit and Predictive Accuracy Assessment

To evaluate model adequacy and compare predictive performance across alternative Bayesian specifications, two fully Bayesian information criteria were employed: the Widely Applicable Information Criterion (WAIC) and Pareto-Smoothed Leave-One-Out cross-validation (PSIS-LOO). Both criteria estimate a model's expected log predictive density (elpd), a measure of how well the model predicts new, unseen data while accounting for model complexity and uncertainty inherent in posterior distributions.

- **Widely Applicable Information Criterion (WAIC)**

WAIC is a generalization of the classical Akaike Information Criterion (AIC) to the Bayesian framework and is asymptotically equivalent to Bayesian cross-validation (Watanabe 2010). It evaluates predictive accuracy by integrating over the full posterior distribution rather than relying on point estimates. WAIC is computed as:

$$WAIC = -2(elpd_{WAIC}) \tag{4.12}$$

where,

$$elpd_{WAIC} = \sum_{i=1}^{N} (log(E_{\theta}[p(y_i|\theta)]) - p_{WAIC,i}) \tag{4.13}$$

and $p_{WAIC} = \sum_i p_{WAIC,i}$ represents the effective number of parameters, defined as the variance of the pointwise log-likelihood across posterior draws. This complexity penalty adjusts for posterior uncertainty and prevents overfitting. A higher $elpd_{WAIC}$ (or equivalently, a lower WAIC value) indicates superior out-of-sample predictive performance.

- **Pareto-Smoothed Importance Sampling LOO-CV**

LOO-CV approximates the predictive accuracy of repeatedly fitting the model while leaving one data point out at a time. Direct LOO is computationally expensive for hierarchical Bayesian models; therefore, the PSIS-LOO estimator (Vehtari et al. 2015) was used. The PSIS procedure improves the stability of importance weights by smoothing the upper tail of their distribution using a generalized Pareto distribution, ensuring numerical reliability even when raw importance weights are heavy-tailed. The LOO predictive metric is:

$$elpd_{LOO} = \sum_{i=1}^{N} log\ (\hat{p}(y_i|y_{-i})) \tag{4.14}$$

where $\hat{p}(y_i|y_{-i})$ is the leave-one-out predictive density. Similar to WAIC, the PSIS-LOO criterion includes an effective complexity term:

$$p_{LOO} = \sum_{i=1}^{N} Var_\theta \left(log\left(p(y_i|\theta)\right)\right) \tag{4.15}$$

which quantifies how much the posterior distribution fluctuates relative to individual data points. The Pareto-k diagnostic was also checked to ensure reliability of PSIS log-likelihood estimates; values $k < 0.7$ indicate stable importance sampling and trustworthy LOO estimates.

Both WAIC and LOO-CV evaluate model quality based on predictive accuracy, not merely goodness-of-fit, making them appropriate for the hierarchical and dynamic Bayesian models used in this study. Unlike classical AIC or BIC, these metrics account for:

I. the full posterior distribution rather than point estimates,
II. the hierarchical structure of the model,
III. correlations induced by temporal lags and spatial dependencies,
IV. uncertainty due to facility-specific random effects.

Because dynamic Bayesian panel and time series models feature correlated likelihood contributions, parameter shrinkage, and non-Gaussian posterior geometry, WAIC and LOO-CV provide more reliable assessments of predictive performance than traditional likelihood-based metrics. In this study, $elpd_{WAIC}$, p_{WAIC}, $elpd_{LOO}$, and p_{LOO} were computed for each model, and the results were used to compare competing specifications. Models with higher elpd values and lower penalized criteria were judged as having superior out-of-sample predictive performance.

4.2 Undesignated Parking During Severe Weather

Undesignated truck parking hotspots along the I-80 corridor were detected using the Density-Based Spatial Clustering of Applications with Noise (DBSCAN) algorithm (Ester et al.

1996), a density-based clustering approach well-suited for identifying spatially cohesive patterns in large, noisy datasets. DBSCAN was chosen because it does not require a priori specification of the number of clusters and can identify clusters of arbitrary geometric shape, while effectively distinguishing noise points, that is isolated parking events not indicative of systematic stopping behavior. These properties are particularly advantageous for analyzing truck parking data, where undesignated stops often occur in irregular spatial configurations along highway shoulders, ramps, or frontage roads.

The input dataset comprised GPS-derived parking events located outside designated facility polygons, representing stops that occurred in informal or ad-hoc areas. To ensure that the analysis captured long-haul rest behavior rather than short operational halts (e.g., fueling, inspections, or brief breaks), only events with parking durations between 1 and 24 hours were retained. Each event record included latitude–longitude coordinates, which were transformed into an appropriate projected coordinate system to enable Euclidean distance computations required by DBSCAN.

DBSCAN was applied to the two-dimensional spatial coordinate space defined by each stop's centroid location. The algorithm was parameterized using a neighborhood search radius (ε) of 1000 meters and a minimum cluster size ($minPts$) of 10 points. The ε parameter defines the maximum distance within which two points are considered part of the same neighborhood, effectively controlling cluster compactness. The choice of 1000 m reflects both the typical spatial extent of informal truck gatherings observed in satellite imagery and practical buffer distances used in prior freight-mobility studies. The $minPts$ value of 10 was selected following the heuristic $minPts \geq 2\ \times$dimensionality (Sander et al. 1998) and verified through sensitivity analysis, ensuring that only locations with repeated stopping activity across multiple trucks and time periods were classified as clusters rather than noise.

4.3 Relationship Between Parking Shortages and Crashes

To rigorously evaluate the statistical relationship between truck parking occupancy and crash occurrence along the I-80 corridor, a sequential inferential framework was applied that integrated correlation analysis and penalized logistic regression modeling. This approach allows for distinguishing between mere statistical association and directional predictive effects, while addressing the rare-event nature of crash data.

4.3.1 Correlation Analysis

Three complementary correlation metrics, Phi coefficient (Φ), Matthews Correlation Coefficient (MCC), and Spearman's Rank Correlation (ρ), were employed to examine whether full parking conditions are statistically associated with crash occurrences. Each method quantifies association from a different statistical perspective, ensuring robustness across data characteristics.

- **Phi Coefficient (Φ)**

The Phi coefficient quantifies the strength of association between two binary variables and is mathematically equivalent to the Pearson correlation coefficient applied to dichotomous outcomes. Its computation is based on the chi-square statistic obtained from a 2×2 contingency table, which summarizes the joint frequencies of crash occurrence (crash = 1, no crash = 0) and parking occupancy status (full = 1, not full = 0). Formally:

$$\Phi = \sqrt{\frac{\chi^2}{N}} \tag{4.16}$$

where χ^2 is the chi-square test of independence statistic and N is the total number of paired observations. The chi-square statistic itself is computed as:

$$\chi^2 = \sum_{i=1}^{2}\sum_{j=1}^{2}\frac{(O_{ij}-E_{ij})^2}{E_{ij}} \tag{4.17}$$

where O_{ij}represents observed cell counts and E_{ij}denotes expected cell counts under the null hypothesis of independence, calculated as:

$$E_{ij} = \frac{(row\ total)_i(column\ total)_j}{N} \tag{4.18}$$

This test evaluates whether the observed joint distribution deviates significantly from what would be expected if crashes and full-occupancy conditions were statistically independent. Phi inherits the same underlying assumptions as the chi-square test: sufficiently large expected frequencies (typically $E_{ij} \geq 5$), mutually exclusive categories, and fixed margins. Under the null hypothesis $H_0\colon \Phi = 0$, there is no association between crashes and full occupancy. Rejecting H_0in favor of the one-sided alternative $H_1\colon \Phi > 0$ indicates a positive dependence structure, meaning that crash occurrence becomes more likely when facilities reach full parking occupancy. Thus, Phi serves as a normalized effect-size measure that complements the chi-square significance test by providing a scale-free index of association strength. Because both variables in this study are binary, Phi is particularly appropriate and interpretable, offering a direct measure of dependence relative to the expected frequencies under independence. Moreover, it provides a useful counterpart to the Matthews Correlation Coefficient (MCC), which is more robust to marginal imbalance, and to Spearman correlation, which captures monotonic rank-based relationships; together, these measures give a comprehensive assessment of crash–occupancy association.

- **Matthews Correlation Coefficient (MCC)**

The MCC provides a more balanced and geometrically interpretable measure of association for imbalanced binary datasets, often preferred in safety analysis where crashes are rare events. It is defined as:

$$MCC = \frac{TP \times TN - FP \times FN}{\sqrt{(TP + FP)(TP + FN)(TN + FP)(TN + FN)}} \tag{4.19}$$

where TP, TN , $FP,$ and FN denote the counts of true positives, true negatives, false positives, and false negatives derived from the binary confusion matrix. The MCC reflects the correlation between observed and predicted binary classifications, producing values from −1 (perfect inverse relationship) to +1 (perfect agreement). A value of 0 indicates no association.

Under H_0: $\text{MCC} = 0$, crashes and occupancy are independent, while H_1: $\text{MMC} > 0$ implies positive co-occurrence consistent with congestion-induced safety risk. Compared with Φ, MCC is less sensitive to class imbalance and therefore provides a more reliable association measure when non-crash observations vastly outnumber crash observations.

- **Spearman's Rank Correlation ($\boldsymbol{\rho}$)**

Spearman's rank correlation was applied to examine potential monotonic dependence between the proportion of full occupancy and the number of crash counts per time–facility pair. It is computed as:

$$\rho = 1 - \frac{6 \sum d_i^2}{n(n^2 - 1)} \tag{4.20}$$

where d_i is the difference between the ranks of paired variables ($\text{OccupancyFull}_i, \text{CrashCount}_i$), and n is the total number of observations. Unlike Pearson correlation, Spearman's ρ captures ordinal monotonicity rather than linearity and is non-parametric, requiring no assumption of normality.

The null hypothesis $H_0: \rho = 0$ indicates no monotonic association, while $H_1: \rho > 0$ suggests that higher occupancy corresponds to higher crash counts in a statistically ordered manner. The combined use of Φ, MCC, and ρ offers a multi-angle assessment across categorical and rank-based dependence structures.

4.3.2 Penalized Logistic Regression (Regularized Estimation)

To validate and quantify the direction and magnitude of the association, a Penalized Logistic Regression (PLR) model was estimated, serving as a parametric robustness check to the non-parametric correlation results. The model was defined as:

$$log\left(\frac{p_{i,t}}{1-p_{i,t}}\right) = \alpha + \beta.OccupancyFull_{i,t} \tag{4.21}$$

where $p_{i,t}$ is the conditional probability of a crash occurring at facility i during time t, and $OccupancyFull_{i,t}$ is a binary indicator equal to 1 when parking occupancy reaches 100%. The parameter β measures the log-odds change in crash probability attributable to full occupancy conditions.

However, estimating this relationship requires careful adjustment for data characteristics, as crash outcomes are extremely rare relative to non-crash states. Crash data typically exhibit rare-event bias, where the outcome of interest (crash occurrence) happens infrequently relative to non-crash observations, leading to upward-biased maximum-likelihood estimates and overstated effect sizes (King and Zeng 2001). To mitigate this issue, a ridge-type L_2 regularization term was incorporated into the log-likelihood function:

$$\ell_p(\beta) = \ell(\beta) - \frac{\lambda}{2}\sum_k \beta_k^2 \tag{4.22}$$

where λ is the penalty parameter governing the degree of shrinkage applied to the coefficient estimates. This penalization constrains coefficient magnitudes, thereby reducing estimator variance, improving numerical stability, and preventing overfitting in small-sample or multicollinear settings. The optimal penalty strength was determined using cross-validated tuning to minimize the out-of-sample deviance and enhance generalization performance.

To further correct for potential bias introduced by the low base rate of crashes, the King & Zeng rare-event (2001) logistic adjustment was applied. This correction modifies the intercept term through a likelihood reweighting procedure based on the empirical crash prevalence, ensuring that predicted probabilities are unbiased and consistent under highly unbalanced binary outcomes. The resulting probability estimates represent Bayes-consistent measures of crash risk conditional on observed full-occupancy states. Hypothesis testing was conducted under the following framework:

- Null hypothesis: $H_0: \beta = 0$ (no effect of parking occupancy on crashes)
- Alternative hypothesis: $H_1: \beta > 0$ (parking shortages increase crash risk)

Inference was based on Wald z-statistics, with standard errors computed using the sandwich (heteroskedasticity-robust) variance–covariance estimator to ensure valid inference under potential variance heterogeneity. Statistical significance was evaluated at the 5% level, and 95% confidence intervals were obtained via asymptotic normal approximations. To facilitate interpretation, marginal effects were calculated as:

$$\frac{\partial p}{\partial OccupancyFul} = p(1-p)\beta \tag{4.23}$$

quantifying the expected change in crash probability associated with a one-unit increase in the full-occupancy indicator, holding all else constant.

Chapter 5 Findings and Discussion

5.1 Inventory of Parking Facilities (Objective 1)

In Chapter 3, Table 3.1 lists the 20 public and 46 private truck parking facilities within a one-mile buffer of I-80, along with their parking capacities. Additional details, including the exit number, mile post, and list of amenities, are provided in Tables A.1 and A.2. A review of this data reveals several important distinctions between public and private facilities. Public facilities, operated by NDOT and spaced approximately 30 to 50 miles apart, typically have fewer than 20 parking spaces and offer only basic services for commercial drivers. In contrast, private truck stops vary widely in size, from small local operations with fewer than 10 spaces to large national-chain travel centers that provide several hundred spaces, and they offer extensive amenities such as fueling stations, restaurants, showers, repair services, convenience stores, and lodging. Although public facilities are smaller and more limited in services, they play an essential role in providing free, accessible parking for drivers who need immediate rest or must stop during weather-related or emergency events (FHWA 2020). Moreover, they fill critical gaps in areas where private truck stops are unavailable, ensuring compliance with HOS regulations and enhancing overall highway safety. Together, public and private facilities form a complementary system within Nebraska’s freight network: public rest areas address safety and compliance needs, whereas private truck stops supply the full range of amenities required for extended driver rest and commercial activity.

5.2 Truck Parking Demand Analysis (Objective 2)

The spatial-temporal analysis of truck parking occupancy was conducted for public and private facilities separately since they differ in terms of size, amenities, and usage pattern. In addition, results derived from NAIP and Google Earth imagery are presented separately, since

NAIP imagery was collected at regular intervals while Google Earth imagery was obtained at irregular intervals.

5.2.1 Temporal Trends at Public Facilities Based on NAIP Data

Figure 5.1 shows the percentage of parking space occupied at each public parking facility between 2010 to 2022 using NAIP images. These percentages are derived from a single image taken during the leaf-on season and at an unspecified time during the day. Figure 5.1(a) shows the facilities accessible to eastbound traffic, and Figure 5.1(b) shows the facilities accessible to westbound traffic.

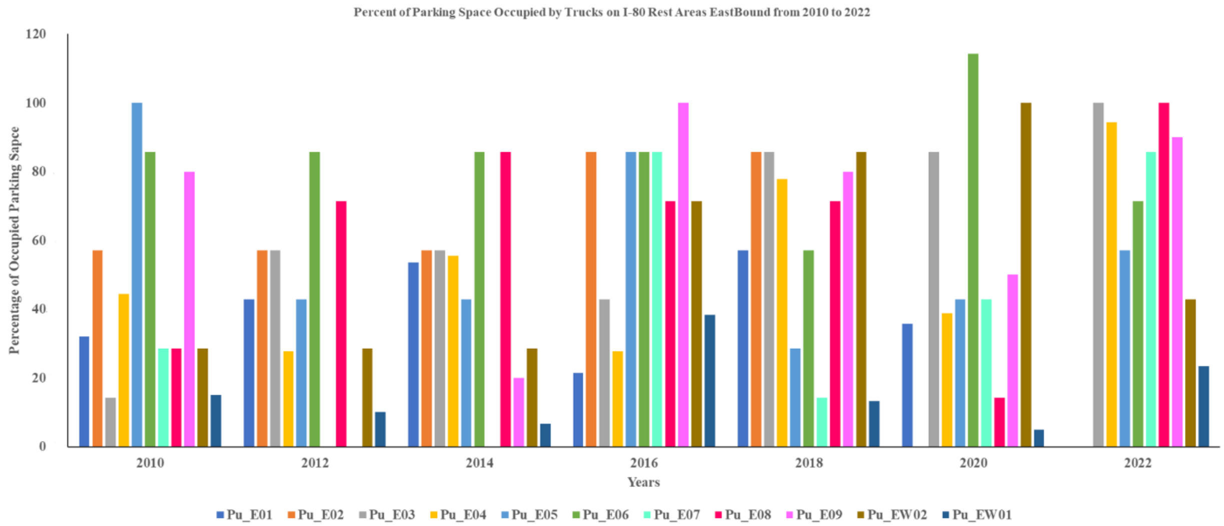

(a) Truck parking facilities on Eastbound I-80

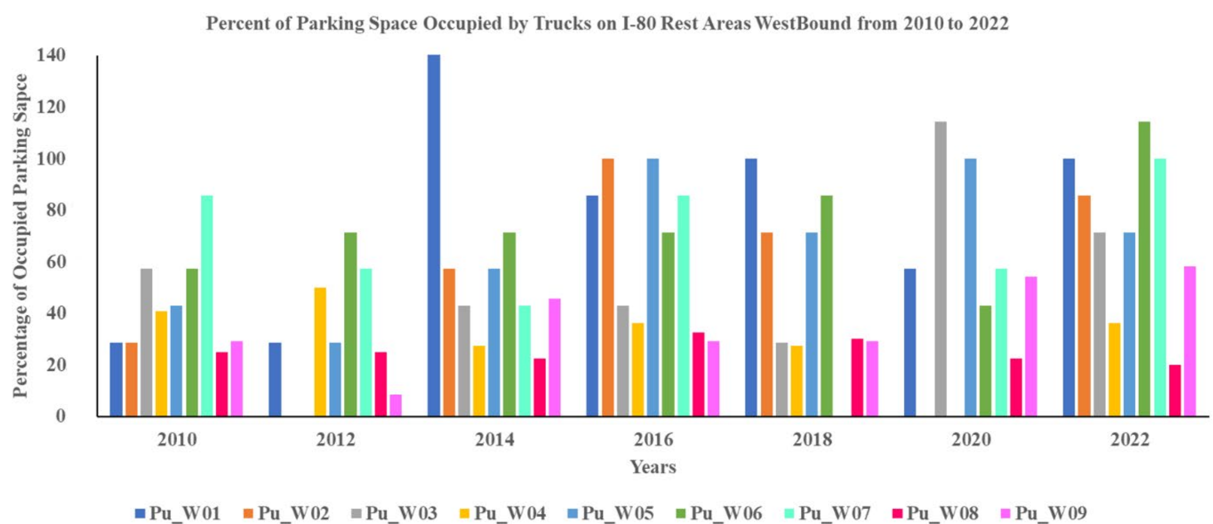

(b) Truck parking facilities on Westbound I-80

Figure 5.1 Percentage of truck parking occupied at each public truck parking facility based on NAIP data.

Among the eastbound parking facilities shown in Figure 5.1(a), at randomly selected times, several facilities had 100% occupancy (Pu_E05 in 2010, Pu_E09 in 2016, Pu_EW02 in 2020, Pu_E03 in 2022, and Pu_E08 in 2022), and one had more trucks parked at its facility than the number of spaces available (Pu_E06 in 2020). Over-parking not only jeopardizes safety but also constitutes a violation of established regulations. A similar finding is found for westbound facilities; however, instead of one facility being observed to have an over-parking issue, there are three, with one exceeding its capacity by 40%.

5.2.2 Temporal Trends at Public Facilities Based on Google Earth data

Figure 5.2 shows the percentage of parking space occupied at each public parking facility between 2010 to 2022 using Google Earth images. Note that some facilities have more images captured than others. For example, the area around Pu_E01 was captured only three times between 2010 and 2022, whereas Pu_E10 was captured 10 times.

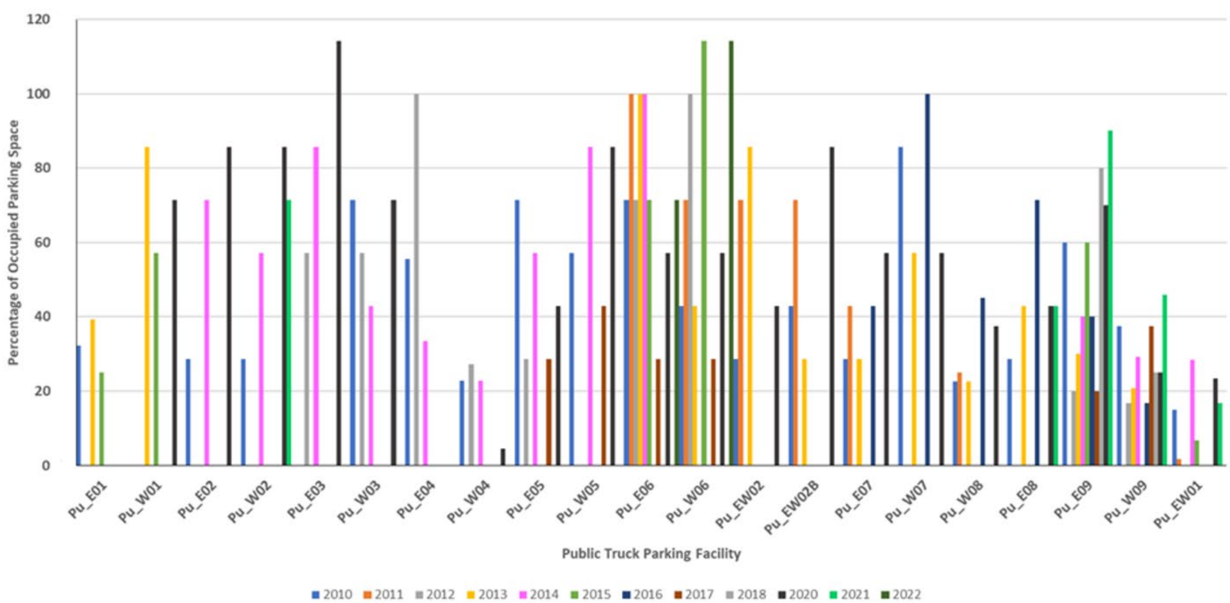

Figure 5.2 Percentage of truck parking occupied at each public truck parking facility based on Google Earth data.

As shown in Figure 5.2, the Google Earth data indicates that Pu_E06 and Pu_W06 have multiple years where parking occupancy was 100% or higher. Other public facilities that experienced 100% occupancy or higher are Pu_E03 in 2020, Pu_E04 in 2012 and Pu_E08 in 2016.

The findings indicate a prevalent trend of high occupancy rates, with most sites consistently exceeding 80% occupancy. This observation underscores the substantial load of truck parking experienced across these public rest areas throughout the study period.

5.2.3 Temporal Trends at Private Facilities Based on NAIP Data

Figure 5.3 shows the percentage of parking space occupied at each private parking facility between 2010 to 2022 using NAIP images. These percentages were derived from a single image taken during the leaf-on season and sometime during the day. Figure 5.3(a) shows the facilities accessible to eastbound traffic and Figure 5.3(b) shows the facilities accessible to westbound traffic.

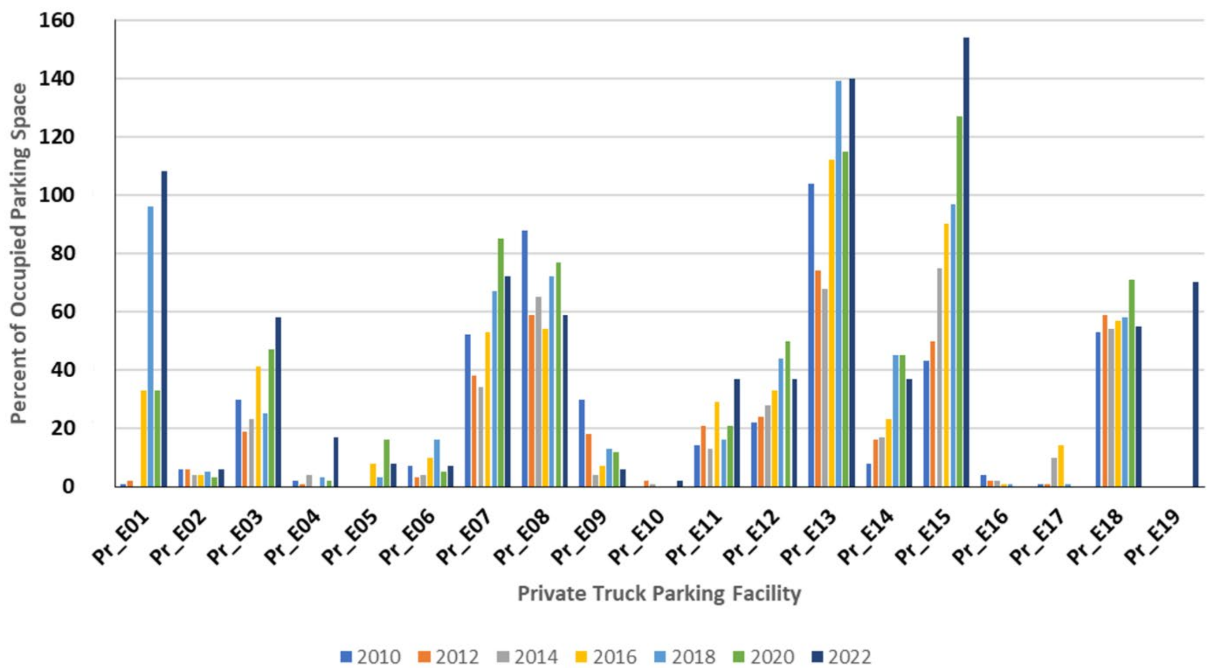

(a) Private parking facility on Eastbound I-80

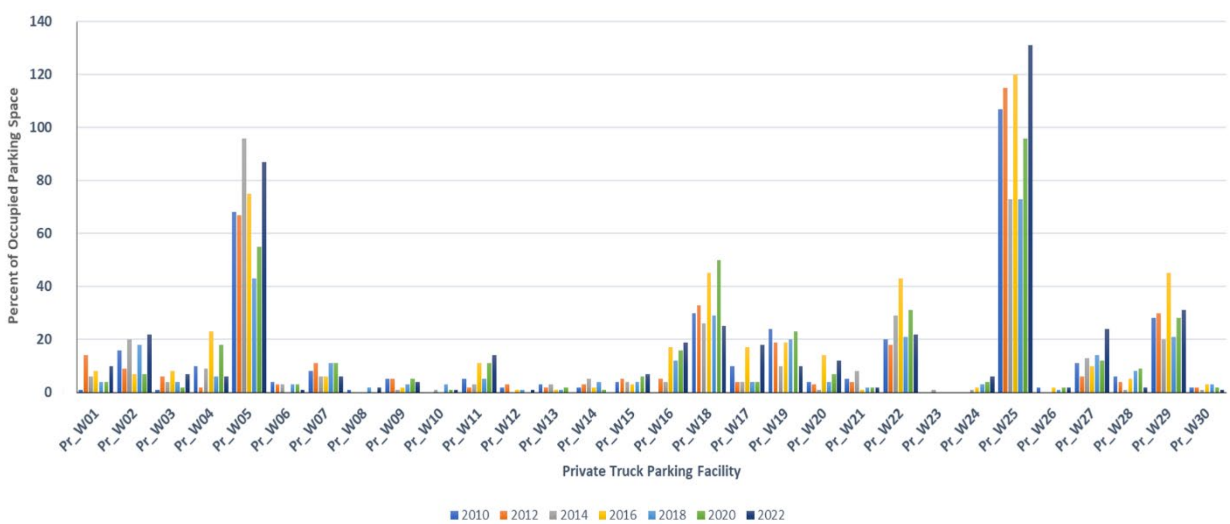

(b) Private parking facility on Westbound I-80

Figure 5.3 The percentage of truck parking occupied at each private truck parking facility based on NAIP Data.

Among the eastbound private facilities shown in Figure 5.3(a), at randomly selected times, several had 100% occupancy or higher: Pr_E01 in 2022, Pr_E13 in 2010, 2016, 2018, 2020, and 2022, and Pr_E15 in 2022 and 2022. Among the westbound private facilities shown in Figure 5.3(b), only Pr_W25 had 100% occupancy or higher. These instances were observed in 2010, 2012, 2016, and 2022.

5.2.4 Temporal Trends at Private Facilities Based on Google Earth Data

Figure 5.4 shows the percentage of parking space occupied at each private parking facility between 2010 to 2022 using Google Earth images. As is the case with public truck parking facilities, some facilities have more images captured than others.

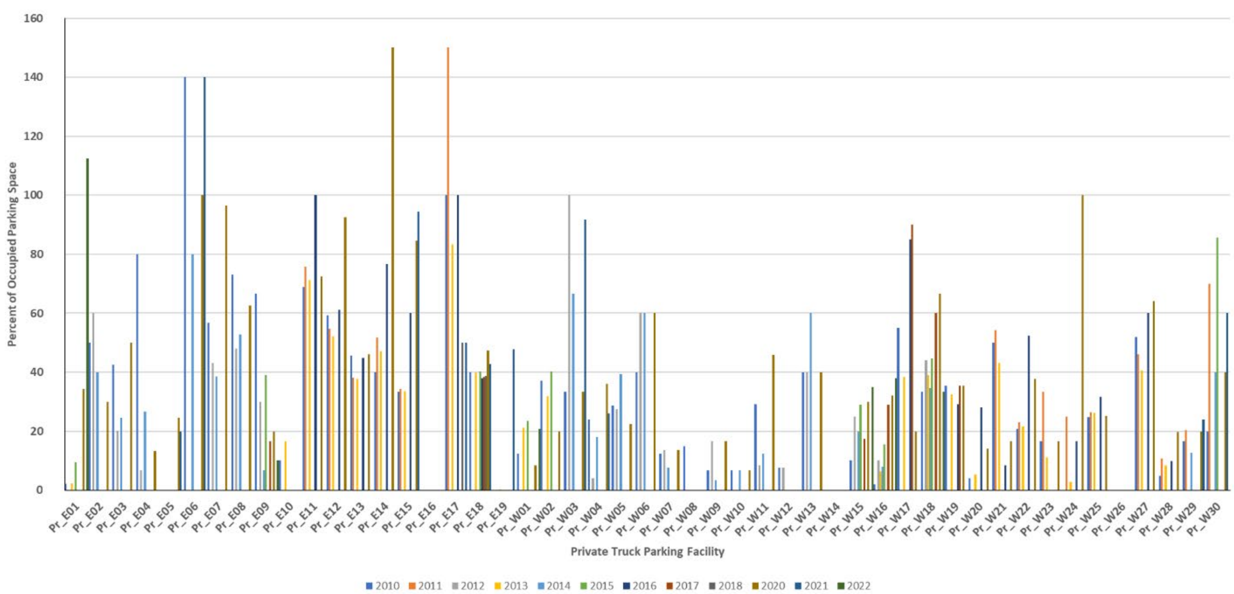

Figure 5.4 The percentage of truck parking occupied at each private truck parking facility based on Google Earth Data.

The Google Earth data in Figure 5.4 indicates that several private facilities experienced 100% occupancy or higher: Pr_E01 in 2022, Pr_E06 in 2010, 2020, 2021, Pr_E11 in 2016, Pr_E14 in 2020, Pr_E17 in 2010, 2011, 2016, Pr_W03 in 2012 and Pr_W24 in 2020.

5.2.5 Spatial and Temporal Trends at Public Facilities Based on NAIP Data

Figure 5.5 shows a heat map of truck parking occupancy for public facilities on (a) eastbound I-80 and (b) westbound I-80 between 2010 and 2022. Figure 5.5(a) shows the spatial distribution of occupancy density, where green represents low occupancy (0 to 20%) and red represents high occupancy (> 100%). The heat map indicates that public facilities located in the eastern part of Nebraska consistently experienced moderate to high occupancy rates: Pu_E06, Pu_E07, Pu_E08, and Pu_E09. The proximity of these facilities to Omaha, the largest city in Nebraska, is likely the reason for the high occupancy rate. This finding suggests that additional parking facilities in this area would alleviate truck parking shortages, thereby improving traffic safety and freight efficiency. For westbound public facilities shown in Figure 5.5(b), the data indicates that two facilities located in western Nebraska, Pu_W01 and Pu_W02, and one facility located in central Nebraska, Pu_W06, show a consistently high occupancy rate. The reason is likely due to the extensive amenities provided at these facilities.

The heat maps in Figure 5.6 show truck parking occupancy for private facilities near (a) eastbound I-80 and (b) westbound I-80. Figure 5.6(a) indicates that several eastbound private facilities in central and eastern Nebraska experienced high occupancy rates: Pr_E05, Pr_E06, Pr_E07, and Pr_E15. In contrast, Figure 5.6(b) indicates that westbound private facilities generally have lower occupancy rates, except for Pr_W04, Pr_W05, and Pr_W13, and Pr_W13.

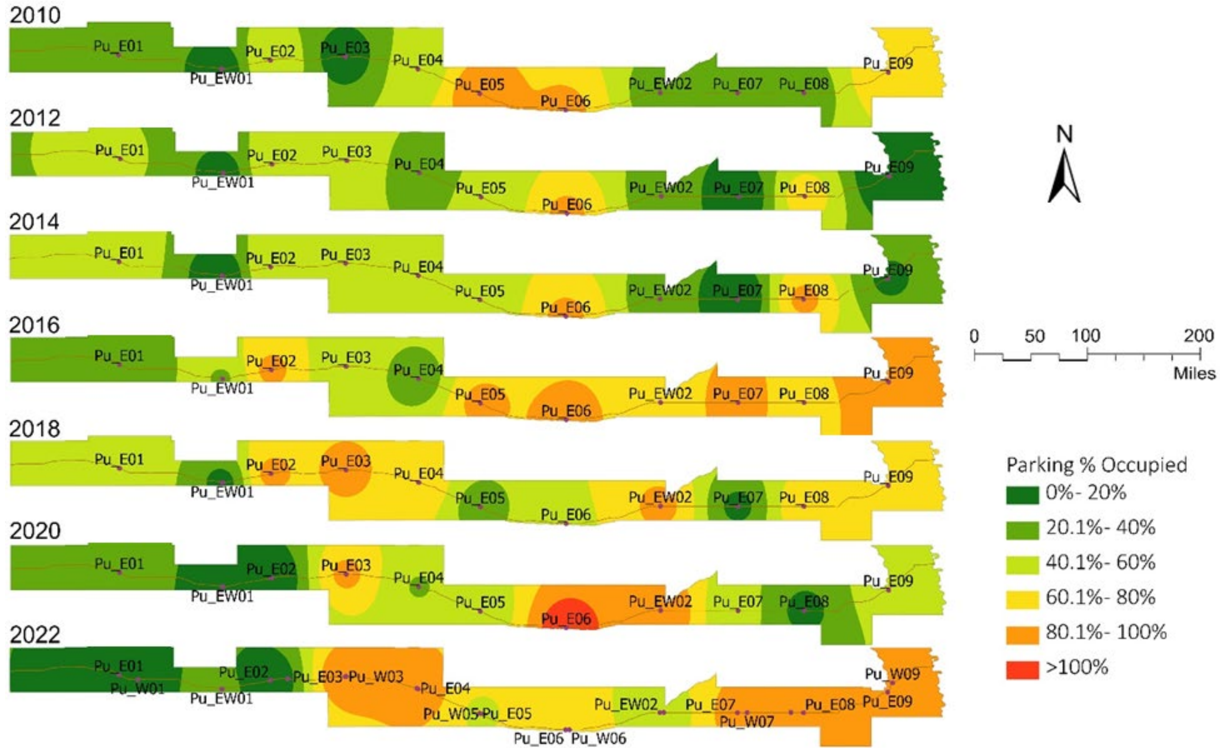

(a) Public parking facility on Eastbound I-80

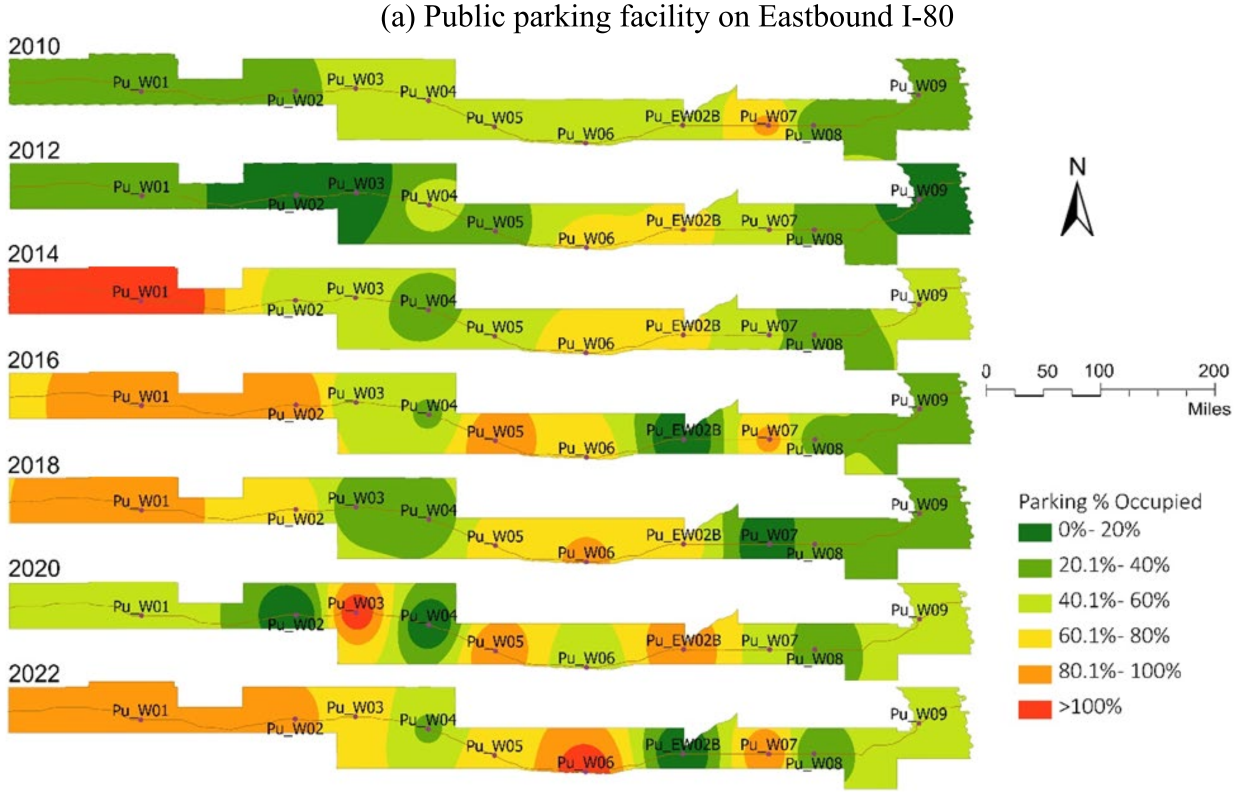

(b) Public parking facility on Westbound I-80

Figure 5.5 Spatiotemporal distribution of truck parking occupancy based on NAIP data.

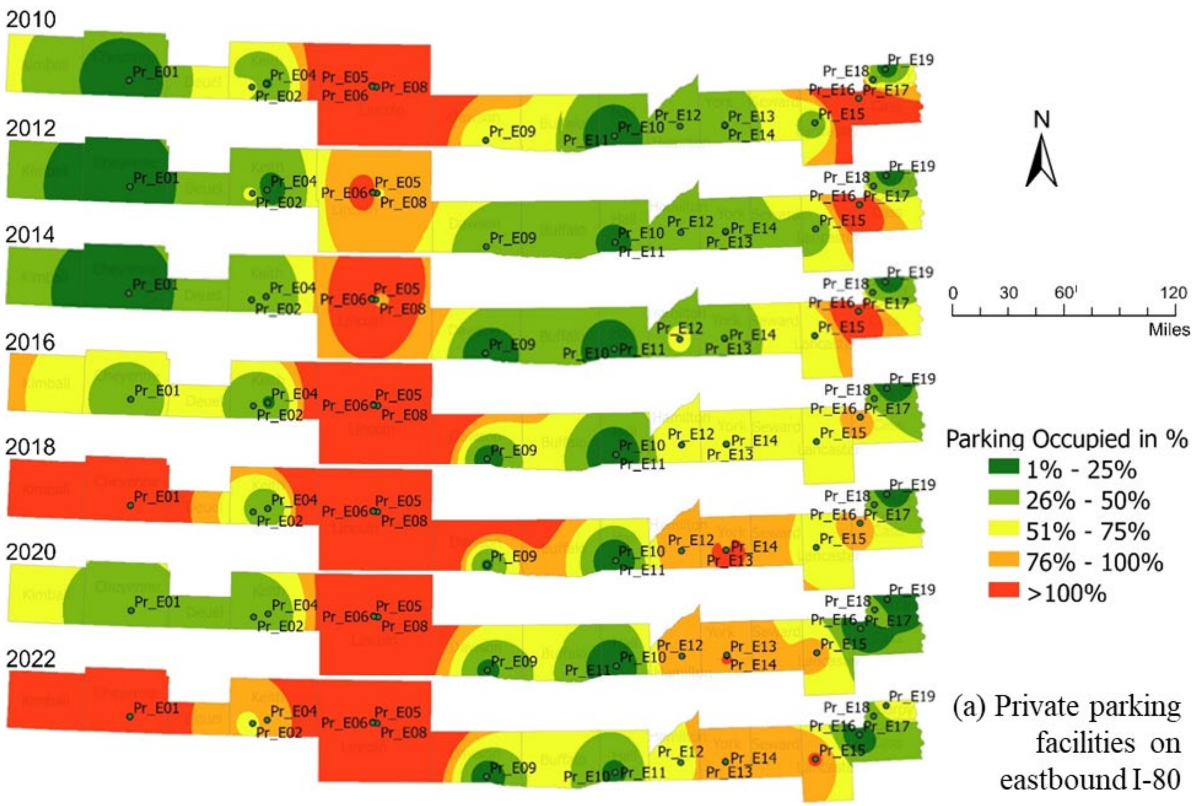

(a) Private parking facility on Eastbound I-80

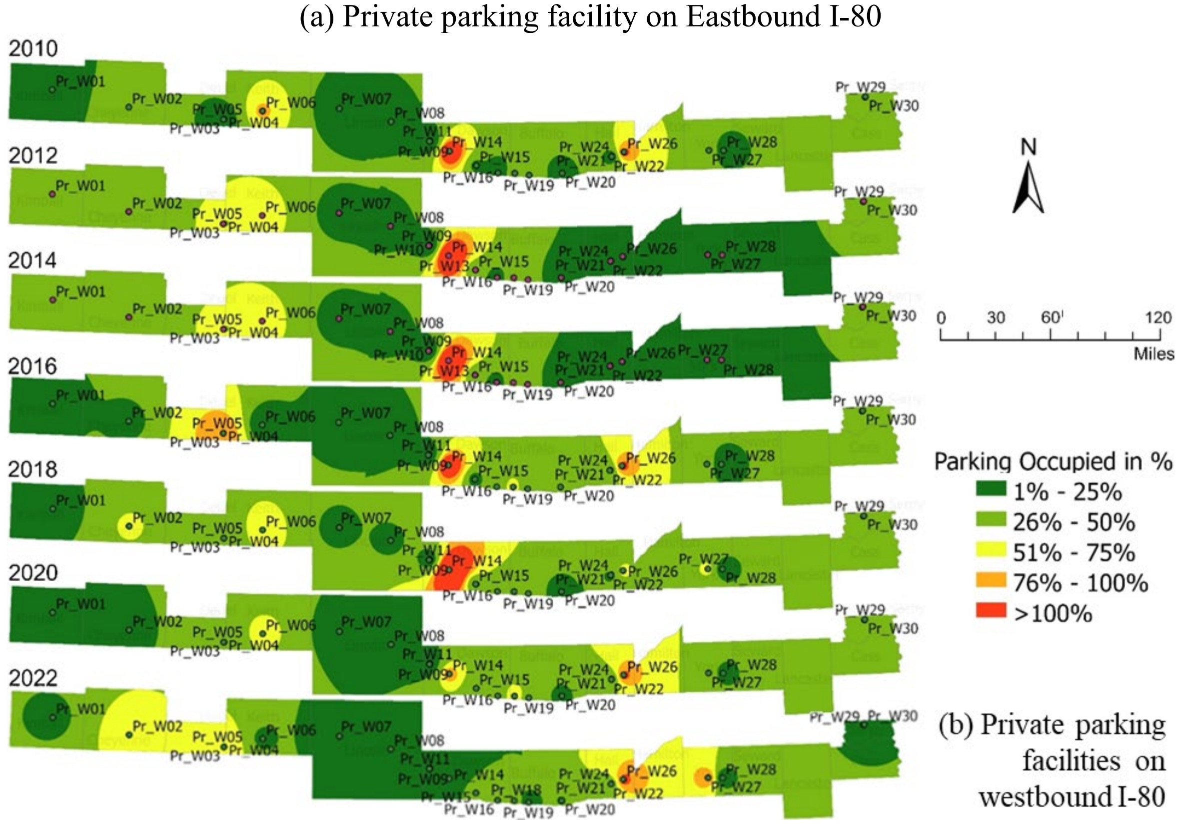

(b) Private parking facility on Westbound I-80

Figure 5.6 Spatiotemporal distribution of truck parking occupancy based on NAIP data.

The spatiotemporal analysis of truck parking occupancy revealed higher average occupancy rates at private facilities compared to public rest areas. This pattern likely reflects the greater capacity and broader range of amenities offered at private truck stops, which attract drivers seeking longer rest periods and additional services. Among public facilities, those near Omaha exhibited consistently high occupancy rates, indicating persistent demand pressures in this area. Sustained parking shortages can lead to unsafe behaviors, such as drivers spending excessive time searching for available spaces or parking in unauthorized locations, which in turn may increase crash risk. These findings highlight areas where additional public or private investment could improve parking availability and enhance safety. Other high-demand public facilities facing similar challenges include Pu_W01 and Pu_W02 in western Nebraska and Pu_W06 in central Nebraska.

5.3 Truck Parking Demand Prediction (Objective 3)

5.3.1 Isolated, Single-Facility: Dynamic Bayesian Time Series Results

This section reports the estimation outcomes of the Dynamic Bayesian Time Series (DBTS) models developed for the five isolated single-facility clusters. These clusters were modeled individually because they are geographically and operationally separated from other parking areas, and their dynamics are therefore best represented through facility-specific time series structures. The results are organized as follows: model diagnostics, interpretation of posterior estimates, assessment of predictive accuracy, and evaluation of model fit.

5.3.1.1 Model Diagnostics

Table 5.1 summarizes the key convergence diagnostics for the DBTS models across the five isolated facilities. The reported statistics include the maximum Gelman–Rubin convergence statistic ($\hat{R}$), the minimum effective sample sizes (ESS) for both bulk and tail distributions, the number of divergent transitions, and whether the Bayesian Fraction of Missing Information (BFMI) exceeded the recommended threshold of 0.90.

Across the five facilities, the diagnostics demonstrate that all models achieved satisfactory convergence. Four models—Pr_E01, Pu_EW01, Pr_W01, and Pu_W02—produced maximum $\hat{R}$ values at or below 1.01, which is well within the standard threshold for reliable convergence. The model for Pu_E06 showed a slightly higher maximum $\hat{R}$ of 1.03 for a subset of hourly time parameters. In the context of latent-state time series models, such deviations are generally considered acceptable when no divergent transitions are detected and $BFMI$ values remain comfortably above the 0.90–0.94 range.

Table 5.1 Convergence diagnostics for Dynamic Bayesian Time Series models

Polygon	Max $\hat{R}$	Min ESS (bulk)	Min ESS (tail)	Divergences	BFMI ≥ 0.94
Pr_E01	1.01	592	512	0	Yes
Pu_EW01	1.00	1150	1284	0	Yes
Pu_E06	1.03	321	499	0	Yes
Pr_W01	1.01	474	677	0	Yes
Pu_W02	1.01	616	890	0	Yes

The effective sample sizes (ESS) indicate that posterior draws are adequate for inference across nearly all parameters. Bulk ESS values ranged from a low of 321 in Pu_E06 to more than 1,100 in Pu_EW01, while tail ESS values followed a similar pattern. Lower ESS values were primarily associated with temporal indicators in the more variable facilities, but even these remained above the minimum acceptable threshold of 300, ensuring that the resulting posterior estimates are statistically reliable.

No divergent transitions were recorded in any of the five models, further confirming numerical stability. Likewise, all models reported $BFMI$ values above the recommended threshold, which demonstrates that Hamiltonian trajectories sufficiently explored the energy landscape during sampling. Together, these diagnostics establish that the estimation process was robust and that posterior draws can be interpreted with confidence. To illustrate this point, Figure 5.7 shows the trace plots of key parameters for Pr_E01. In these plots, each "chain" represents an independent Markov process initialized at a different starting point, and well-behaved chains should overlap, fluctuate around a constant mean, and mix rapidly across the parameter space. The chains in Figure 5.7 display precisely these characteristics: they show stable mixing, minimal autocorrelation, and no signs of pathological behavior such as drifting, sticking, or sudden jumps. This visual evidence, combined with the quantitative diagnostics reported in Table 5.1, confirms the reliability of the DBTS model estimates and provides a strong foundation for interpreting the posterior distributions and subsequent forecasting results.

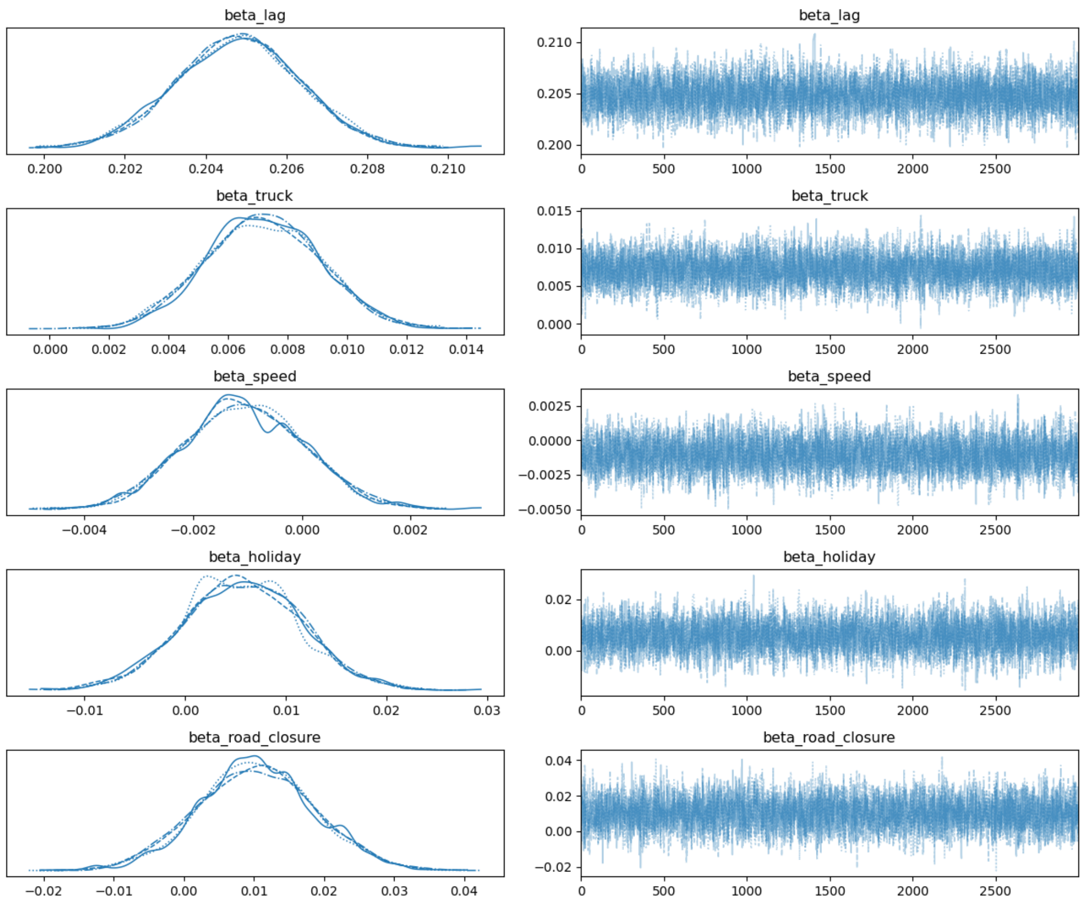

Figure 5.7 Trace plots for selected parameters in the Pr_E01 model, indicating effective mixing across chains.

- **Posterior Estimates and Interpretation of Key Drivers**

The posterior estimation results provide insight into the temporal persistence and external drivers of truck parking occupancy across the five isolated facilities. As summarized in Table 5.2, the posterior mean coefficient of the lagged occupancy term (β_{lag}) is consistently positive and statistically significant in all models, confirming strong temporal dependence. This finding indicates that occupancy levels in any given hour are strongly influenced by the previous hour, a finding that aligns with previous studies' conclusions (Sadek et al. 2020; Sasaki et al. 2023; Yang et al. 2022). Notably, the strength of this variable varies across sites, with the largest effect observed in Pu_W02 ($\beta_{lag} = 0.424$) and the weakest in Pr_W01 ($\beta_{lag} = 0.097$) suggesting site-specific differences in how strongly past occupancy influences current parking conditions.

Table 5.2 Posterior Means of Coefficients across Parking Clusters

Parameter	Pr_E01	Pu_EW01	Pu_E06	Pr_W01	Pu_W02
β_{lag}	0.205	0.272	0.216	0.097	0.424
β_{truck}	0.007	0.010	–0.004	0.002	0.008
β_{speed}	–0.001	0.003	0.001	–0.002	0.001
$\beta_{holiday}$	0.006	–0.047	–0.001	0.002	–0.026
$\beta_{road\_closure}$	0.010	–0.002	–0.007	0.004	0.015

The posterior mean coefficient for the upstream truck volume (β_{truck}) variable is mostly positive, but small in magnitude. For example, Pu_EW01 exhibits the strongest positive association (0.010), while Pu_E06 shows a slight negative effect (–0.004). These results suggest that while truck volume contributes to explaining parking demand, its influence varies by location and may depend on factors such as facility accessibility, available amenities, and driver familiarity with the site.

The posterior mean coefficient for average speed variable (β_{speed}) is close to zero across all models and not statistically significant. This finding is consistent with that from Slavova (2022), who reported that traffic slowdowns often stem from exogenous factors, such as work zones, roadway geometry, or congestion, rather than from parking demand decisions.

The posterior mean coefficient for the Holiday variable ($\beta_{holiday}$) shows weak and inconsistent effects across facilities. Three facilities, such as Pu_EW01, have negative coefficients, but the associated intervals include zero, indicating that the estimated effects are not statistically significant. This finding suggests that while some facilities may experience reduced demand during holidays, others continue to serve rerouted or long-haul trips.

The posterior mean coefficient for road closures ($\beta_{road\_closure}$) shows mixed effects across the five facilities, with positive values at Pr_E01, Pr_W01, and Pu_W02, and negative values at Pu_EW01 and Pu_E06. The corresponding credible intervals include zero, indicating that these variables are not statistically significant at the 95% confidence level. This finding suggests that road closures will redistribute parking demand to other facilities rather than increase or decrease overall parking activity.

Beyond these covariates, temporal indicators (hour of day, day of week, month of year) were incorporated into the models to capture scheduling regularities in freight operations. Although the 95% highest density intervals for these variables include zero, the posterior means reveal systematic directional patterns. Figure 5.8 summarizes these effects across facilities. Hourly patterns (Figure 5.8a) reveal that occupancy demand peaks during late evening and overnight hours (22:00–05:00), with Pu_EW01 and Pu_W02 showing the strongest positive deviations (up to +0.25). Midday hours (12:00–15:00) exhibit negative effects, particularly at Pu_W02, where values dip below –0.12. Day-of-week effects (Figure 5.8b) show systematically higher occupancy during weekends, particularly at Pr_E01 where coefficients approach +0.30. Seasonal patterns (Figure 5.8c) highlight elevated occupancy during winter and early spring months (December–April). For instance, Pr_E01 records positive posterior means around +0.20 in January and April, while demand in summer months (July–August) stabilizes at moderate levels across most facilities.

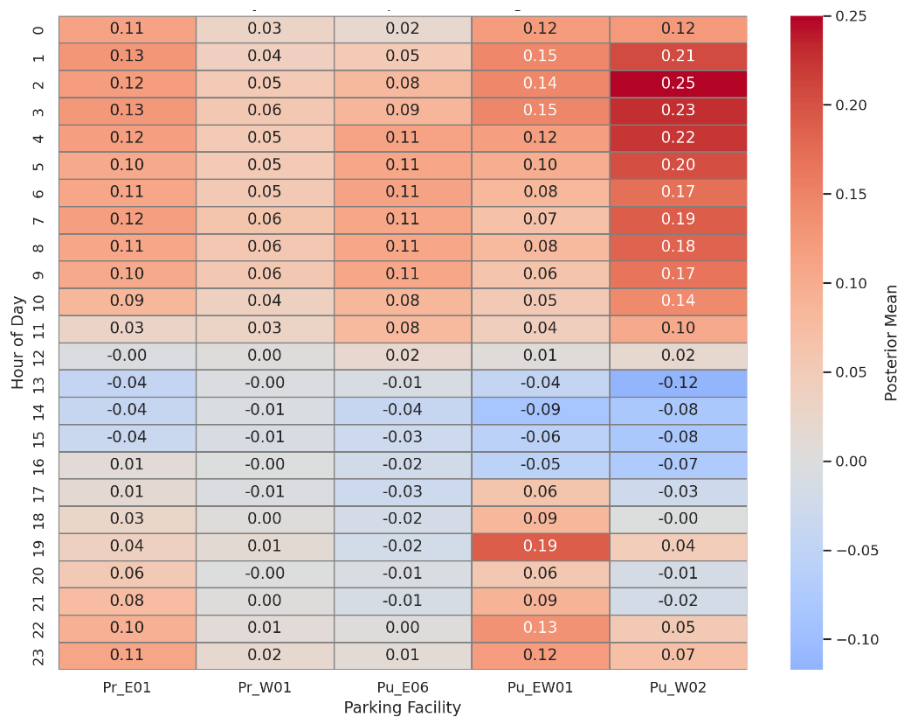

(a) Hour-of-day effects

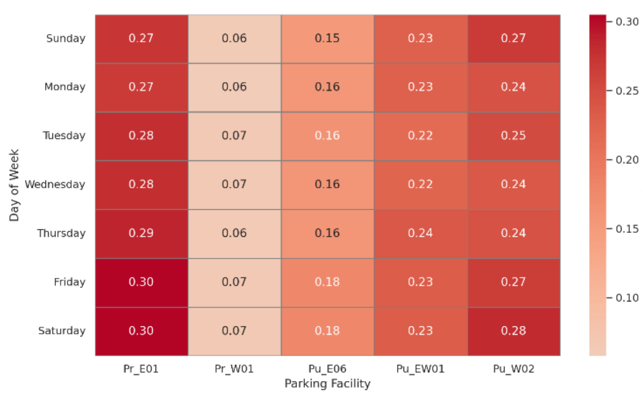

(b) Day-of-week effects

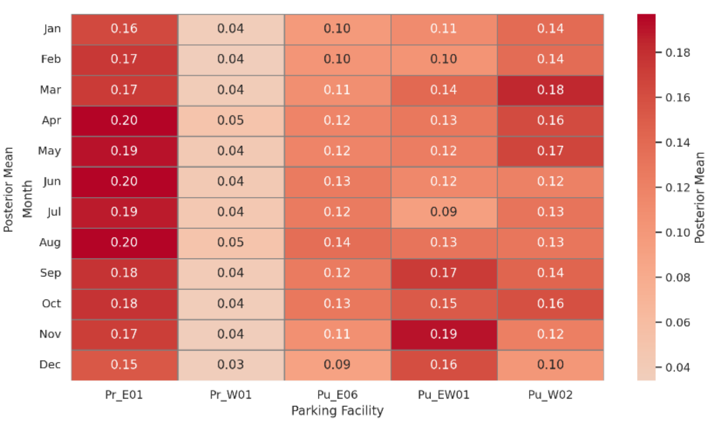

(c) Month-of-year effects

Figure 5.8 Heatmaps of posterior means for temporal effects across five parking facilities.

- **Posterior Predictive Checks (PPC)**

Posterior Predictive Checks (PPC) were applied to assess how well the models reproduced the observed occupancy distributions. Figure 5.9 presents the PPC density plot for facility Pr_E01, which serves as a representative example. In this figure, the observed occupancy distribution is plotted in black, the posterior predictive mean is shown as an orange dashed line, and 100 simulated posterior draws are shown in blue. The close alignment between the predictive mean and the peak of the observed distribution, combined with the broad coverage of the simulated draws, indicates that the model is well-calibrated for this site. Both the location and spread of the occupancy distribution are successfully reproduced, suggesting that the temporal structure and covariate effects embedded in the model adequately capture the underlying dynamics at this facility.

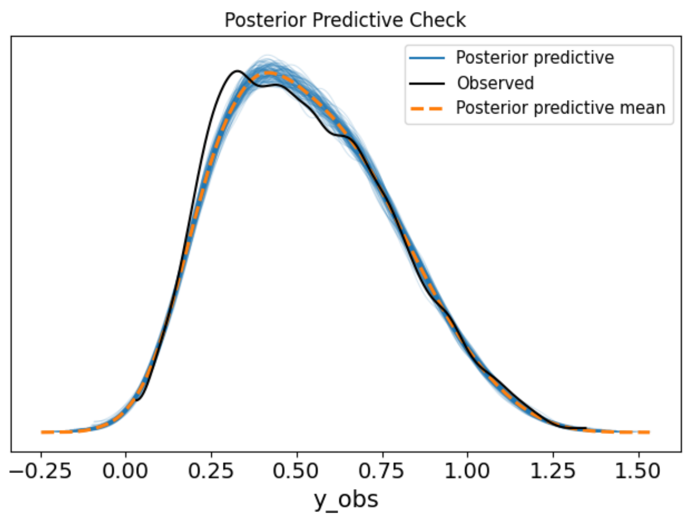

Figure 5.9 Posterior predictive check for parking area Pr_E01 as an illustrative example

While the Pr_E01 model illustrates a strong match, the PPC results for the other four isolated facilities—Pu_EW01, Pu_E06, Pr_W01, and Pu_W02—showed more nuanced outcomes. Specifically, all models were able to reproduce the general distributional shape and central tendency of occupancy, but they struggled to capture the sharp spike at zero occupancy that was frequently observed in the raw data. This discrepancy is attributable to the high prevalence of zero values in the dataset, a common challenge in freight parking applications where facilities may experience prolonged intervals of no activity.

Quantitative evaluation confirms that the underestimation of zero occupancy did not substantially undermine predictive performance. Even in the weakest-performing case (Pu_W02), more than 62% of the observed zero-occupancy intervals were matched by posterior predictions below 0.1, which can be treated as practically equivalent to zero. Across all five models, the mean absolute error (MAE) for zero-occupancy hours remained below 0.18, demonstrating that predictions were acceptably accurate even in this difficult region of the distribution. These results show that the DBTS models are able to reproduce not only the average occupancy dynamics but also the variability and uncertainty inherent in truck parking demand.

Overall, the PPC analysis confirms that the Bayesian time series framework yields predictive distributions that are consistent with observed occupancy patterns. Although replicating zero spikes accurately remains a challenge, the models successfully capture the key statistical structures, including peak location, spread, and uncertainty coverage, supporting their suitability for interpretation and forecasting in subsequent analyses.

- **Predictive Accuracy**

Table 5.3 reports the performance statistics in terms of Root Mean Squared Error ($RMSE$) and the coefficient of determination (R^2). The R^2 values range from 0.74 to 0.87, demonstrating that the models successfully explained a substantial portion of the observed variation in occupancy. $RMSE$ values are generally low, ranging from 0.0647 to 0.2739, which confirms the ability of the models to produce forecasts that are closely aligned with actual observations.

Table 5.3 Predictive performance of Bayesian time series models

Group / Polygon	RMSE	R^2
Pr_E01	0.0896	0.8719
Pu_EW01	0.1815	0.7745
Pu_E06	0.0935	0.8745
Pr_W01	0.0647	0.7359
Pu_W02	0.2739	0.7498

Among the single/isolated facilities, Pr_E01 and Pu_E06 achieved the strongest performance, with R^2 values of 0.8719 and 0.8745, respectively, and $RMSE$ values below 0.10. These results indicate that the models at these sites captured occupancy dynamics with high fidelity. In contrast, Pr_W01 showed the lowest R^2 (0.7359), although its $RMSE$ was the smallest (0.0647), suggesting that while the model's explanatory power was weaker, the magnitude of prediction errors was small in absolute terms.

The facility Pu_W02 exhibited the largest RMSE (0.2739), reflecting challenges in reproducing the high volatility and frequent zero-occupancy intervals at this location. Nevertheless, its R^2 remained acceptable at 0.7498, confirming that the model is still able to capture general patterns of variation despite these complexities.

Overall, the results demonstrate that the DBTS framework provides reliable predictive performance across different facility types. Both high-demand and low-demand scenarios were adequately represented, underscoring the robustness of the modeling approach. To further ensure statistical validity, convergence diagnostics and sample quality metrics were revisited, and all models satisfied the required thresholds ($\hat{R} < 1.01$, $ESS > 400$, low Monte Carlo error), thereby confirming that the predictive estimates are statistically sound.

- **Model Fit Evaluation Using WAIC and LOO**

Model adequacy was examined using WAIC and LOO-CV, and the corresponding results are summarized in Table 5.4. The metrics capture out-of-sample predictive performance while also reflecting the effective complexity of each model.

Table 5.4 WAIC and LOO Metrics for Dynamic Bayesian Time Series Models

Facility	$elpd_{WAIC}$	p_{WAIC}	$elpd_{Loo}$	p_{Loo}
Pr_E01	8641.65	68.20	8641.57	68.28
Pu_EW01	1043.75	54.08	1043.73	54.09
Pu_E06	8269.26	69.17	8268.94	69.49
Pr_W01	11506.03	60.19	11506.00	60.21
Pu_W02	–1136.96	53.32	–1136.99	53.35

The results show consistently high elpd values for four of the five facilities, demonstrating strong out-of-sample predictive performance and stable parameterization. The exception is Pu_W02, where both WAIC and LOO yield negative elpd values. This reflects the atypical occupancy distribution at the site, dominated by prolonged periods of zero or near-zero occupancy, as previously noted in the posterior predictive checks. Despite this, the relatively low effective parameter count ($p_{WAIC} \approx 53$) suggests that the model remains parsimonious and does not suffer from overfitting.

Among the other facilities, Pr_W01 achieved the highest elpd values under both WAIC and LOO, highlighting its superior calibration and predictive strength. Pr_E01 and Pu_E06 also show robust fit, with effective parameter counts around 68–69, balancing flexibility with model stability. The close agreement between WAIC and LOO across all facilities further validates the consistency of these results, reinforcing the reliability of the DBTS framework for capturing demand dynamics in isolated parking areas.

5.3.1.2 Forecasting Application

The estimated Dynamic Bayesian Time Series (DBTS) models are not only effective for retrospective interpretation but can also be used as operational forecasting tools for future parking occupancy. Given their autoregressive formulation and probabilistic estimation via posterior distributions, the models can generate both point forecasts and credible intervals for upcoming hours under varying traffic, temporal, and operational conditions. This capability enables proactive management of parking capacity by anticipating near-term changes in demand rather than reacting to them after occurrence. For demonstration, the final estimated DBTS model for facility Pr_E01, expressed in terms of posterior mean coefficients, can be written as follows:

$$y_t \sim \mathcal{N}(\mu_t, \sigma^2)$$

$$\begin{aligned}
\mu_t \ = \ & [0.11, 0.13, 0.12, 0.13, 0.12, 0.10, 0.11, 0.12, 0.11, 0.10, 0.09, 0.03, \text{-0.00} \\
& -0.04, -0.04, -0.04, 0.01, 0.01, 0.03, 0.04, 0.06, 0.08, 0.10, 0.11]^T \gamma_{h(t)} \\
& + \ [0.27, 0.27, 0.28, 0.28, 0.29, 0.30, 0.30]^T \delta_{d(t)} \\
& + [0.16, 0.17, 0.17, 0.20, 0.19, 0.20, 0.19, 0.20, 0.18, 0.18, 0.17, 0.15]^T \eta_{m(t)} \\
& + 0.205\, y_{t-1} \ + \ 0.007\, V_t \ - \ 0.001\, S_t \ + \ 0.006\, H_t \ + \ 0.010\, R_t
\end{aligned} \tag{5.1}$$

where y_t denotes the hourly parking occupancy rate, and μ_t is its conditional mean. The terms $\gamma_{h(t)}$, $\delta_{d(t)}$, and $\eta_{m(t)}$ represent the hour-of-day, day-of-week, and month-of-year effects selected by the corresponding temporal index at time t. The variable $y_{t-1}$is the lagged occupancy capturing autoregressive persistence, V_t is the hourly truck volume, S_t is the average traffic speed, H_t is a holiday indicator (1 on federal holidays, 0 otherwise), and R_t is a road-closure indicator (1 when flow drops below 50 vehicles per hour due to weather or operational disruption). Finally, σ^2 is the residual variance of the Normal likelihood.

5.3.2 Multi-Facility Cluster Analysis: Dynamic Bayesian Panel Model with Temporal and Spatial Effects Results

This subsection presents the estimation outcomes of the Dynamic Bayesian Panel Models developed for the fifteen multi-facility clusters identified along I-80. Unlike the isolated single-facility models, these clusters capture the interdependent nature of truck parking behavior across neighboring facilities within a 19-mile radius. By incorporating both temporal and spatial effects, the models provide a more realistic representation of corridor-wide demand dynamics and allow for the evaluation of how occupancy at one facility influences, and is influenced by, conditions at adjacent sites.

The hierarchical and unbalanced structure of the dataset necessitated preliminary specification tests to validate the use of panel-based modeling. Within each cluster, a Chow test was first conducted to examine whether a pooled model could adequately describe the data. In every case, the null hypothesis of parameter homogeneity was rejected, indicating substantial cross-facility heterogeneity and supporting the adoption of a panel framework. These results align with expectations in the truck parking context, where differences in facility size, location, and amenities contribute to systematically distinct demand profiles.

To further guide model specification, Hausman tests were performed to distinguish between fixed- and random-effects formulations. Although the test results did not indicate statistically significant differences between the two approaches, the fixed-effects specification was chosen for simplicity and interpretability. This choice also allows for control of unobserved, time-invariant facility attributes, such as access design, visibility from the highway, and availability of specific amenities, that may influence parking demand but are not directly captured by the observed variables.

Building on these specification checks, the Dynamic Bayesian Panel Models were estimated under two complementary configurations: one excluding spatial lags and one incorporating facility-level spatial effects. This dual specification enables a direct assessment of the role of spatial interactions in improving model performance and in identifying redistribution patterns across facilities.

5.3.2.1 Model Diagnostics

The estimation process for all fifteen multi-facility clusters was evaluated under both temporal and spatiotemporal configurations with respect to convergence diagnostics, sampling behavior, and numerical stability. Across all clusters, the Markov Chain Monte Carlo (MCMC) simulations converged properly, and no irregular or divergent sampling behavior was observed. The maximum $\hat{R}$ values for all parameters in all clusters were equal to 1.00, confirming complete convergence of the Markov chains to the target posterior distribution. This value is well below the commonly accepted threshold of 1.01, validating the stability of the estimation process.

The effective sample sizes (ESS) were consistently large across all clusters. Bulk ESS values typically exceeded 2,000 and, in some westbound clusters, were greater than 10,000. These high ESS values indicate sufficient statistical independence among posterior draws and stable parameter estimation. Tail ESS values also surpassed recommended thresholds, confirming reliable estimation in the distributional extremes and the accuracy of uncertainty intervals.

No divergent transitions were detected in any model, indicating that the parameter space was smooth and the Hamiltonian step sizes were properly tuned. All models reported BFMI values greater than 0.90, demonstrating adequate exploration of the energy landscape by the Hamiltonian Monte Carlo sampler. Collectively, the absence of divergences, high BFMI values, and consistent $\hat{R}$ statistics confirm that the models were computationally stable and statistically reliable.

Between the two configurations, the models incorporating spatial effects generally exhibited higher effective sample sizes and lower variability across chains. This pattern suggests improved posterior geometry and numerical efficiency when spatial heterogeneity across facilities within a cluster was explicitly modeled. Such improvements were most evident in large clusters containing multiple parking facilities, confirming that the inclusion of spatial structure enhances estimation stability.

Table 5.5 presents a representative subset of results for four clusters (two eastbound and two westbound) estimated under both model configurations, with and without spatial effects. The reported diagnostics follow the same pattern observed across all clusters, confirming that all models met standard Bayesian convergence criteria.

Table 5.5 Representative convergence diagnostics for selected clusters

Cluster	**Parameter**	**$\hat{R}$ (Spatial/Non-Spatial)**	**ESS (bulk) Spatial/Non-Spatial**	**ESS (tail) Spatial/Non-Spatial**	**BFMI (Spatial/Non-Spatial)**
E_cluster 1	β_{lag}	1.00 / 1.00	2707 / 4633	4068 / 5525	Yes / Yes
E_cluster 1	β_{truck}	1.00 / 1.00	1669 / 4626	3293 / 6147	Yes / Yes
E_cluster 1	β_{speed}	1.00 / 1.00	2696 / 3901	3745 / 5302	Yes / Yes
E_cluster 1	$\beta_{holiday}$	1.00 / 1.00	2996 / 3729	5101 / 5194	Yes / Yes
W_cluster 1	β_{lag}	1.00 / 1.00	12298 / 5509	7407 / 3628	Yes / Yes
W_cluster 1	β_{truck}	1.00 / 1.00	12600 / 5402	6937 / 4064	Yes / Yes
W_cluster 1	β_{speed}	1.00 / 1.00	12168 / 5792	6770 / 4556	Yes / Yes
W_cluster 1	$\beta_{holiday}$	1.00 / 1.00	14301 / 5104	7345 / 4733	Yes / Yes

For illustration, Figure 5.10 presents the trace plots and posterior distributions of the key parameters in the largest cluster, W_cluster 4 model, which includes ten parking facilities. The trace plots show stable sampling behavior with consistent mixing and no evidence of autocorrelation or irregular drift, confirming full convergence of the MCMC chains.

The posterior densities for β_{lag}, β_{truck}, β_{speed}, and $\beta_{holiday}$ are unimodal, symmetric, and narrowly concentrated, indicating precise parameter estimation. In particular, β_{lag} remains concentrated between 0.224 and 0.229, with an average of about 0.226, while β_{truck} centers between 0.004 and 0.005, and β_{speed} exhibits a narrow symmetric spread around –0.001. The

$\beta_{holiday}$ coefficient is confined within –0.005 to 0.015, and beta_road_closure shows slightly broader dispersion around zero.

The $\beta_{spatial\_polygon}$ coefficient displays multiple distinct posterior modes ranging from approximately –0.01 to 0.03, corresponding to the individual parking facilities within the cluster. Each spatial component remains stable and well-mixed across iterations, confirming convergence. The overall behavior in Figure 5.10 is consistent with the diagnostic results in Table 5.5, validating the numerical stability of the estimation for this cluster.

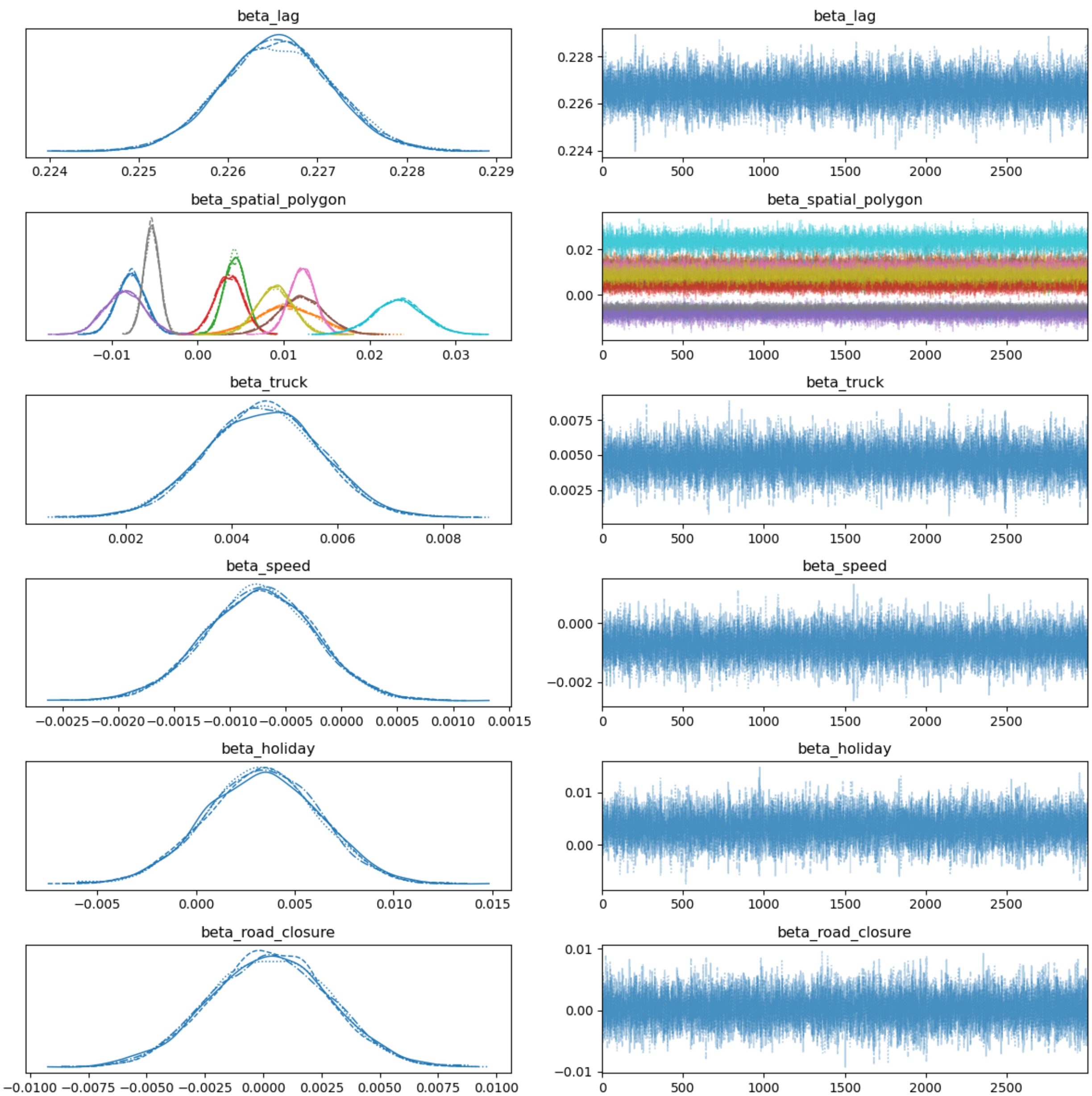

Figure 5.10 Trace plots and posterior densities of key parameters in the W_cluster 4 model

- **Posterior Estimates and Interpretation of Key Drivers**

Due to the large number of estimated coefficients across the fifteen multi-facility clusters, full numerical results are not presented here. Instead, we summarize key patterns and highlight statistically significant effects, defined as those with 95% highest density intervals (HDIs) that do not include zero. To illustrate, one representative cluster is analyzed in detail at the end of this section.

Among all clusters, the β_{lag} coefficient, representing temporal dependency, was consistently positive and significantly different from zero in both model settings. This confirms strong temporal autocorrelation in parking occupancy, aligned with findings from Sasaki et al. (2023) and Yang et al. (2022). Models including spatial effects exhibited lower dispersion in this coefficient, suggesting improved estimation precision through spatial information.

The truck volume coefficient (β_{truck}) was positive and significant in over 80% of clusters, with stronger and more precise estimates in the spatial models, highlighting the benefit of accounting for spatial interactions in identifying traffic-related effects.

The average speed coefficient (β_{speed}) showed varied behavior. In some clusters (e.g., W_cluster 4 and E_cluster 9), it was significantly negative, while in others it hovered around zero. These differences suggest that speed reduction does not universally translate to higher parking demand, potentially due to road geometry or other non-demand-related delays (Slavova et al. 2022).

The holiday coefficient ($\beta_{holiday}$) was generally weak and unstable across clusters. However, spatial models produced tighter HDI intervals for clusters with weekend-oriented demand patterns (e.g., W_cluster 9 and E_cluster 3), yielding more reliable estimates.

The effect of road closures ($\beta_{road\_closure}$) varied across the multi-facility clusters in both magnitude and sign. For example, clusters such as E_cluster 1 and W_cluster 4 exhibited negative posterior mean coefficients, whereas others like E_cluster 5 showed positive coefficient estimates. However, in all cases, the 95% highest density intervals (HDIs) included zero, indicating no statistically significant effects. As discussed in the single-facility analysis, this uncertainty may stem from the localized nature of road closures and heterogeneous driver responses. In some cases, such disruptions lead to spatial redistribution of parking demand rather than a net change in overall demand (Mathew et al. 2024).

Although temporal indicators, such as hour-of-day, day-of-week, and month-of-year, were included in the model, the 95% HDIs for their coefficients included zero in most clusters, suggesting a lack of strong statistical evidence for distinct calendar effects. Nonetheless, these temporal variables were retained to control for latent calendar-based fluctuations that may not be fully captured by other dynamic covariates and to preserve comparability with earlier studies in freight and parking demand modeling (Anastasopoulos and Mannering 2011). Furthermore, systematic and predictable differences in traffic flow across days of the week and seasons have been documented in the literature, even under weak statistical support (Crawford et al. 2017). In hierarchical Bayesian frameworks, retaining weakly informative predictors can also enhance model stability and reduce underfitting, especially for out-of-sample forecasting (Gelman et al. 2021; Jr et al. 2013).

Following the interpretation of primary covariate effects, the analysis next examines spatial heterogeneity and its contribution to explaining inter-facility variations in parking occupancy. The posterior distribution of spatial coefficients varied substantially across clusters. Table 5.6 summarizes the number of facilities in each cluster with 95% certainty (i.e., HDI 95% not including zero):

Table 5.6 Summary of significant spatial coefficients (95% HDI not including zero) by cluster

Cluster	Total Spatial Coefficients	Significant Coefficients	Percentage (%)
E_cluster_1	2	1	50.0
E_cluster_2	6	6	100.0
E_cluster_3	2	0	0.0
E_cluster_4	3	2	67.0
E_cluster_5	3	3	100.0
E_cluster_6	2	2	100.0
E_cluster_7	4	4	100.0
W_cluster_1	3	3	100.0
W_cluster_2	3	3	100.0
W_cluster_3	3	2	67.0
W_cluster_4	10	10	100.0
W_cluster_5	2	2	100.0
W_cluster_6	2	1	50.0
W_cluster_7	2	1	50.0
W_cluster_8	2	1	50.0

As shown in Table 5.6, clusters such as E_cluster 2, E_cluster 5, W_cluster 2, and W_cluster 4 exhibited the highest rates of facilities with reliable spatial effects (100%), while clusters like E_cluster 3 showed no significant spatial influence. These variations likely stem from factors such as facility proximity and density, which intensify spatial interactions in clusters with closely spaced lots (e.g., E_cluster 2); ownership type, since private facilities with restricted access can influence nearby public lots by either diverting trucks away (competition) or absorbing excess demand (complementarity); amenity differences, where services like food, restrooms, or showers enhance a facility's spatial draw; and directional placement, where upstream facilities may either reduce or reinforce demand at downstream ones depending on accessibility and attractiveness (Xiao and Jaller 2025).

To provide a more concrete understanding of facility-specific spatial effects, an illustrative example from E_cluster2 is presented. This cluster includes two private parking facilities, Pr_E03 and Pr_E04, both located eastbound along I-80. The two private lots are located across the road from each other. Table 5.7 reports key parameter estimates, with a focus on the spatial coefficients for the two facilities:

Table 5.7 Summary of E_cluster 2 model statistics

Variable	Mean	Std. Dev.	95% HDI	$\hat{R}$
β_{lag}	0.319	0.001	[0.318, 0.321]	1.00
$\beta_{spatial\_polygon}[0]$	-0.100	0.024	[-0.144, -0.055]	1.00
$\beta_{spatial\_polygon}[1]$	-0.098	0.010	[-0.117, -0.079]	1.00
β_{truck}	0.009	0.001	[0.007, 0.012]	1.00
β_{speed}	0.000	0.001	[-0.001, 0.001]	1.00
$\beta_{holiday}$	0.003	0.003	[-0.003, 0.009]	1.00
$\beta_{road\_closure}$	-0.002	0.005	[-0.011, 0.007]	1.00

Both spatial coefficients are negative and highly certain (95% HDI entirely below zero), indicating a strong competitive spatial interaction between the two facilities. In practical terms, when occupancy increases in one facility, demand in the neighboring facility is likely to decrease. Given their close proximity and their location on opposite sides of the road, drivers are unlikely to switch between the two once a choice is made, reinforcing the competitive dynamic.

In addition to spatial effects, the analysis of temporal coefficients in E_cluster 2 reveals that incorporating spatial structure slightly reduces the magnitude of temporal fluctuations. As shown in Figure 5.11(a) to 5.11(c), posterior mean estimates for most months, days of the week, and hours of the day are lower in the spatial model compared to the non-spatial counterpart. For instance, the effect for August decreases from 0.115 to 0.100, and the effect for Saturday (day 6) drops from 0.202 to 0.179. Moreover, hourly fluctuations during midday and afternoon periods approach zero in the spatial model. Although the 95% highest density intervals for temporal coefficients include zero in both models, indicating insufficient statistical evidence to confirm their effects with 95% certainty, the observed differences in posterior means suggest that part of the temporal variation may reflect underlying spatial interactions among neighboring parking facilities.

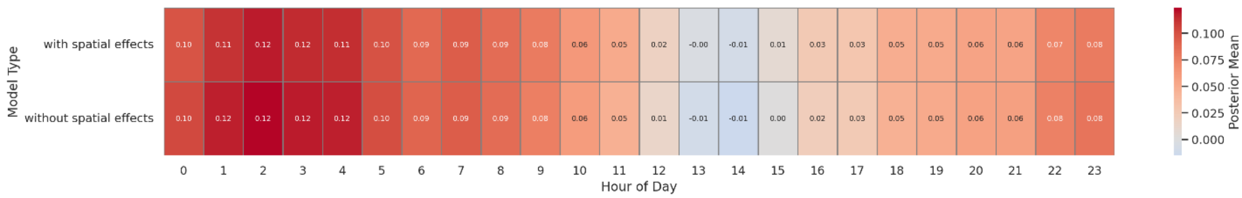

(a) Hour-of-day effects

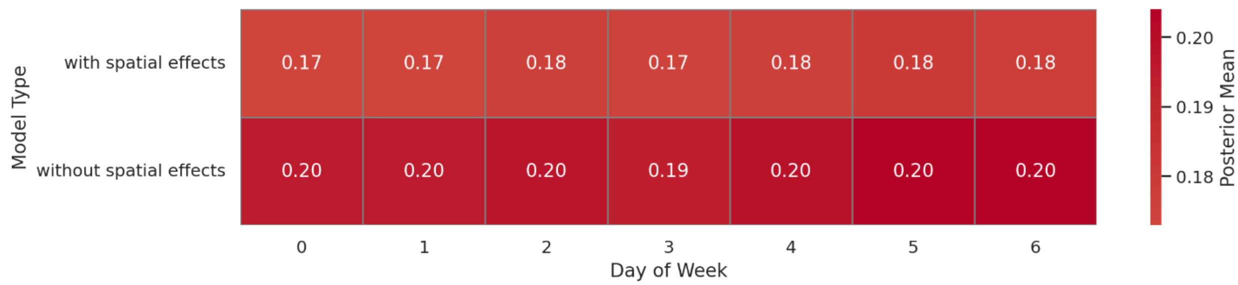

(b) Day-of-week effects

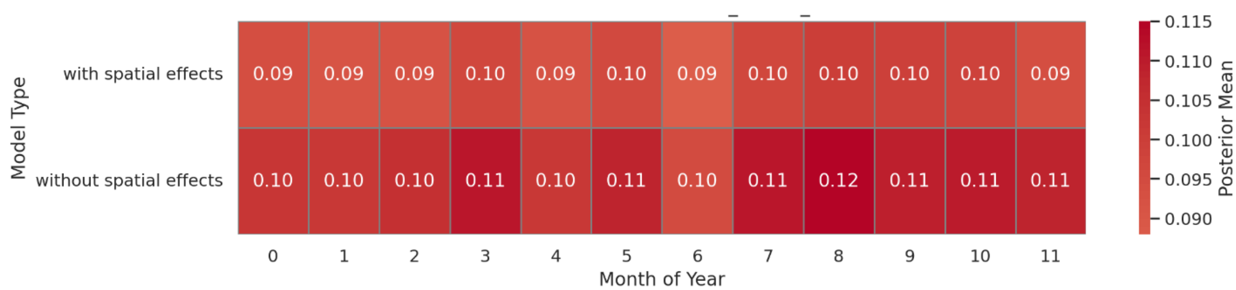

(c) Month-of-year effects

Figure 5.11 Posterior means of temporal indicators for E_cluster 2, with and without spatial effects

- **Posterior Predictive Checks (PPC)**

To evaluate the adequacy and reliability of the Bayesian dynamic panel models, both spatial and non-spatial, posterior predictive checks (PPC) were systematically performed across all 15 identified clusters. The PPC results demonstrated that the models effectively replicated key statistical features of the occupancy distribution, including the peak density location, overall dispersion, and uncertainty bounds.

Figure 5.12 presents the posterior predictive check (PPC) for E_cluster 2. The plot compares the distribution of the observed occupancy data (black curve) with the distribution of occupancy values simulated from the fitted spatial DBTS model (blue curve), along with the posterior predictive mean (orange dashed curve). The sharp peak near zero in the observed distribution reflects the frequent low-occupancy periods characteristic of these facilities, while the posterior predictive distribution closely tracks this pattern, indicating that the model successfully reproduces both the central tendency and the overall shape of the empirical data. The close alignment between the observed density and the posterior predictive densities demonstrates good model fit and suggests that the model captures the dominant features of occupancy dynamics for this cluster.

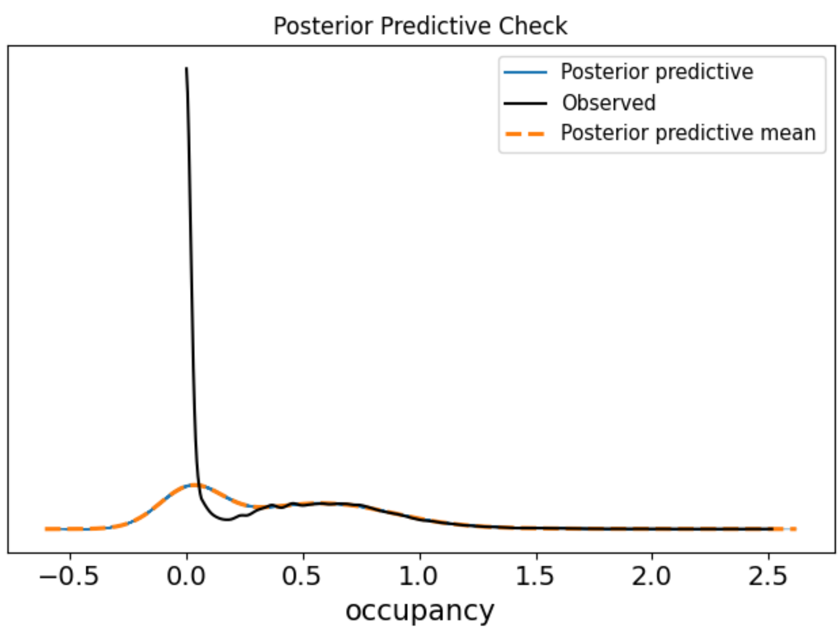

Figure 5.12 Posterior predictive density for E_cluster_2 under the spatial model

Beyond overall fit, the spatial model produced sharper posterior predictive densities and better uncertainty calibration compared with its non-spatial counterpart. This improvement highlights the analytical value of explicitly modeling spatial dependence when capturing localized patterns of parking demand.

Despite these strengths, a recurring challenge across all clusters was the systematic underestimation of the sharp spike observed at zero occupancy. This pronounced spike, driven by the high prevalence of zero values in the empirical distribution, was only partially recovered in the posterior predictions, particularly in the non-spatial model. However, the spatial model exhibited a notable improvement in approximating these zero-inflation dynamics: in E_cluster 2, more than 72% of time intervals with true zero occupancy were predicted with values below 0.1. In contrast, the corresponding coverage in the non-spatial model was approximately 65%.

These results underscore that while exact replication of observed zeros remains difficult, especially under limited information and data sparsity, the spatial Bayesian model consistently produced near-zero predictive values that are operationally sufficient for planning and decision-making purposes.

- **Predictive Accuracy**

Building upon the time-series evaluation discussed earlier, the same predictive accuracy metrics were extended to the panel context. Table 5.8 presents a comprehensive comparison of the spatial and non-spatial Bayesian panel models across all 15 clusters. Spatial models consistently yielded lower RMSE values and higher R^2 values across all clusters. Additionally 12 out of the 15 clusters resulted in fewer or equal numbers of divergent transitions, indicating improved numerical stability and smoother posterior geometry when spatial dependencies were modeled.

Table 5.8 Comparison of predictive accuracy and sampling stability between spatial and non-spatial Bayesian panel models

Cluster	RMSE (Spatial / Non-Spatial)	R^2 (Spatial / Non-Spatial)	Divergence (Spatial / Non-Spatial)
E_cluster_1	0.0545 / 0.0545	0.8524 / 0.8522	25 / 31
E_cluster_2	0.1257 / 0.1270	0.8937 / 0.8915	0 / 0
E_cluster_3	0.1502 / 0.1502	0.7388 / 0.7388	29 / 32
E_cluster_4	0.1337 / 0.1337	0.7445 / 0.7442	2 / 1
E_cluster_5	0.1085 / 0.1090	0.7771 / 0.7750	18 / 30
E_cluster_6	0.1379 / 0.1381	0.7450 / 0.7445	12 / 21
E_cluster_7	0.1130 / 0.1140	0.9047 / 0.9031	0 / 2
W_cluster_1	0.0982 / 0.0985	0.8527 / 0.8520	9 / 10
W_cluster_2	0.1404 / 0.1406	0.7618 / 0.7609	13 / 7
W_cluster_3	0.1562 / 0.1564	0.7538 / 0.7531	9 / 9
W_cluster_4	0.1390 / 0.1392	0.7687 / 0.7680	0 / 0
W_cluster_5	0.1117 / 0.1127	0.8621 / 0.8595	16 / 13
W_cluster_6	0.1570 / 0.1571	0.7318 / 0.7316	6 / 7
W_cluster_7	0.1018 / 0.1020	0.8172 / 0.8164	5 / 11
W_cluster_8	0.1942 / 0.1943	0.6600 / 0.6595	9 / 26

While the numerical differences in some clusters appear minor, the consistently improved RMSE and R^2 values, alongside reduced or equal divergent transitions in 12 clusters, reinforce the value of modeling spatial interactions between nearby parking facilities. These enhancements not only boost predictive accuracy but also improve computational robustness and sampling efficiency.

To ensure the statistical reliability of these results, convergence diagnostics and posterior quality metrics were thoroughly examined. All models satisfied key Bayesian standards: $\hat{R}$ values less than 1.01, effective sample sizes above 400, and Monte Carlo standard errors were sufficiently small relative to posterior uncertainty. These indicators confirm the robustness and reliability of the estimated posterior distributions.

- **Model Fit Evaluation Using WAIC and LOO**

To evaluate relative model performance and generalization capability, the spatial and non-spatial Bayesian panel models were compared using two widely accepted Bayesian criteria: the Widely Applicable Information Criterion (WAIC) and Leave-One-Out Cross-Validation (LOO-CV). Table 5.9 summarizes the results for both spatial and non-spatial specifications across the fifteen clusters.

Table 5.9 WAIC and LOO Metrics for Bayesian Panel Models (With vs. Without Spatial Effects)

Cluster	**$elpd_{WAIC}$ (Spatial / Non-Spatial)**	**p_{WAIC} (Spatial / Non-Spatial)**	**$elpd_{LOO}$ (Spatial / Non-Spatial)**	**p_{LOO} (Spatial / Non-Spatial)**
E_cluster 1	26053.14 / 26044.45	67.29 / 63.76	26053.08 / 26044.43	67.35 / 63.77
E_cluster 2	34344.68 / 33805.20	79.22 / 72.04	34344.66 / 33805.15	79.24 / 72.09
E_cluster 3	8296.27 / 8298.55	65.44 / 62.92	8296.24 / 8298.52	65.47 / 62.95
E_cluster 4	15535.51 / 15525.82	67.08 / 63.68	15535.50 / 15525.79	67.08 / 63.71
E_cluster 5	21016.74 / 20896.79	73.86 / 70.65	21016.68 / 20896.73	73.91 / 70.71
E_cluster 6	9793.18 / 9775.71	62.49 / 60.87	9793.18 / 9775.68	62.49 / 60.90
E_cluster 7	26606.82 / 26322.95	77.22 / 72.72	26606.79 / 26322.99	77.25 / 72.68
W_cluster 1	23625.44 / 23565.48	76.02 / 72.84	23625.45 / 23565.56	76.01 / 72.75
W_cluster 2	14245.69 / 14197.59	77.07 / 72.40	14245.65 / 14197.59	77.10 / 72.40
W_cluster 3	11441.44 / 11408.48	71.65 / 67.88	11441.38 / 11408.49	71.71 / 67.87
W_cluster 4	48495.26 / 48374.92	87.95 / 76.52	48495.22 / 48374.87	87.99 / 76.57
W_cluster 5	13485.47 / 13325.66	62.73 / 60.62	13485.41 / 13325.69	62.79 / 60.59
W_cluster 6	7521.80 / 7520.11	63.59 / 60.53	7521.78 / 7520.10	63.61 / 60.53
W_cluster 7	15111.23 / 15074.81	71.34 / 68.61	15111.29 / 15074.82	71.28 / 68.61
W_cluster 8	3800.04 / 3787.52	60.68 / 59.15	3800.02 / 3787.49	60.70 / 59.17

Across 14 of the 15 clusters, spatial models achieved higher $elpd_{WAIC}$ and $elpd_{LOO}$ values, signaling improved predictive performance on held-out data. Notably, the largest performance gains were observed in clusters with known spatial heterogeneity, such as E_cluster

2, E_cluster 7, and W_cluster 4. In contrast, E_cluster 3 is the only case where the spatial model slightly underperforms the non-spatial one, suggesting minimal spatial dependence within that cluster.

Importantly, the effective number of parameters (p_{WAIC} and p_{LOO}), which reflect model complexity, remained stable between the spatial and non-spatial variants. This indicates that the performance gains of the spatial model were not due to overfitting or excessive flexibility. In fact, in multiple clusters (e.g., W_cluster 6, E_cluster 1), the spatial models achieved better predictive accuracy with fewer or equal effective parameters, highlighting both their efficiency and parsimony.

Collectively, these results validate the inclusion of spatial effects in panel-based modeling frameworks. The consistent, albeit sometimes modest, improvements in predictive fit support the hypothesis that incorporating facility-level geographic interactions leads to more generalizable and robust models. These findings complement the RMSE and R^2 results discussed earlier and reinforce the spatial model's suitability for spatiotemporal forecasting of truck parking occupancy.

5.3.2.2 Forecasting Application

As in the case with Dynamic Bayesian Time Series models, the dynamic Bayesian panel models can also be used for short-term forecasting of occupancy levels of clustered facilities. In most clusters, the model produced well-calibrated point forecasts with narrow credible intervals, reflecting its effectiveness in capturing near-term demand fluctuations under varying traffic and temporal conditions. As an illustration, in E_cluster 6, which includes two adjacent facilities, Pu_E08 and Pr_E15, the model accurately reproduced hourly occupancy variations by incorporating historical observations and facility-specific characteristics. The final predictive equation for this cluster, based on posterior mean estimates, is presented below:

$$
\begin{aligned}
&y_{1t} \sim \mathcal{N}(\mu_{1t}, \sigma^2) \\
\mu_{1t} \; = \; & 0.26 + [0.08, 0.09, 0.10, 0.09, 0.08, 0.08, 0.07, 0.06, 0.06, 0.06, 0.04, 0.02, \text{-}0.01 \\
& -0.03, -0.04, -0.03, -0.03, -0.01, 0.00, 0.02, 0.03, 0.03, 0.04, 0.05]^T \gamma_{h(t)} \\
& + [0.13, 0.13, 0.12, 0.12, 0.12, 0.13, 0.13]^T \delta_{d(t)} \\
& + [0.08, 0.07, 0.06, 0.08, 0.06, 0.06, 0.06, 0.07, 0.06, 0.07, 0.06, 0.07]^T \eta_{m(t)} \\
& + 0.22\, y_{1,t-1} - 0.01 SL_{1t} \; + \; 0.02\, V_{1t} \; - \; 0.00\, S_{1t} \; + \; 0.01\, H_{1t} \; + \; 0.00\, R_{1t}
\end{aligned}
\tag{5.2}
$$

$$
\begin{aligned}
&y_{2t} \sim \mathcal{N}(\mu_{2t}, \sigma^2) \\
\mu_{1t} \; = \; & 0.26 + [0.08, 0.09, 0.10, 0.09, 0.08, 0.08, 0.07, 0.06, 0.06, 0.06, 0.04, 0.02, \text{-}0.01 \\
& -0.03, -0.04, -0.03, -0.03, -0.01, 0.00, 0.02, 0.03, 0.03, 0.04, 0.05]^T \gamma_{h(t)} \\
& + [0.13, 0.13, 0.12, 0.12, 0.12, 0.13, 0.13]^T \delta_{d(t)} \\
& + [0.08, 0.07, 0.06, 0.08, 0.06, 0.06, 0.06, 0.07, 0.06, 0.07, 0.06, 0.07]^T \eta_{m(t)} \\
& + 0.22\, y_{2,t-1} + 0.02 SL_{2t} \; + \; 0.02\, V_{2t} \; - \; 0.00\, S_{2t} \; + \; 0.01\, H_{2t} \; + \; 0.00\, R_{2t}
\end{aligned}
\tag{5.3}
$$

where y_{1t} and y_{2t} denote the hourly parking occupancy rates at facilities 1 and 2, respectively, and μ_{1t} and μ_{2t} are their corresponding conditional means under the Normal likelihood with common variance σ^2. The vectors $\gamma_{h(t)}$, $\delta_{d(t)}$, and $\eta_{m(t)}$ represent the hour-of-day, day-of-week, and month-of-year effects selected by the temporal index at time t. The terms $y_{1,t-1}$ and $y_{2,t-1}$ are the lagged occupancies capturing autoregressive persistence at each facility, while SL_{1t} and SL_{2t} are the spatial lags of occupancy, defined as weighted averages of neighboring-facility occupancies within the 19-mile interaction range. The variables V_{1t} and V_{2t} denote upstream hourly truck volumes, S_{1t} and S_{2t} are the corresponding average upstream speeds, H_{1t} and H_{2t}

are holiday indicators (1 on federal holidays, 0 otherwise), and R_{1t} and R_{2t} are road-closure indicators (1 when flow drops below 50 trucks per hour due to weather or operational disruptions, 0 otherwise).

5.4 Undesignated Truck Parking During Inclement Weather (Objective 4)

Table 5.10 provides a summary of undesignated truck parking events along the I-80 corridor in 2022, categorized by type of location. As described in the Methods chapter, these estimates are derived from GPS records and adjusted using expansion factors. Recall that undesignated parking refers to any stop occurring outside truck parking facilities and only includes reconstructed stop intervals with durations between 1 and 24 hours.

Across the full year, a total of 223,181 undesignated parking events were recorded. Among these, the vast majority occurred in off-network locations, accounting for over 214,000 events (96.0%), while ramps represented the second-largest category with nearly 7,482 events (3.4%). Parking on shoulders and entry/exit areas was relatively smaller, with 1,087 (0.5%) and 443 (0.2%) events, respectively.

During periods of severe weather conditions defined operationally by NDOT as documented events of heavy snowfall, blowing snow, freezing rain, or high winds reported in the ATR daily reports for specific highway segments and time intervals, often accompanied by reduced traffic volumes, hazardous surface conditions, and, in some cases, temporary road closures, 5,166 undesignated parking events were identified. Among this, off-network parking dominated, with 4,823 events (93.4%), while ramps accounted for 268 events (5.2%). Shoulders and entry/exit areas were relatively fewer, with 71 (1.4%) and 4 (0.1%) events, respectively. This breakdown indicates that while undesignated parking occurred in multiple types of locations, off-network locations were consistently the most common setting, both under normal and adverse weather conditions.

Table 5.10 Undesignated Truck Parking Events along the I-80 Corridor by Parking Type (2022)

Scope	Parking Type	Number of Undesignated Parking Events
All Year	All Types	223,181
	Entry/Exit Areas	443
	Off-Network Locations	214,169
	Ramps	7,482
	Shoulders	1,087
Severe Weather Conditions	All Types	5,166
	Entry/Exit Areas	4
	Off-Network Locations	4,823
	Ramps	268
	Shoulders	71

To further examine the spatial distribution of undesignated truck parking during severe weather conditions, a clustering analysis was conducted using DBSCAN. The resulting hotspots are presented in Figure 5.13, where marker size reflects the relative share of total events and color intensity represents the local density of undesignated stops within each hotspot (i.e., darker colors correspond to areas where trucks stopped more frequently).

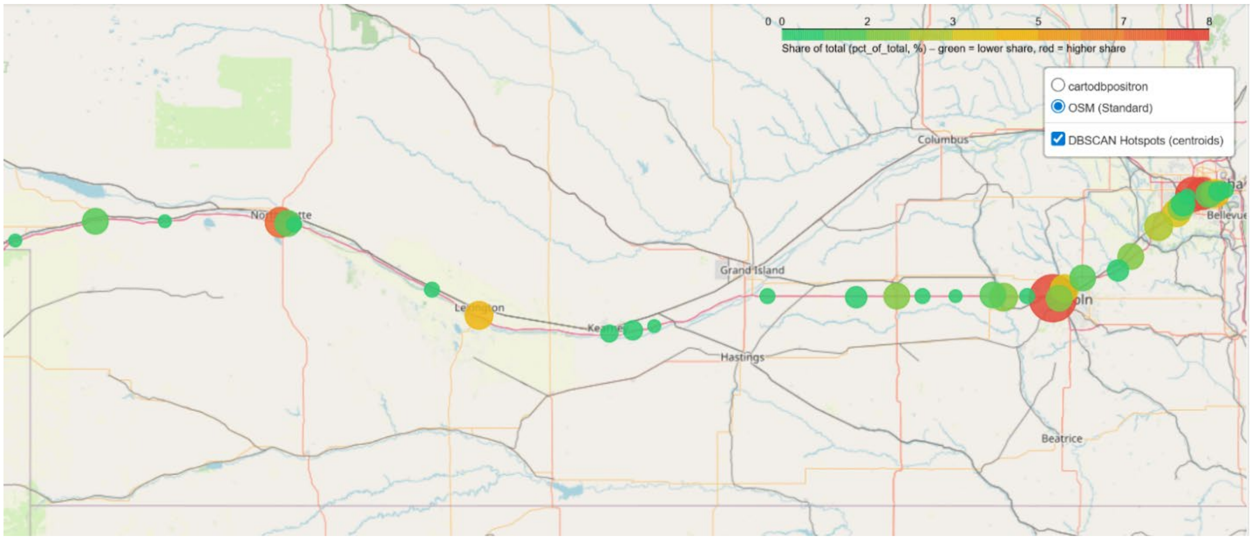

Figure 5.13 DBSCAN Hotspots of Undesignated Truck Parking during Severe Weather along the I-80 Corridor (2022)

A complete summary of all clusters is provided in Table 5.11, ordered by share of total events, including the number of parking occurrences, average and median parking duration, and the geographic centroid of each cluster.

Table 5.11 DBSCAN Hotspots of Undesignated Parking during Severe Weather (2022), Ordered by Share of Total

Rank	Region ID	Approx. Location	Number of Parking Events	% of Total	Avg. Duration (min)	Median Duration (min)
1	3	Lincoln – Central	1,273	25.9%	263	165
2	5	Lincoln – East	596	12.1%	167	105
3	20	Omaha – Central	382	7.8%	159	101
4	1	North Platte	356	7.2%	141	120
5	0	Kearney Corridor	215	4.4%	194	117
6	15	Omaha – West	212	4.3%	136	104
7	14	Lincoln – Northwest	193	3.9%	215	134
8	18	Lincoln – South Suburb	181	3.7%	135	95

9	13	Lincoln – Southwest	143	2.9%	194	124
10	7	Sidney – Central	125	2.6%	245	91
11	21	York – Central	125	2.5%	185	122
12	4	Grand Island	111	2.3%	155	92
13	22	Lincoln – Northeast	96	1.9%	130	116
14	9	Seward	93	1.9%	214	110
15	8	Lincoln – West	93	1.9%	167	94
16	23	Ogallala – Central	71	1.4%	270	119
17	29	North Platte – West	69	1.4%	260	204
18	10	Omaha – East	59	1.2%	102	81
19	11	Lincoln – Southeast	59	1.2%	182	148
20	25	York Corridor	55	1.1%	165	129
21	24	Lincoln – West Suburb	48	1.0%	166	140
22	28	Lincoln – Far Southwest	44	0.9%	250	148
23	12	York – West	39	0.8%	205	88
24	32	Hastings – Central	32	0.7%	193	98
25	17	Omaha – Corridor	30	0.6%	113	120
26	37	Kearney – West	22	0.5%	71	69
27	26	Lincoln – Far West	19	0.4%	142	129
28	34	Lincoln – North	19	0.4%	271	258
29	16	Omaha – North	19	0.4%	85	75
30	2	Hastings – East	18	0.4%	224	168
31	6	North Platte – East	17	0.3%	495	548
32	27	Lexington	16	0.3%	277	296
33	19	York – Far West	15	0.3%	134	142
34	38	Western Nebraska	13	0.3%	98	98
35	36	Sidney – West	13	0.3%	212	212
36	31	Ogallala – West	13	0.3%	285	105
37	33	Wyoming Border	13	0.3%	123	123
38	30	Hastings – West	12	0.2%	396	415
39	35	York – South	11	0.2%	145	145

The results indicate that undesignated parking during inclement weather was concentrated in five primary clusters. The largest hotspot (Region 3) is located around Lincoln and accounts for 1,273 events, or 25.9% of the total, with an average parking duration of 263 minutes. Other notable clusters were identified east of Lincoln (Region 5: 596 events, 12.1%) and within the Omaha metropolitan area (Region 20: 382 events, 7.8%). In central Nebraska, clusters were observed near North Platte (Region 1: 356 events, 7.2%) and in Kearney (Region 0: 215 events, 4.4%).

Together, these five clusters represented nearly 60% of all undesignated parking events during severe weather conditions. Other clusters, while individually smaller (each contributing less than 4%), were distributed along the corridor, particularly west of Lincoln (Regions 14, 15, and 18), as well as in areas near Grand Island, Lexington, and Ogallala. Median parking durations across most clusters exceeded 100 minutes, with some regions (e.g., Regions 23 and 29) showing median durations above 200 minutes, indicating that drivers often remained stopped for extended periods until conditions improved.

These findings highlight that during severe weather; drivers most frequently resorted to undesignated parking near major urban centers such as Lincoln and Omaha and along central corridor locations including North Platte and Kearney. In contrast, the western portion of the corridor exhibited fewer but still notable smaller clusters.

5.5 Impact of Truck Parking on Truck Crashes (Objective 5)

Table 5.12 provides a summary of truck-involved crashes along the I-80 corridor in 2022 that occurred within parking facilities and within a 10-mile downstream buffer of each facility. The table also reports the total number of truck-involved crashes, and distribution by travel direction.

Table 5.12 Truck-Involved Crashes along I-80 (2022)

Category	Number of Crashes
Within Parking Facilities – Public	26
Within Parking Facilities – Private	12
Total Within Parking Facilities	38
Within 10 Miles Downstream of Facilities	795
Total Number of Truck-Involved Crashes	1610
Eastbound Direction	808
Westbound Direction	802

Figure 5.14 illustrates the spatial distribution of crash rates along the I-80 corridor, computed by dividing the number of crashes occurring within each ATR's influence area by the total number of trucks recorded at that ATR and scaling the result per 100,000 trucks. Although crashes occurred throughout the length of I-80, several locations exhibited notably elevated crash rates. The highest concentration was found in the eastern portion of the state, between Omaha and Lincoln, where a crash rate exceeding 26.83 per 100,000 trucks was observed. In central Nebraska, comparatively dense clusters were identified near North Platte (11.06), Sidney (9.19), and Lexington (8.01), indicating localized segments of increased crash risk along the corridor.

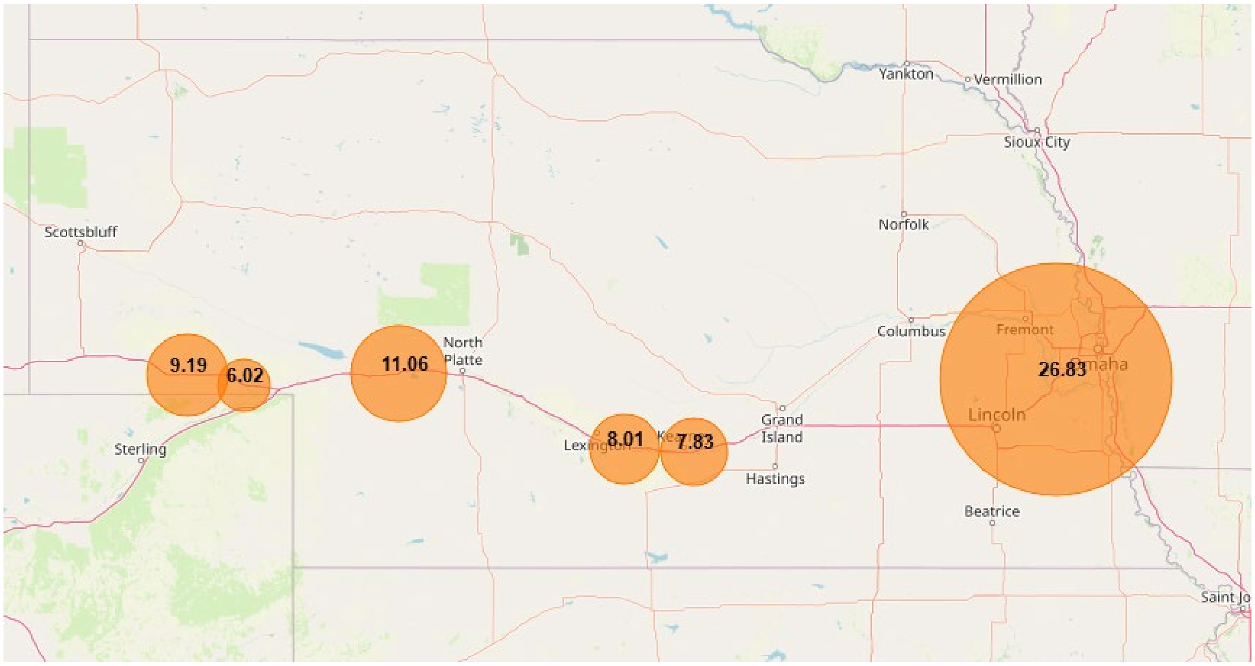

Figure 5.14 Spatial distribution of truck-involved crash rates along the I-80 corridor in 2022

To assess the association between truck parking occupancy and truck-involved crashes, two approaches were considered. The first examined whether crashes within a 10-mile downstream buffer were statistically associated with the full parking occupancy status of the upstream facility at the corresponding hour. The second broadened the spatial scope by considering crashes occurring between two consecutive facilities. Given the rarity of crashes relative to the total number of hourly observations, a matched-sample approach was employed to ensure balanced representation across crash and non-crash hours. The final dataset comprises 1,356 hourly instances, 226 with at least one crash and 1,130 randomly selected non-crash hours, enabling stable estimation of crash likelihood as a function of upstream parking conditions. Using this matched dataset, a series of correlation analyses were performed to examine potential associations between parking conditions and observed truck-involved crashes, considering both binary and continuous data representations.

5.5.1 Relationship between Truck Parking Occupancy and Crashes within 10 Miles Downstream

First, a chi-square test of independence was performed between two binary variables: CrashBinary (indicating whether at least one crash occurred during a given hour) and OccupancyFull (indicating whether the parking facility was at or above capacity). The test yielded a phi coefficient of 0.000 and a p-value of 1.000, suggesting no statistical association between full occupancy and crash occurrence. In other words, crash incidence appears unrelated to whether the corresponding upstream facility was at capacity.

To validate this result, a more robust method for binary classification problems was utilized, the Matthews correlation coefficient (MCC). The MCC was nearly zero (-1.4×10^{-5}), reinforcing the lack of a systematic relationship between crash occurrence and parking status.

Finally, a Spearman rank-order correlation was computed to assess the association between the continuous occupancy rate and crash count. The coefficient was -1.3×10^{-5} with a p-value of 0.993, again indicating no statistically meaningful monotonic relationship.

Collectively, these findings consistently indicate an absence of any substantive correlation between truck parking occupancy and downstream truck-involved crashes. A summary of the statistical results is provided in Table 5.13.

Table 5.13 Correlation Measures between Parking Occupancy and Truck-Involved Crashes Within 10 Miles Downstream

Measure	Coefficient Value	p-value
Phi Coefficient	0.0000	1.000
Matthews Correlation Coefficient	-0.000014	—
Spearman Correlation	-0.000013	0.993

To further verify this relationship, a penalized logistic regression model was estimated using the full set of hourly observations. The outcome variable was CrashBinary, and the sole explanatory variable was the binary indicator OccupancyFull, capturing whether a facility was at or above capacity. This approach enables estimation of the effect of occupancy status on crash likelihood while accounting for rare-event bias and potential overfitting.

As shown in Table 5.14, the coefficient for OccupancyFull was negative but statistically insignificant ($p = 0.993$), implying no evidence that full facilities are associated with higher downstream crash risk. The corresponding odds ratio of 0.997, with a 95% confidence interval ranging from 0.49 to 2.02, reinforces this conclusion. An odds ratio close to 1 indicates that the likelihood of a truck-involved crash is nearly the same regardless of whether the upstream parking facility was full or not. Taking together with the preceding correlation tests, the regression results provide consistent evidence that, at an hourly level, upstream parking occupancy status is not associated with truck-involved crashes within 10 miles downstream of the facility.

Table 5.14 Penalized Logistic Regression Results for 10-Mile Downstream Scenario

Variable	**Coefficient**	**Std. Error**	**z**	**p-value**	**Odds Ratio**	**95% CI (Lower)**	**95% CI (Upper)**
Constant	-7.4853	0.068	-110.49	0.000	0.0006	0.0005	0.0006
OccupancyFull	-0.0032	0.360	-0.009	0.993	0.997	0.492	2.019

5.5.2 Relationship between Truck Parking Occupancy and Crashes Between Two Consecutive Facilities

To investigate whether truck parking shortages are associated with truck-involved crashes immediately beyond the 10-mile downstream buffer, the analysis is repeated to consider crashes between two consecutive facilities. This expanded spatial lens allows for a more comprehensive understanding of how upstream parking shortages may impact crashes across longer distances.

Due to the extreme imbalance in the original dataset, where truck-involved crashes occurred in only 417 of over 403,000 hourly inter-facility observations, a matched-sample strategy was again adopted. All 417 crash hours were retained, and 2,085 non-crash hours were randomly selected to construct a balanced dataset of 2,502 hourly instances. This approach improves the stability and interpretability of the subsequent statistical models.

First, a chi-square test of independence was performed between two binary indicators: CrashBinary (denoting whether at least one crash occurred during a given hour) and OccupancyFull (indicating whether the upstream facility was at or above capacity). The test yielded a phi coefficient of 0.0007 with a p-value of 0.654, providing no statistical evidence of association between full occupancy and downstream crash occurrence.

Next, the Matthews Correlation Coefficient (MCC) was calculated to validate the binary relationship. The MCC value was 0.0009, further reinforcing the absence of any systematic connection between occupancy status and crash outcomes.

Finally, a Spearman rank-order correlation was computed to examine the potential monotonic relationship between the continuous occupancy rate and the crash count. The resulting coefficient was 0.0009 ($p = 0.561$), indicating no statistically significant monotonic trend.

Collectively, these findings consistently indicate an absence of any substantive correlation between truck parking occupancy and downstream truck-involved crashes. A summary of the statistical results is provided in Table 5.15.

Table 5.15 Correlation Measures between Parking Occupancy and Truck-Involved Crashes Between Two Consecutive Facilities

Measure	Coefficient	p-value
Phi Coefficient	0.0007	0.654
Matthews Correlation Coefficient	0.0009	—
Spearman Correlation	0.0009	0.561

A penalized logistic regression model was also estimated using the full hourly dataset, including 417 crash events and over 400,000 non-crash instances. The binary dependent variable (CrashBinary) captured the presence of one or more crashes during a given hour, while the key independent variable was the binary indicator OccupancyFull. Despite the large sample size, the model yielded a log-likelihood of –3282.9 with a pseudo-R^2 of 0.000049, indicating negligible explanatory power.

As shown in Table 5.16, the coefficient for OccupancyFull was positive but not statistically significant ($p = 0.562$), with a 95% confidence interval that spans both sides of zero. The estimated odds ratio of 1.15 [0.71, 1.88] suggests a weak and imprecise association.

Table 5.16 Penalized Logistic Regression Results for Between Facilities Scenarios

Variable	Coefficient	Std. Error	z	p-value	Odds Ratio	95% CI (Lower)	95% CI (Upper)
Constant	-6.8779	0.050	-137.490	0.000	0.0006	0.0005	0.0006
OccupancyFull	0.1438	0.248	0.580	0.562	1.1546	0.7105	1.8765

As is the case when considering only up to 10 miles downstream, the correlation tests and regression results provide consistent evidence that, at an hourly level, upstream parking occupancy status is not associated with truck-involved crashes between two consecutive parking facilities.

Chapter 6 Conclusions and Recommendations

6.1 Conclusions

The inventory developed under Objective 1 identified 66 truck parking facilities within a one-mile buffer (0.5 mile on each side) along Nebraska's I-80 corridor, comprising 20 public and 46 private facilities. The findings highlight the dominant role of private facilities in providing parking capacity and amenities, complemented by a network of public rest areas that support essential safety and regulatory functions. This inventory provides a comprehensive baseline of truck parking supply along I-80 and serves as a foundation for subsequent analyses of parking demand, utilization, and safety outcomes. It also offers NDOT and its partners an up-to-date reference for planning and prioritizing future truck parking improvements.

The spatiotemporal analysis conducted under Objective 2 revealed clear geographic and temporal patterns of truck parking demand along Nebraska's I-80 corridor between 2010 and 2022. Public rest areas near Omaha (Pu_E06, Pu_E07, Pu_E08, and Pu_E09) consistently exhibited high occupancy rates, reflecting the influence of proximity to major freight and population centers. Similarly, westbound facilities Pu_W01 and Pu_W02 in western Nebraska and Pu_W06 in central Nebraska frequently operated at or above capacity, likely due to the extensive amenities they provide. Private facilities also demonstrated sustained high occupancy in several eastbound locations (Pr_E05, Pr_E06, Pr_E07, and Pr_E15). These findings point to localized shortages and suggest that targeted investments, capacity expansion, and improved utilization of existing sites are needed. The results provide NDOT with a data-driven basis for prioritizing truck parking improvements and coordinating with private partners to enhance safety and freight efficiency along I-80.

The modeling conducted under Objective 3 applied a Dynamic Bayesian framework to predict hourly truck parking occupancy. The framework simultaneously captures temporal and spatial dependencies among nearby facilities. Facilities were analyzed either individually or in clusters if they are located within 19 miles of each other. For single facilities, Dynamic Bayesian Time Series models were utilized, and for the clustered facilities, Dynamic Bayesian Panel models with time fixed effects and distance-based spatial lags were utilized. For both types of models, the lagged occupancy variable consistently emerged as the most influential predictor of current occupancy, while truck volume showed positive and statistically significant effects in most clusters. Variables such as speed and holiday indicators exhibited weaker or less consistent effects. Incorporating spatial effects substantially improved model performance: across all spatial models, $RMSE$ values ranged from 0.054 to 0.274, indicating lower prediction error, and corresponding R^2 values ranged from 0.66 to 0.89. These results confirm that truck parking occupancy follows predictable temporal cycles and exhibits spatial spillover effects to nearby facilities. Overall, the proposed models successfully reproduced key temporal dynamics and high-demand peaks, demonstrating strong operational applicability for real-time forecasting and corridor-level demand management.

The analysis conducted under Objective 4 examined undesignated parking behavior during road closures and severe weather events using DBSCAN-based clustering of truck GPS data. Four primary areas of undesignated parking were identified: entry and exit areas of facilities, off-road sites, ramps, and highway shoulders. These areas were concentrated near Omaha, Lincoln, and central Nebraska, where there is limited parking capacity and high truck volumes. As expected, severe weather events force drivers to park in undesignated or unsafe locations. These findings suggest the need for adaptive management strategies, such as temporary staging areas, real-time parking and weather information systems, and coordination with local enforcement, to support CMV drivers during disruptive weather events.

The analysis conducted under Objective 5 tested the hypothesis that truck parking shortages are associated with a higher likelihood of truck-involved crashes. Correlation analyses did not reveal a significant relationship between parking occupancy levels and crash frequency within ten miles downstream of a facility or between adjacent facilities along the I-80 corridor. Similar results were obtained from the regression analysis. This outcome is likely influenced by data limitations, as the analysis relied on parking estimates derived from GPS-based sampling and expansion factors rather than direct measurements of actual parking demand. A more accurate assessment would be possible with detailed, sensor-based parking utilization data.

6.2 Recommendations

To address persistent truck parking shortages along Nebraska's I-80 corridor, several coordinated policy and planning actions are recommended.

6.2.1 Strengthening Public–Private Coordination

The inventory underscores a structural imbalance in the corridor's parking infrastructure: many public rest areas maintain a small footprint, often fewer than 20 spaces, which effectively shifts the primary burden of capacity to private operators. Given that private facilities already provide the majority of parking capacity along the corridor, NDOT may consider strengthening public–private coordination strategies to ensure long-term alignment between freight demand and parking supply. NDOT is already pursuing this direction through public–private partnerships (PPPs) and locally led initiatives to better support the state's freight strategy. Continued collaboration among NDOT, local governments, private operators, and community stakeholders is essential to identify feasible expansion sites and determine appropriate facility scale. Providing data, technical support, and forecasting tools to private stakeholders could enable more informed investment decisions and enhance corridor-wide efficiency.

6.2.2 Targeted Capacity Expansion Strategy

Targeted expansion should be prioritized in locations exhibiting sustained high occupancy, particularly in the Omaha and Lincoln regions. A useful framework for communicating this strategy to stakeholders is the "busy lung" analogy developed during this research. Adding targeted capacity in congested nodes like Omaha and Lincoln can relieve pressure across the broader corridor network rather than requiring system-wide investment. NDOT is exploring how this targeted approach can guide long-term infrastructure and freight efficiency goals. In western and central Nebraska, including the Pu_W01, Pu_W02, and Pu_W06 areas, selective investments may also help mitigate recurring capacity constraints.

6.2.3 Managing Undesignated Parking During Disruptions

The analysis shows that a substantial proportion of undesignated parking during severe weather occurs in large commercial parking lots. This suggests that drivers rely on these locations as informal staging areas during I-80 closures. NDOT may consider evaluating the feasibility of voluntary coordination agreements with major retailers in high-demand areas to formalize temporary staging use and reduce unsafe shoulder and ramp parking during disruptive events.

Based on the hotspot analysis from Objective 4, priority consideration should be given to the most severe undesignated parking clusters, particularly the Lincoln–Central, Lincoln–East, Omaha–Central, North Platte, and Kearney areas, which together accounted for nearly 60% of all undesignated parking during severe weather. Coordination through existing planning processes and partnerships can ensure that new or upgraded facilities meet operational needs and complement local development objectives (SCAN Team 20-02 2022).

Adaptive management strategies, including temporary staging areas, real-time parking and weather information systems, and coordination with local enforcement, should be further explored to improve corridor resilience during severe weather.

6.2.4 Advancing Predictive Demand Management

The Dynamic Bayesian framework developed in this study, which achieved R^2 values as high as 0.89 and successfully captured spatial spillover effects between neighboring facilities, provides a strong methodological foundation for future demand management tools. NDOT is exploring how to integrate higher-resolution weather and roadway sensor data into this framework as such data becomes available, particularly through the Variable Speed System sensor installations currently underway along I-80. To inform this effort more broadly, NDOT could review successful PPP and technology deployment models from other states and engage peer agencies to identify cost-effective strategies suited to Nebraska's context.

6.2.5 Data Improvements to Support Future Analyses

Future NDOT-sponsored research would benefit from access to several key datasets. Direct measurements of truck parking occupancy from sensor-based or camera-assisted monitoring systems would substantially improve demand model estimation and validation. The finding from Objective 5, that parking occupancy levels were not statistically associated with crash frequency, is a meaningful contribution that challenges common anecdotal assumptions about the relationship between full parking facilities and crash risk. However, this result is likely influenced by the reliance on GPS-based occupancy estimates rather than observed data, and a more accurate assessment would be possible with sensor-based utilization records. Continuous hours-of-driving information would also be essential for more robust safety analyses. Understanding how long drivers have been operating before reaching a facility, and how close they are to their Hours-of-

Service (HOS) limits, would allow NDOT to assess whether parking shortages disproportionately affect fatigued drivers and may reveal more nuanced safety impacts that the current dataset could not detect. Such data is not available in the current ATRI GPS dataset, which provides location, speed, and timestamps but does not include electronic logging device (ELD) records. Finally, access to higher-resolution weather and environmental data, such as roadway surface temperature, precipitation type, visibility, and friction factors, would enable analysis of intermediate conditions rather than just the extremes of "normal" and "severe." Ensuring that researchers have access to sensor data from the Variable Speed System installations, either in real time or archived form, would greatly enhance future analytical capabilities.

References

Anastasopoulos, Panagiotis Ch., and Fred L. Mannering. 2011. "An Empirical Assessment of Fixed and Random Parameter Logit Models Using Crash- and Non-Crash-Specific Injury Data." *Accident Analysis & Prevention* 43 (3): 1140–47. https://doi.org/10.1016/j.aap.2010.12.024.

Anderson, Jason C., Salvador Hernandez, Eric L. Jessup, and Eric North. 2018. "Perceived Safe and Adequate Truck Parking: A Random Parameters Binary Logit Analysis of Truck Driver Opinions in the Pacific Northwest." *International Journal of Transportation Science and Technology* 7 (1): 89–102. https://doi.org/10.1016/j.ijtst.2018.01.001.

ATR. 2023. "Critical Issues in the Trucking Industry – 2023." *ATRI*, October. https://truckingresearch.org/wp-content/uploads/2023/10/ATRI-Top-Industry-Issues-2023.pdf.

Baltagi, Badi H. 2021. *Econometric Analysis of Panel Data*. Springer Texts in Business and Economics. Springer International Publishing. https://doi.org/10.1007/978-3-030-53953-5.

Betancourt, Michael. 2016. "Diagnosing Suboptimal Cotangent Disintegrations in Hamiltonian Monte Carlo." Version 1. Preprint, arXiv. https://doi.org/10.48550/ARXIV.1604.00695.

Boggs, Alexandra M., Amin Mohamadi Hezaveh, and Christopher R. Cherry. 2019. "Shortage of Commercial Vehicle Parking and Truck-Related Interstate Ramp Crashes in Tennessee." *Transportation Research Record: Journal of the Transportation Research Board* 2673 (10): 153–63. https://doi.org/10.1177/0361198119849586.

Boris, Caroline, and Rebecca M Brewster. 2016. "Managing Critical Truck Parking Case Study – Real World Insights from Truck Parking Diaries." *ATRI*, December. https://truckingresearch.org/wp-content/uploads/2016/12/ATRI-Truck-Parking-Case-Study-Insights-12-2016.pdf.

Bürkner, Paul-Christian. 2017. "Brms: An *R* Package for Bayesian Multilevel Models Using *Stan*." *Journal of Statistical Software* 80 (1). https://doi.org/10.18637/jss.v080.i01.

Crawford, F., D.P. Watling, and R.D. Connors. 2017. "A Statistical Method for Estimating Predictable Differences between Daily Traffic Flow Profiles." *Transportation Research Part B: Methodological* 95 (January): 196–213. https://doi.org/10.1016/j.trb.2016.11.004.

Ester, Martin, Hans-Peter Kriegel, Jörg Sander, and Xiaowei Xu. 1996. "A Density-Based Algorithm for Discovering Clusters in Large Spatial Databases with Noise." *In Proceedings of the Second International Conference on Knowledge Discovery and Data Mining (KDD'96)*, 226–31.

FHWA. 2020. "National Coalition on Truck Parking December 1, 2020 Presentation - FHWA Office of Operations."

https://ops.fhwa.dot.gov/Freight/infrastructure/truck_parking/coalition/2020/mtg/mtg12012020_jasons_law.htm.

Gelman, Andrew, Jennifer Hill, and Aki Vehtari. 2021. *Regression and Other Stories*. Cambridge University Press.

Haque, Khademul, Sabyasachee Mishra, Rajesh Paleti, Mihalis M. Golias, Afrid A. Sarker, and Karlis Pujats. 2017. "Truck Parking Utilization Analysis Using GPS Data." *Journal of Transportation Engineering, Part A: Systems* 143 (9): 04017045. https://doi.org/10.1061/JTEPBS.0000073.

Hoffman, Matthew D., and Andrew Gelman. 2014. "The No-U-Turn Sampler: Adaptively Setting Path Lengths in Hamiltonian Monte Carlo." *Journal of Machine Learning Research* 15 (1): 1593–623.

Hwang, Ho-Ling, Hyeonsup Lim, Shih-Miao Chin, et al. 2021. *Freight Analysis Framework Version 5 (FAF5) Base Year 2017 Data Development Technical Report*. ORNL/TM-2021/2154. Oak Ridge National Laboratory (ORNL), Oak Ridge, TN (United States). https://doi.org/10.2172/1844893.

Jr, David W. Hosmer, Stanley Lemeshow, and Rodney X. Sturdivant. 2013. *Applied Logistic Regression*. John Wiley & Sons.

King, Gary, and Langche Zeng. 2001. "Logistic Regression in Rare Events Data." *Political Analysis* 9 (2): 137–63. https://doi.org/10.1093/oxfordjournals.pan.a004868.

LeSage, James, and Robert Kelley Pace. 2009. *Introduction to Spatial Econometrics*. 0 ed. Chapman and Hall/CRC. https://doi.org/10.1201/9781420064254.

Mathew, Jijo K., Jairaj Desai, Edward D. Cox, and Darcy M. Bullock. 2024. "Application of Connected Truck Data to Evaluate Spatiotemporal Impact of Rest Area Closures on Ramp Parking." *Journal of Transportation Technologies* 14 (03): 289–307. https://doi.org/10.4236/jtts.2024.143018.

Minnesota Department of Transportation. 2019. *Minnesota Statewide Truck Parking Study: Final Report*. Technical Report. Office of Freight and Commercial Vehicle Operations, Minnesota Department of Transportation. https://www.dot.state.mn.us/ofrw/freight/PDF/truckparking/final-report.pdf.

Nebraska Department of Transportation. 2023. *Nebraska State Freight Plan*. U.S. Department of Transportation, Federal Highway Administration. https://dot.nebraska.gov/media/wjtcwygp/ne-state-freight-plan-2023-usdot-approved.pdf.

Sadek, Bassel A., Elliot W. Martin, and Susan A. Shaheen. 2020. "Forecasting Truck Parking Using Fourier Transformations." *Journal of Transportation Engineering, Part A: Systems* 146 (8): 05020006. https://doi.org/10.1061/JTEPBS.0000397.

Salvatier, John, Thomas V. Wiecki, and Christopher Fonnesbeck. 2016. “Probabilistic Programming in Python Using PyMC3.” *PeerJ Computer Science* 2 (April): e55. https://doi.org/10.7717/peerj-cs.55.

Sander, Jörg, Martin Ester, Hans-Peter Kriegel, and Xiaowei Xu. 1998. “Density-Based Clustering in Spatial Databases: The Algorithm GDBSCAN and Its Applications.” *Data Mining and Knowledge Discovery* 2 (2): 169–94. https://doi.org/10.1023/A:1009745219419.

Sasaki, Yuya, Junya Takayama, Juan Ramón Santana, Shohei Yamasaki, Tomoya Okuno, and Makoto Onizuka. 2023. “Predicting Parking Lot Availability by Graph-to-Sequence Model: A Case Study with SmartSantander.” *2023 24th IEEE International Conference on Mobile Data Management (MDM)*, July, 73–80. https://doi.org/10.1109/MDM58254.2023.00023.

SCAN Team 20-02. 2022. *Successful Approaches for Facilitating Truck Parking Accommodations Along Major Freight Corridors*. SCAN 20-02. SCAN Team Report, NCHRP Project 20-68A, Scan 20-02. National Cooperative Highway Research Program (NCHRP), Transportation Research Board (TRB). https://onlinepubs.trb.org/onlinepubs/nchrp/docs/SCAN20-02.pdf.

Shao, Wei, Yu Zhang, Pengfei Xiao, et al. 2024. “Transferrable Contextual Feature Clusters for Parking Occupancy Prediction.” *Pervasive and Mobile Computing* 97 (January): 101831. https://doi.org/10.1016/j.pmcj.2023.101831.

Slavova, Stefani, Jean Paul Sebastian Piest, and Wouter van Heeswijk. 2022. “Predicting Truck Parking Occupancy Using Machine Learning.” *Procedia Computer Science*, The 13th International Conference on Ambient Systems, Networks and Technologies (ANT) / The 5th International Conference on Emerging Data and Industry 4.0 (EDI40), vol. 201 (January): 40–47. https://doi.org/10.1016/j.procs.2022.03.008.

Vehtari, Aki, Andrew Gelman, and Jonah Gabry. 2015. “Practical Bayesian Model Evaluation Using Leave-One-out Cross-Validation and WAIC.” *arXiv Preprint* arXiv: 1507.04544. https://doi.org/10.48550/ARXIV.1507.04544.

Vehtari, Aki, Andrew Gelman, Daniel Simpson, Bob Carpenter, and Paul-Christian Bürkner. 2021. “Rank-Normalization, Folding, and Localization: An Improved Rˆ for Assessing Convergence of MCMC (with Discussion).” *Bayesian Analysis* 16 (2). https://doi.org/10.1214/20-BA1221.

Watanabe, Sumio. 2010. “Asymptotic Equivalence of Bayes Cross Validation and Widely Applicable Information Criterion in Singular Learning Theory.” *Journal of Machine Learning Research* 11: 3571–94.

Xiao, Runhua Ivan, and Miguel Jaller. 2025. “Spatial Analysis and Predictive Modeling Framework of Truck Parking and Idling Impacts on Environmental Justice Communities.” *Journal of Transport Geography* 127 (July): 104263. https://doi.org/10.1016/j.jtrangeo.2025.104263.

Yang, Hao (Frank), Ruimin Ke, Zhiyong Cui, Yinhai Wang, and Karthik Murthy. 2022. "Toward a Real-time Smart Parking Data Management and Prediction (SPDMP) System by Attributes Representation Learning." *International Journal of Intelligent Systems* 37 (8): 4437–70. https://doi.org/10.1002/int.22725.

Zhang, Weijia, Hao Liu, Yanchi Liu, Jingbo Zhou, Tong Xu, and Hui Xiong. 2022. "Semi-Supervised City-Wide Parking Availability Prediction via Hierarchical Recurrent Graph Neural Network." *IEEE Transactions on Knowledge and Data Engineering* 34 (8): 3984–96. https://doi.org/10.1109/TKDE.2020.3034140.

Zhao, Ziyao, Yi Zhang, and Yi Zhang. 2020. "A Comparative Study of Parking Occupancy Prediction Methods Considering Parking Type and Parking Scale." *Journal of Advanced Transportation* 2020 (February): 1–12. https://doi.org/10.1155/2020/5624586.

Appendix A Truck Parking Facility Attribute Tables

Table A.1 List of public truck parking facilities along I-80 in Nebraska with additional attributes

CODE	Name	Exit #	Mile Post	Available Parking Spaces	Amenities
Pu_E01	Sidney RA EB	I-80E	51	34	6 picnic shelters, 4 picnic tables, and a children's play area
Pu_W01	Sidney RA WB	I-80W	61.37	7	6 picnic shelters, 4 picnic tables, and a children's play area
Pu_EW01	Interch. 101 EB & WB	I-80E/W	101	60	No amenities available
Pu_W02	Ogallala RA WB	I-80W	132.55	7	8 picnic tables, children's play area, and a summer tourist information station
Pu_E03	Sutherland RA EB	I-80E	159.6	7	10 picnic tables, children's play area, and a summer tourist information station
Pu_W03	Sutherland RA WB	I-80W	159.94	7	7 picnic tables, children's play area, and a summer tourist information station
Pu_W04	Brady RA WB	I-80W	194	22	10 picnic shelters, children's play area, and a summer tourist information station
Pu_E04	Brady RA EB	I-80E	194.35	18	6 picnic shelters, 4 picnic tables, children's play area, and a summer tourist information station
Pu_E05	Cozad RA EB	I-80E	226.73	7	6 picnic shelters, 4 picnic tables, and a children's play area, a family/alternate restroom, and a tourist information station

CODE	Name	Exit #	Mile Post	Available Parking Spaces	Amenities
Pu_W05	Cozad RA WB	I-80W	227.46	7	6 picnic shelters, 4 picnic tables, and a children's play area, a family/alternate restroom, and a tourist information station
Pu_E06	Kearney RA EB	I-80E	269	7	5 picnic shelters, 2 picnic tables,children's play area, a family/alternate restroom, and a tourist information station
Pu_W06	Kearney RA WB	I-80W	270.94	7	6 picnic shelters, 4 picnic tables,children's play area, a family/alternate restroom, and a tourist information station.
Pu_EW02	Grand Island RA EB	I-80E	314.93	7	7 picnic shelters, 2 picnic tables, children's play area, a family/alternate restroom, and a summer tourist information station
Pu_EW02B	Grand Island RA WB	I-80W	316.52	7	7 picnic shelters, 2 picnic tables, a family/alternate restroom, and a summer tourist information station
Pu_E07	York RA EB	I-80E	350.8	8	6 picnic shelters, 4 picnic tables, children's play area, a family/alternate restroom, and a summer tourist information station

CODE	Name	Exit #	Mile Post	Available Parking Spaces	Amenities
Pu_W07	York RA WB	I-80W	355.23	9	6 picnic shelters, 2 picnic tables, children's play area, a family/alternate restroom, and a summer tourist information station
Pu_W08	Goehner RA WB	I-80W	375	56	Open with all services
Pu_E08	Blue River RA EB	I-80E	381	7	8 picnic shelters, children's play area, and a family/alternate restroom
Pu_E09	Platte River RA EB	I-80E	425	16	6 picnic shelters, 6 picnic tables, children's play area, and a summer tourist information station
Pu_W09	Melia Hill RA WB	I-80W	431.6	26	9 picnic shelters, Family/alternate restroom, and a summer tourist information station

Table A.2 List of private truck parking facilities along I-80 in Nebraska with additional attributes

Code	Name	Address	Mile Marker	Available Parking Spaces	Amenities
Pr_W01	Travel Shop	1700 S Highway 71, Kimball	21.0	48	Truck Parking; Store; Self Service;
Pr_E01	Love's Travel Stop #625	645 Chase DR, Sidney	60.0	96	24 Hour Diesel, 24 Hour Fast Food, Atm, Bulk Def, Cat Scales, Cng, Convenience Store, Dat Check Cashing, Deli, Document Scanning, Dot Inspections, Dump Station, Fast Food, Lng, Love's Travel Stop, Metered Propane, Money Orders, Motel, Natso Check Link, Oil And Lube, Parking,Lighted Area, Paved Lot, Pet Area, Propane Bottles, Public Fax / Copier, Road Service, Rv Gasoline, Rv Parking, Scales - Certified, Showers, Tire Repair, Trip Pack Locations, Truck Repairs, Trucker Store, Ups Box, Western Union, Wifi
Pr_W02	Sapp Brothers Travel Center	2914 Upland PKWY, Sidney	60.0	35	24 Hour Diesel, 24 Hour Fast Food, Atm, Bulk Def, Convenience Store, Deli, Fast Food, Gift Shop, Motel, Paved Lot, Public Fax / Copier, Rv Gasoline, Rv Parking, Sapp Brothers, Showers, Trailer Drop, Trucker Store, Ups Box, Walking Trail, Wifi
Pr_W03	Truck & Travel	100 Frontage RD, Big Springs	107.5	6	24 Hour Diesel, Atm, Convenience Store, Deli, Motel, Natso Check Link, Parking,Lighted Area, Public Fax / Copier, Rv Gasoline, Rv Parking, Showers, Trucker Store, Truckers Lounge, Wifi
Pr_W05	Flying J Travel	109 Circle Rd, Big Springs	107.5	244	Truck Parking; Store; Showers; Laundromat; Lounge; Self Service;

Code	Name	Address	Mile Marker	Available Parking Spaces	Amenities
	Center #904				
Pr_E02	Happy Jack	675 Rd West F S, Brule	120.0	10	Truck Parking; Restaurant/Deli; Store; Showers; Laundromat; Self Service
Pr_E03	Travel Centers Of America	103 Prospector Dr, Ogallala	127.0	94	24 Hour Diesel, Atm, Bulk Def, Can Wire Money Out, Cat Scales, Convenience Store, Deli, Document Scanning, Dot Inspections, Fedex Box, Game Room, Laundry, Money Orders, Natso Check Link, Oil And Lube, Parking,Lighted Area, Paved Lot, Pet Area, Propane Bottles, Public Fax / Copier, Receive Prepaid Permits, Religious Services - Chapel, Reserved Parking, Restaurant, Rv Gasoline, Rv Parking, Scales - Certified, Showers, Tire Repair, Trailer Drop, Travel Centers Of America, Trip Pack Locations, Truck Repairs, Trucker Store, Truckers Lounge, Western Union
Pr_E04	Fat Dogs - Ogallala	100 Prospector DR, Ogallala	127.0	15	Diesel Fueling Bays, Gasoline Fueling Bays, ATM, Convenience Store, Fast Food, RV Gasoline, WIFI, WALK-IN BEER CAVE – Wine and Spirits, Souvenirs, Men & Women's Apparel, Nebraska Collegiate Apparel
Pr_W06	Sapp Brothers	101 Stage Coach Road, Ogallala	128.0	5	Truck Parking; Store; Showers; Self Service
Pr_W07	Western Convenience Truck Stop	814 N Spur 56c, Hershey	167.0	80	24 Hour Diesel, Atm, Bulk Def, Cng, Convenience Store, Deli, Document Scanning, Gift Shop, Laundry, Parking,Lighted Area, Paved Lot, Propane Bottles, Public Fax / Copier, Receive

Code	Name	Address	Mile Marker	Available Parking Spaces	Amenities
					Prepaid Permits, Restaurant, Safe Haven / Hazmat, Scales - Certified, Showers, Trailer Drop, Truckers Lounge
Pr_E05	Fat Dogs Gulf	102 Holiday Frontage RD, North Platte	81.0	65	24 Hour Diesel, Atm, Bulk Def, Convenience Store, Deli, Document Scanning, Fast Food, Paved Lot, Public Fax / Copier, Red Diesel, Showers, Wifi
Pr_E06	Time Saver #7	3220 S Jeffers ST, North Platte	81.0	0	Fuel, Convenience Store, Fastfood
Pr_E08	Flying J Travel Plaza	3400 Newberry Rd, North Platte	179.0	123	24 Hour Diesel, 24 Hour Restaurant, Atm, Boss Shop, Bulk Def, Can Wire Money Out, Cat Scales, Convenience Store, Deli, Document Scanning, Dump Station, Fedex Box, Flying J Travel Plaza, Laundry, Metered Propane, Motel, Oil And Lube, Paved Lot, Propane Bottles, Public Fax / Copier, Reserved Parking, Restaurant, Road Service, Rv Gasoline, Rv Parking, Scales - Certified, Showers, Tire Repair, Towing, Trailer Drop, Trip Pack Locations, Truck Repairs, Truckers Lounge, Ups Box, Western Union, Wifi
Pr_E07	Love's Travel Stop #390	3211 NewberryRD, North Platte	179.0	88	24 Hour Diesel, 24 Hour Fast Food, Atm, Bulk Def, Cat Scales, Convenience Store, Dat Check Cashing, Deli, Document Scanning, Dot Inspections, Dump Station, Fast Food, Fedex Box, Love's Travel Stop, Metered Propane, Natso Check Link, Oil And Lube, Parking,Lighted Area, Paved Lot, Pet Area, Propane Bottles, Public Fax / Copier, Road Service, Rv Gasoline, Rv

Code	Name	Address	Mile Marker	Available Parking Spaces	Amenities
					Parking, Scales - Certified, Showers, Tire Repair, Trailer Drop, Trip Pack Locations, Truck Repairs, Trucker Store, Ups Box, Wifi
Pr_W08	Ranchland Convenience Store	8849 South Spur 56A, Maxwell	190.0	20	Truck Parking; Restaurant/Deli; Store; Self Service;
Pr_W09	Cubby's	416 Platte River RD, Gothenburg	211.0	30	Atm, Convenience Store, Deli, Motel, Pet Area, Public Fax / Copier, Wifi
Pr_W10	Plaza Shell	416 Platte River Rd, Gothenburg	211.0	15	Truck Parking; Store; Self Service;
Pr_W11	Cubby's	301 S Lake AVE, Gothenburg	211.0	24	24 Hour Diesel, 24 Hour Fast Food, Atm, Bulk Def, Convenience Store, Deli, Fast Food, Parking,Lighted Area, Paved Lot, Red Diesel, Showers, Trailer Drop, Wifi
Pr_W12	I - 80 Pit Stop	301 Lake Ave, Gothenburg	214.0	40	Truck Parking; Restaurant/Deli; Store; Showers; Self Service;
Pr_W14	Casey's General Store	510 S Meridian Ave, Cozad	222.0	0	Truck Parking; Restaurant/Deli; Store; Showers; Self Service;
Pr_W13	Gas N Shop	510 S Meridian AVE, Cozad	222.0	5	Convenience Store, Truck Parking
Pr_E09	Nebraska Land Tire Truck Center	3004 Plum Creek Parkway, Lexington	237.0	60	Truck parking, Restaurant, Truck repair, Diesel
Pr_W15	Ampride	2700 Plum Creek PKWY, Lexington	237.0	20	24 Hour Diesel, Atm, Convenience Store, Deli, Parking,Lighted Area, Propane Bottles, Public Fax / Copier, Trailer Drop
Pr_W16	Jay Brothers	74975 RD 444, Overton	248.0	50	Atm, Convenience Store, Parking,Lighted Area, Red Diesel, Restaurant, Rv Gasoline, Showers, Wifi

Code	Name	Address	Mile Marker	Available Parking Spaces	Amenities
Pr_W18	Bosselmans Fuel Stop	5085 Buffalo Creek Rd, Elm Creek	257.0	20	24 Hour Diesel, Atm, Bulk Def, Can Wire Money Out, Cat Scales, Convenience Store, Dat Check Cashing, Deli, Document Scanning, Fast Food, Fedex Box, Game Room, Laundry, Money Orders, Motel, Paved Lot, Pilot Travel Center, Propane Bottles, Receive Prepaid Permits, Reserved Parking, Rv Gasoline, Rv Parking, Scales - Certified, Showers, Trip Pack Locations, Trucker Store, Truckers Lounge, Western Union, Wifi
Pr_W17	Pilot Travel Center #901	5085 BUFFALO Creek RD, Elm Creek	257.0	75	Truck Parking; Restaurant/Deli; Store; Showers; Lounge; Self Service;
Pr_W19	Sapp Brothers	380 Odessa Rd, Odessa	264.0	65	Truck Parking; Restaurant/Deli; Store; Showers; Laundromat; Repair Svcs; Lounge; Towing; Self Service;
Pr_W20	Fort Kearney Trading Post - Gibbon	1730 NE 10, Gibbon	280.0	50	24 Hour Diesel, Atm, Convenience Store, Deli, Fast Food, Paved Lot, Public Fax / Copier, Receive Prepaid Permits, Rv Gasoline, Rv Parking, Trailer Drop
Pr_E10	Bosselman Fuel Stop	11775 S Nebraska Hwy 11, Wood River	300.0	10	Truck Parking; Restaurant/Deli; Store; Showers; Laundromat; Lounge; Self Service
Pr_E11	Pilot Travel Center #912	11775 S NE-11, Wood River	300.0	29	Atm, Bulk Def, Can Wire Money Out, Convenience Store, Dat Check Cashing, Deli, Document Scanning, Fast Food, Laundry, Money Orders, Natso Check Link, Paved Lot, Pilot Travel Center, Propane Bottles, Public Fax / Copier, Receive Prepaid Permits, Reserved Parking, Rv Gasoline, Rv

Code	Name	Address	Mile Marker	Available Parking Spaces	Amenities
					Parking, Showers, Subway, Trailer Drop, Trip Pack Locations, Trucker Store, Truckers Lounge, Ups Box, Western Union, Wifi
Pr_W21	Travel Centers Of America	8033 W Holling Rd, Alda	306.0	12	Truck Parking; Restaurant/Deli; Store; Showers; Laundromat; Repair Svcs; Lounge; Scales; Oil Change; Self Service;
Pr_W22	Grand Maverick Truck Stop	PO Box 337, Grand Island	306.0	82	Truck Parking; Self Service;
Pr_W24	Gas N Shop	8976 S Alda RD, Wood River	306.0	6	24 Hour Diesel, Atm, Convenience Store, Document Scanning, Parking,Lighted Area, Public Fax / Copier, Rv Gasoline, Rv Parking, Wifi
Pr_W23	Git 'N Split	8976 S Alda Rd, Wood River	306.0	6	Truck Parking; Store; Self Service;
Pr_W25	Pilot Travel Center #902 - Bosselman's	3335 W Wood River RD, Grand Island	312.0	400	Atm, Bridgestone Tires, Bulk Def, Can Wire Money Out, Cat Scales, Convenience Store, Dat Check Cashing, Deli, Document Scanning, Dump Station, Fast Food, Fedex Box, Firestone Tires, Goodyear Tires, Laundry, Metered Propane, Michelin Tires, Money Orders, Motel, Natso Check Link, Oil And Lube, Parking,Lighted Area, Paved Lot, Pilot Travel Center - Dealer, Propane Bottles, Public Fax / Copier, Receive Prepaid Permits, Religious Services - Chapel, Restaurant, Rv Gasoline, Rv Parking, Scales - Certified, Showers, Subway, Tire Repair, Trailer Drop, Trip Pack Locations, Truck Repairs, Trucker Store, Truckers Lounge, Ups Box, Western Union, Wifi

Code	Name	Address	Mile Marker	Available Parking Spaces	Amenities
Pr_W26	Bosselman Travel Center	Interstate 80 Big Springs Rd, Big Springs	312.0	0	Truck Parking; Restaurant/Deli; Store; Showers; Laundromat; Repair Svcs; Lounge; Scales; Oil Change; Truck Wash; Motel; Self Service;
Pr_E12	Love's Travel Stop #309	1539 Madison AVE, Aurora	332.0	54	24 Hour Diesel, 24 Hour Fast Food, Atm, Bulk Def, Cat Scales, Convenience Store, Dat Check Cashing, Deli, Document Scanning, Dump Station, Fast Food, Laundry, Love's Travel Stop, Metered Propane, Natso Check Link, Oil And Lube, Parking,Lighted Area, Paved Lot, Pet Area, Propane Bottles, Road Service, Rv Gasoline, Rv Parking, Scales - Certified, Showers, Tire Repair, Trailer Drop, Trip Pack Locations, Truck Repairs, Trucker Store, Wifi
Pr_W27	Sapp Brothers	3432 S Lincoln Ave, York	353.0	25	Truck Parking; Restaurant/Deli; Store; Showers; Laundromat; Scales; Self Service;
Pr_E14	Crossroads Fuel Stop	5018 S Lincoln Ave, York	353.0	30	Truck Parking; Restaurant/Deli; Store; Showers; Lounge; Self Service;
Pr_E13	Petro Stopping Center	4700 S Lincoln Ave, York	353.0	250	24 Hour Diesel, Atm, Bulk Def, Can Wire Money Out, Cat Scales, Convenience Store, Dat Check Cashing, Deli, Document Scanning, Dot Inspections, Dump Station, Fast Food, Fedex Box, Game Room, Laundry, Money Orders, Natso Check Link, Oil And Lube, Parking,Lighted Area, Paved Lot, Pet Area, Petro, Propane Bottles, Public Fax / Copier, Receive Prepaid Permits, Reserved Parking, Restaurant, Road Service, Rv Gasoline, Rv Parking, Safe Haven / Hazmat,

Code	Name	Address	Mile Marker	Available Parking Spaces	Amenities
					Scales - Certified, Showers, Tire Repair, Trailer Drop, Trip Pack Locations, Truck Repairs, Truck Wash, Trucker Store, Truckers Lounge, Ups Box, Western Union, Wifi
Pr_W28	Akal Travel Center	915 Road South, Waco	360.0	61	Truck Parking, Resturent, Diesel
Pr_E15	Shoemake's Travel Plaza	151 SW 48th St, Lincoln	395.0	150	Parking, truck stop, diesel, food, shower, mobile repair shop, truck repair shop, truck wash, tank wash, vehicle inspection
Pr_E17	Rite Way 66	13014 238TH ST, Greenwood	421.0	2	Truck Parking
Pr_E18	Flying J Travel Plaza -	15010 South Highway 31, Gretna	433.0	150	24 Hour Diesel, 24 Hour Restaurant, Atm, Boss Shop, Bulk Def, Can Wire Money Out, Cat Scales, Cng, Convenience Store, Dat Check Cashing, Deli, Dump Station, Fedex Box, Flying J Travel Plaza, Game Room, Laundry, Metered Propane, Money Orders, Natso Check Link, Parking,Lighted Area, Paved Lot, Propane Bottles, Public Fax / Copier, Receive Prepaid Permits, Reserved Parking, Restaurant, Rv Gasoline, Rv Parking, Scales - Certified, Showers, Tire Repair, Towing, Trailer Drop, Trip Pack Locations, Truck Repairs, Trucker Store, Truckers Lounge, Ups Box, Wifi
Pr_W29	Sapp Brothers	9905 Sapp Brothers Dr, Omaha	441.0	150	Truck Parking; Restaurant/Deli; Store; Showers; Laundromat; Repair Svcs; Lounge; Scales; Oil Change; Self Service

Code	Name	Address	Mile Marker	Available Parking Spaces	Amenities
Pr_E19	Love's Travel Stop #730	14375 Cornhusker RD, Omaha	440.0	107	24 Hour Diesel, 24 Hour Fast Food, Atm, Bulk Def, Cat Scales, Convenience Store, Dat Check Cashing, Document Scanning, Dot Inspections, Fast Food, Game Room, Laundry, Love's Travel Stop, Metered Propane, Natso Check Link, Oil And Lube, Parking, Patrolled, Parking,Lighted Area, Paved Lot, Pet Area, Propane Bottles, Public Fax / Copier, Receive Prepaid Permits, Road Service, Rv Gasoline, Rv Parking, Showers, Tire Repair, Trip Pack Locations, Truck Repairs, Ups Box, Wifi

Appendix B Underutilized Truck Parking Facilities

ID	Name	Spaces
Pu_E01	Sidney RA EB	34
Pr_E02	Happy Jack	10
Pr_W06	Sapp Brothers	5
Pr_W13	Gas N Shop	5
Pr_W18	Bosselmans Fuel Stop	20
Pr_W10	Plaza Shell	15
Pr_E10	Bosselman Fuel Stop	10
Pr_W12	I-80 Pit Stop	40
Pr_W23	Git 'N Split	6
Pr_W24	Gas N Shop	6
Pr_W25	Pilot Travel Center #902 – Bosselman's	400
Pr_W26	Bosselman Travel Center	0